UNIVERSITY OF SOUTHAMPTON

FACULTY OF NATURAL AND ENVIRONMENTAL SCIENCES

Chemistry

Synthesis of PAMAM dendrimers and investigation of their interaction with POPC/POPG lipids

by

HASSAN GNEID

Thesis for the degree of Master of Philosophy

September 2014

’رب زدني علما‘طه:114

‘O My Lord, increase my knowledge’, Taha:114

’ انما يخشى الله من عباده العلماء’فاطر:28

‘It is only those who have knowledge amongst His Slaves that fear Allah’, Fatir:28

To those whom are well missed in my life and whom I wish they were still with us to share another happy moment of achievement I dedicate this work: my dad 3/2/1990 and my grandmother ‘mama Rajab’ 5/1/2013

UNIVERSITY OF SOUTHAMPTON

ABSTRACT

FACULTY OF NATURAL AND ENVIRONMENTAL SCIENCES

Chemistry

Thesis for the degree of Master of Philosophy

SYNTHESIS OF PAMAM DENDRIMERS AND INVESTIGATION OF THEIR INTERACTION WITH POPC/POPG LIPIDS

Hassan Gneid

PAMAM dendrimers are three dimensional organic polymers synthesised by repetitive steps to achieve a controlled size and shape with a choice of surface functional groups. One of the potential applications of dendrimers is for drug/gene delivery which requires the dendrimer to interact with the cellular membranes. This study is designed to probe the interactions between PAMAM dendrimers and lipid bilayers.

To investigate these interactions PAMAM dendrimers up to the third generation were synthesised. ^{31}P and ^{1}H-^{1}H NOESY NMR studies between these dendrimer and POPC/POPG-derived lipids were then carried out. The results obtained from the NMR experiments were then compared with those from fluorescence studies using a surface-labelled PAMAM dendrimer and the nature of the dendrimer-lipid bilayer interactions was also explored using molecular dynamics modelling.

The solid-state NMR study in a controlled buffer at pH 7.2 revealed that the larger dendrimer (third generation) interacts strongly with a bilayer containing POPG, but not with a bilayer containing only POPC, and no interaction between the smaller dendrimer (zero generation) was observed with either POPC or POPG. This was confirmed with the fluorescence experiments, as changes in the emission intensity of a labelled dendrimer were mainly detected for negatively charged species (SDS and POPG) and rather less for zwitterionic, neutral or cationic species (1,2-dodecyldiol, CTAB and POPC). The coarse-grained molecular dynamic simulations showed that the 3rd generation PAMAM dendrimer can interact with the surface of the membrane when dendrimer is positively charged, but not when the dendrimer is uncharged.

These studies demonstrate how the positive charges and size of the dendrimer influence the interaction with negatively charged lipid, which can have an impact on both the dendrimer's cellular uptake and potential toxicity.

Contents

List of tables

List of figures

nm in aqueous solution. The extinction coefficient of **3G-dansyl** shows the value 10,969 $M^{-1}cm^{-1}$, about twice the value for the single dansyl and as there is a linear relation between the number of the dansyls attached to the PAMAM dendrimer,[146] this suggests that the ratio in **3G-dansyl** is 2:1 dansyl:dendrimer. . 97

List of schemes

DECLARATION OF AUTHORSHIP

I, Hassan Gneid

declare that the thesis entitled

"Synthesis of PAMAM dendrimers and investigation of their interaction with POPC/POPG lipids"

and the work presented in the thesis are both my own, and have been generated by me as the result of my own original research. I confirm that:

- this work was done wholly or mainly while in candidature for a research degree at this University;
- where any part of this thesis has previously been submitted for a degree or any other qualification at this University or any other institution, this has been clearly stated;
- where I have consulted the published work of others, this is always clearly attributed;
- where I have quoted from the work of others, the source is always given. With the exception of such quotations, this thesis is entirely my own work;
- I have acknowledged all main sources of help;

- where the thesis is based on work done by myself jointly with others, I have made clear exactly what was done by others and what I have contributed myself;
- none of this work has been published before submission.

Signed: ……..

Date:……

Acknowledgements

A few years back, when I decided I needed to get back to education and increase both my knowledge and skills, it sounded as an unreachable dream due to the commitments I had in life. Although I was surrounded by a mix of doubtful and supportive people, I had doubts myself but I still made up my mind and after that anything else was not going to be good enough. When I set myself a target I fully commit myself to chase this target and even years before the official starting date I had to overcome any obstructions preventing me from achieving this target, be it personal, financial or otherwise.

This did mean without any doubt a lot of sacrifices, as during a changing time in life you lose some and win some. To all those who without your support these words would not have ever been written, to all those who came in at different stages during this project and helped me one way or another, it would not have been possible for me to achieve what I set myself to achieve and my dream would have stayed as dream. Therefore, to all of you, there would never be enough words to thank you for your contributions and your help, but please do accept my grateful words in an achievement you all took part in as much as I did.

I would like to start by thanking my supervisor Dr. Martin Grossel for giving me the opportunity to work in his group and helping me through my research. I would also like to thank my group, both the current and previous members, for their help and support (Nick, Dom, Darren, Gavin (Bingjia), Adam, Gareth and Alyaa) and also the visitors and project students I worked with (Emma and Dan). I would like to thank Dr. Syma Khalid and her group in computational chemistry for their help and in particular I would like to thank Jamie for his help. I also should thank Dr. Phil Williamson and Andy Hutchin in the biology

department for their help during the project and a particular thanks goes to Dr. Stuart Findlow in the biology department for running my samples on solid state NMR and teaching me how to analysis the results. Additionally, I would like to thank the mass spectroscopy and the NMR departments in University of Southampton for their help. I would like to mention a number of great people I met at Southampton University: the Gale group whom I had great time joining them in tea breaks (Nathalie, Issy, Wim, Stuart, Jenny, Louise, Mike, Xin and Francesca), also my friends Azzam, Faisal, Sameer, Feras, Amar and the members in the ISOC society for their support. I would like to thank my friend Mazen Alhareri and my previous tutors from undergraduate education for providing me with refereeing letters, namely Dr. Farouk Kandil and Dr. François Qrabit.

I would like to thank a number of people whose contributions on a personal level were more than essential in reaching my target. Special thank you goes for my dearest friend Emma Britts, or as she would like to be called *'miss perfect of course :)'* quoting from her text message on my mobile, without your help achieving my MPhil would have been impossible. Thank you Em.

I would like to thank my Brother Yousif for his continuous love and support, my sister Hanan for all her crucial food supplies during my MPhil without which I would have starved, and my sister's family who always were there for me (her husband Simon, the two young men Adam and Colin, and the young princess Areej).

I would like to thank my greatest gain during my MPhil, my beautiful fiancée Dr. Nathalie Busschaert, for all the help and the support at both personal and professional level.

Finally I have to end with thanking my inspiration and the source of the endless love and care in my life and who always believed in my capability and supported me when things were tougher: my mother.

Definitions and Abbreviations

˚C	degrees centigrade
λ_{em}	fluorescence emission maximum
µL	microlitre
µm	micrometer
18-C-6	18-Crown-6
^{31}P	phosphorous NMR
Å	Ångstrom
a.u.	atomic units
AFM	atomic force microscopy
Ar	aryl
Boc	tert-butoxycarbonyl (protecting group for amines)
br	broad resonance (NMR)
Bu	butyl
calcd	calculated
$CDCl_3$	deuterated chloroform
CG	coarse-grained [simulations]
COSY	correlation spectroscopy
d	doublet (NMR)
D_2O	deuterated water
DCC	*N*,*N*′-dicyclohexylcarbodiimide
DCM	dichloromethane
DLS	dynamic light scattering
DMPC	1,2-dimyristoyl-*sn*-glycero-3-phosphocholine
DNA	deoxyribonucleic acid
DOPE	dioleylphosphoethanolamine

DPPA	1,2-dipalmitoyl-*sn*-glycero-3-phosphatidic acid
DPPC	1,2-dipalmitoyl-*sn*-glycero-3-phosphocholine
DSC	differential scanning calorimetry
EDA	ethylene diamine
EDTA	ethylenediaminetetraacetic acid
EM	Erythromycin
EPR	electron paramagnetic resonance
eq	equivalents
ESI	electrospray ionisation
EtOH	ethanol
FCS	fluorescence correlated spectroscopy
FTIR	Fourier transform infra-red spectroscopy
G	generation [PAMAM dendrimer]
g	gram
GPC	gel permeation chromatography
GUVs	giant unilamellar vesicles
HBT	1-hydroxybenzotriazole
HRMS	high resolution mass spectroscopy
Hz	Hertz
IR	infrared spectroscopy
ITC	isothermal titration calorimetry
J	coupling constant (NMR)
L	litre
LDPE	low density polyethylene
LRMS	low resolution mass spectroscopy
L_α	Liquid crystaline fluid phase [of phospholipid bilayers]
L_β	Gel phase [of phospholipid bilayers]
m	multiplet (NMR) or *meta*
M	molar (moles per litre)
m/z	mass to charge ratio
MA	methyl acrylate
MAS	magic spectroscopy angle
MD	molecular dynamics [simulations]
Me	methyl
MeOH	methanol

MHz	megahertz
min	minute(s)
mL	millilitre
mM	millimolar
mmol	millimole(s)
mol	mole(s)
Mp	melting point
ms	milliseconds
MS	mass spectroscopy
nm	nanometer
NMR	nuclear magnetic resonance
NOESY	nuclear Overhauser effect spectroscopy
ns	nanosecond
PAMAM	polyamidoamine
PDB	protein database
PEG	poly(ethylene glycol)
PEI	polyethyleneimine
PFBP	polyfluorene-alt-biphenylene
Ph	phenyl
pK_a	acid dissociation constant
POM	polarizing optical microscopy
POPC	1-palmitoyl-2-oleoyl-*sn*-glycero-3-phosphocholine
POPG	1-palmitoyl-2-oleoyl-*sn*-glycero-3-phosphoglycerol
PPh_3	triphenylphosphine
PPI	polypropyleneimine
ppm	parts per million
PVC	poly(vinyl chloride)
q	quartet (NMR)
qu	quintet (NMR)
RNA	ribonucleic acid
RT	room temperature
s	singlet (NMR) or seconds
SAXS	small angle X-ray sattering
SDS	sodium dodecyl sulphate
SLB	supported lipid bilayer

t	triplet (NMR) or time
T_1	spin-lattice relaxation time
T_2	spin-spin relaxation time
TEM	transmission electron microscopy
THF	tetrahydrofuran
TLC	thin layer chromatography
TMV	tobacco mosaic virus
TOB	tobramycin
TOCSY	total correlation spectroscopy
Tris	tris(hydroxymethyl)aminomethane
UV	ultraviolet [light]
Vis	visible [light]
w/w	Weight-to-weight ratio

Chapter 1: Introduction

Dendrimers are a relatively new class of the much older and better-known polymers, polymer definition according to the Oxford English Dictionary is *"a compound with a molecular structure in which a (usually large) number of similar polyatomic units are bonded together"*.[1] As the field of dendrimers was originally a small niche field within polymer chemistry, a short introduction to polymers will be given in this chapter. However, dendrimers are now a well-established area within chemistry and have many potential applications in a range of areas, from optoelectronics to biomedicine. A comprehensive overview of the synthesis, properties and applications of dendrimers will therefore also be given in this chapter.

1.1 From polymers to dendrimers

Polymers are traditionally categorised depending on their overall structure into three main categories linear, branched or network polymers,[2, 3] but are also often classified as homo-polymers (prepared using only one type of monomer unit) or co-polymers (prepared using different types of monomer units, each of which are present in the backbone of the polymer). Linear polymers represent one of the most common types of polymer and many examples of linear polymers exist, e.g. poly (vinyl chloride) (PVC) (see **Scheme 1(a)**). Branched polymers, such as low density polyethylene (LDPE), share a similar structure to linear polymers, but with additional side chains. It is the presence of these side chains that makes branched polymers less flexible than

linear polymers (see **Scheme 1(b)**). Finally there are network polymers which are linear or branched polymers with covalent cross-links between the chains, where increased cross-linking leads to an increase in strength of the network polymer, e.g. a cross-linked silicone polymer network (see **Scheme 1(c)**).[4]

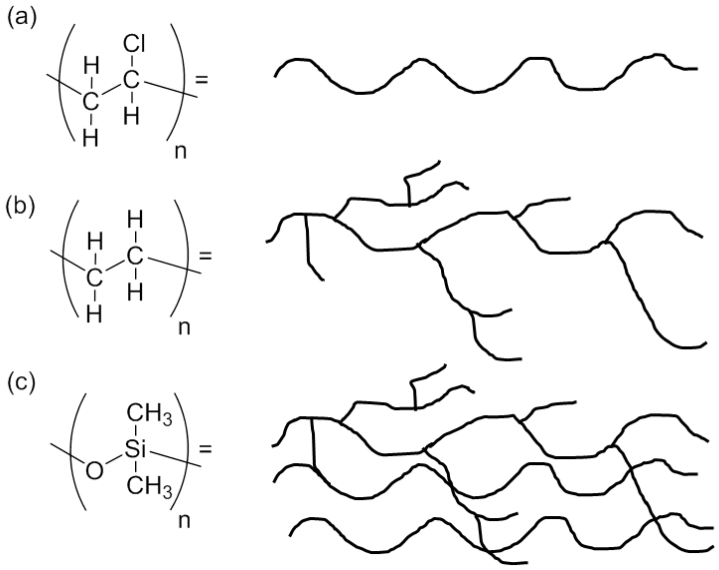

Scheme 1 Classic polymers categories: (a) linear polymer poly (vinyl chloride) (PVC), (b) branched polymer low density polyethylene (LDPE), (c) network polymer cross-linked silicone polymer

Many other types of polymers classification have emerged over the years and only the most common will be discussed here. Comb polymers are polymers joined with a large number of overhanging chains. Examples include polystyrene main chains with poly(ethylene oxide) side chains (see **Scheme 2(a)**)[5, 6]. Another class of polymers is the ladder polymers, which contain a backbone consisting of multiple rings. Hiroto and co-workers, for example, have synthesised a ladder polymer via a condensation reaction between resorcinol and an alkanedial (see **Scheme 2(b)**).[7, 8]

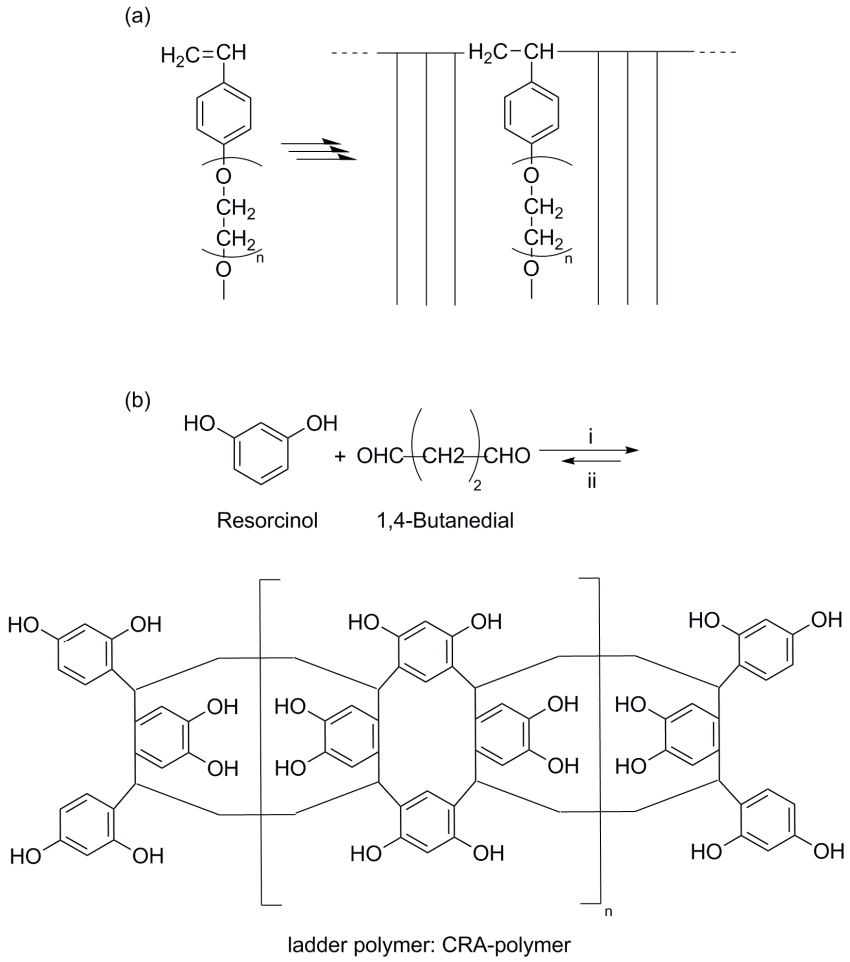

Scheme 2 Examples of polymers with unique structures: (a) comb polymer formed of polystyrene as a backbone with poly(ethylene oxide) side chains, (b) ladder polymer synthesised by the condensation reaction of resorcinol and 1,4-butanedial, i) HCl, ii) 80°C, 48h in ethanol.

Furthermore, an interest in supramolecular polymers and polymeric supramolecular assemblies has developed in recent years. Supramolecular polymers differ from traditional polymers in that non-covalent interactions play an important role in this type of system. One class of supramolecular polymers are the polyrotaxanes,[9, 10] which are systems where a polymer backbone threads through multiple rings such as in the polyfluorene-alt-biphenylene (PFBP), a conjugated polymer threaded through β-cyclodextrin macrocycles developed by Sforazzini *et al.* (see **Figure 1(a)**).[11] Polycatenanes[10, 12] are another type of supramolecular polymer consisting of interlocking rings and examples can be found in the work of Stoddart and co-workers who synthesised a polycatenane using the polyesterification of a [2]catenane (see **Figure 1(b)**). [13]

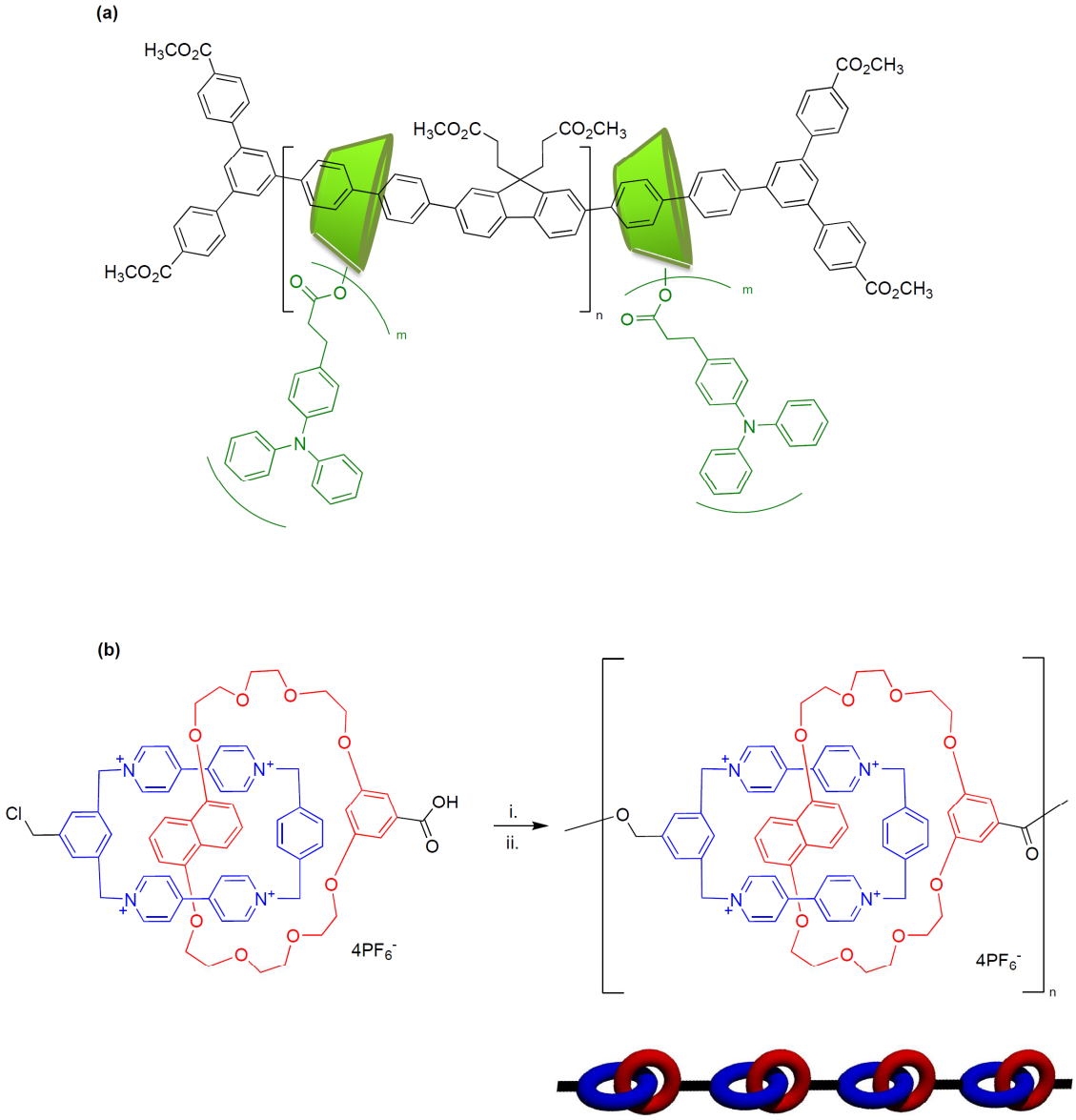

Figure 1 Supramolecular polymers: (a) polyrotaxanes, green cone represent β-cyclodextrin,[11] (b) polycatenanes synthesised by Stoddart and co-workers, i) LiBr, 2,6-Lutidine, MeCN, ii) NH_4PF_6, H_2O.[13]

Branched polymers gradually evolved into hyperbranched polymers, opening the door to a fourth main class of polymers now known as '*dendrimers*'. The first step towards dendrimer synthesis was reported in 1978 when Vögtle and co-workers described a repetitive reaction sequence leading to a multiply branched heptaamine (which they referred to as a '*cascade*' or '*non-skid-chain*' structure).[14] Shortly after that, in 1979, Tomalia and colleagues had a breakthrough in building highly branched supermolecules they referred to as 'starburst polymers' by alternately adding acrylate and diamine monomers to a

central molecule (see **Figure 3(c)** for the starburst polymer first developed by Tomalia). Since these first publications the interest around the subject has grown exponentially and a new type of polymeric architecture has been established, the so-called dendrimers.[15-17] The term dendrimer is generated by combining the two greek words of *dendron,* which means tree, and *meros,* which means part. Thus, dendrimers are highly branched polymers with multi-functional reactive end groups and strongly controlled structure and size.[16] Around the same time as Tomalia's initial work, Newkome *et al.* used a simple mathematical progression to discover a series of branched polymers that are able to give a cascade-like structure and can act as micelles. Newkome and co-workers referred to their compounds as arborols (from the latin word *arbor,* meaning tree) but arborols were later identified as a sub-category of dendrimers.[18, 19] Since the pioneering work of Vögtle, Tomalia and Newkome, the interest in the synthesis, properties and applications of dendrimers has been rapidly increasing, as can be seen from the growing number of publications related to dendrimers in the last thirty years (See **Figure 2**).

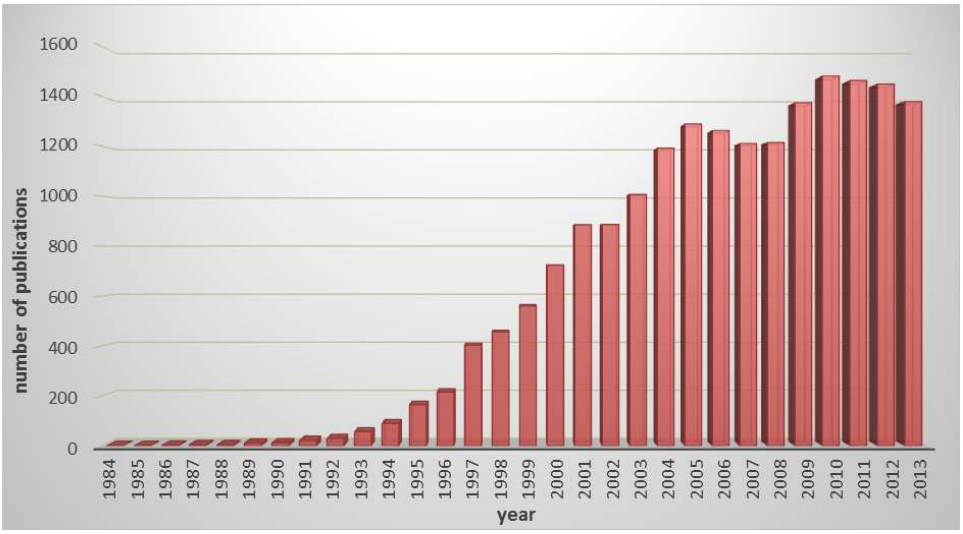

Figure 2 The growing number of publications per year related to dendrimers. Figure generated using SciFinder using 'dendrimer' as keyword.

While the development of dendrimers was partly driven by their potential applications, it is also important to point out that the growing interest in dendrimers was driven by to the possibility of achieving what has been a

chemists' dream for many decades, i.e. synthesising and building well-defined, and both shape and size controlled 'supermolecules' that can imitate what already exists naturally in biological systems. The difficulty in obtaining well-defined molecules similar to those found in biology can be illustrated by comparing one of the highest molecular-weight synthesised samples of polystyrene with a molecular weight ($40x10^6$ g/mol)[20] to the small simple tobacco mosaic virus (TMV) which has a well-defined shape.[21] TMV can be considered as a massive supermolecule with a specific structure, function, size and shape. It consists of a self-assembled structure of 2,130 protein monomers and a 6395 nucleotide units long positive RNA strand with the shape of a helical rod 3,000 Å in length and 180 Å in diameter, while each protein monomer on its own has a defined size and shape consisting of a bundle of four α-helices (see **Figure 3(a)**).[22-24] On the other hand, polystyrene has an undefined random coil shape,[25] i.e. the free rotation around the bonds means that a statistical distribution of various sizes and shapes of the polymer chain are possible[26] (see **Figure 3(b)**). Unlike polymers, Tomalia and colleagues showed that small dendrimers have an ellipsoidal shape, while larger dendrimers adopt a spherical shape as a result of the steric hindrance between the surface groups (see **Figure 3(c)**).[27] The ability to define the dendrimer size and shape could be viewed as the missing link between the classical undefined shaped polymers and the well-defined molecules found in biology.

While **Figure 3** shows that dendrimers start to approach the well-defined shape of biological molecules, their size is also comparable to that of natural molecules. **Figure 4** displays the various size scales from atoms to networks and shows that dendrimers are bigger than conventional organic molecules, but are comparable in size to the biologically relevant micelles and proteins.[15] This well-defined size and shape comparable to biological macromolecules has contributed greatly to the popularity and applications of dendrimers. However, the development of strategies for synthetizing such rigorously controlled structures has not been easy and many years of research were needed to optimize the synthesis of dendrimers, as will be discussed in the next section.

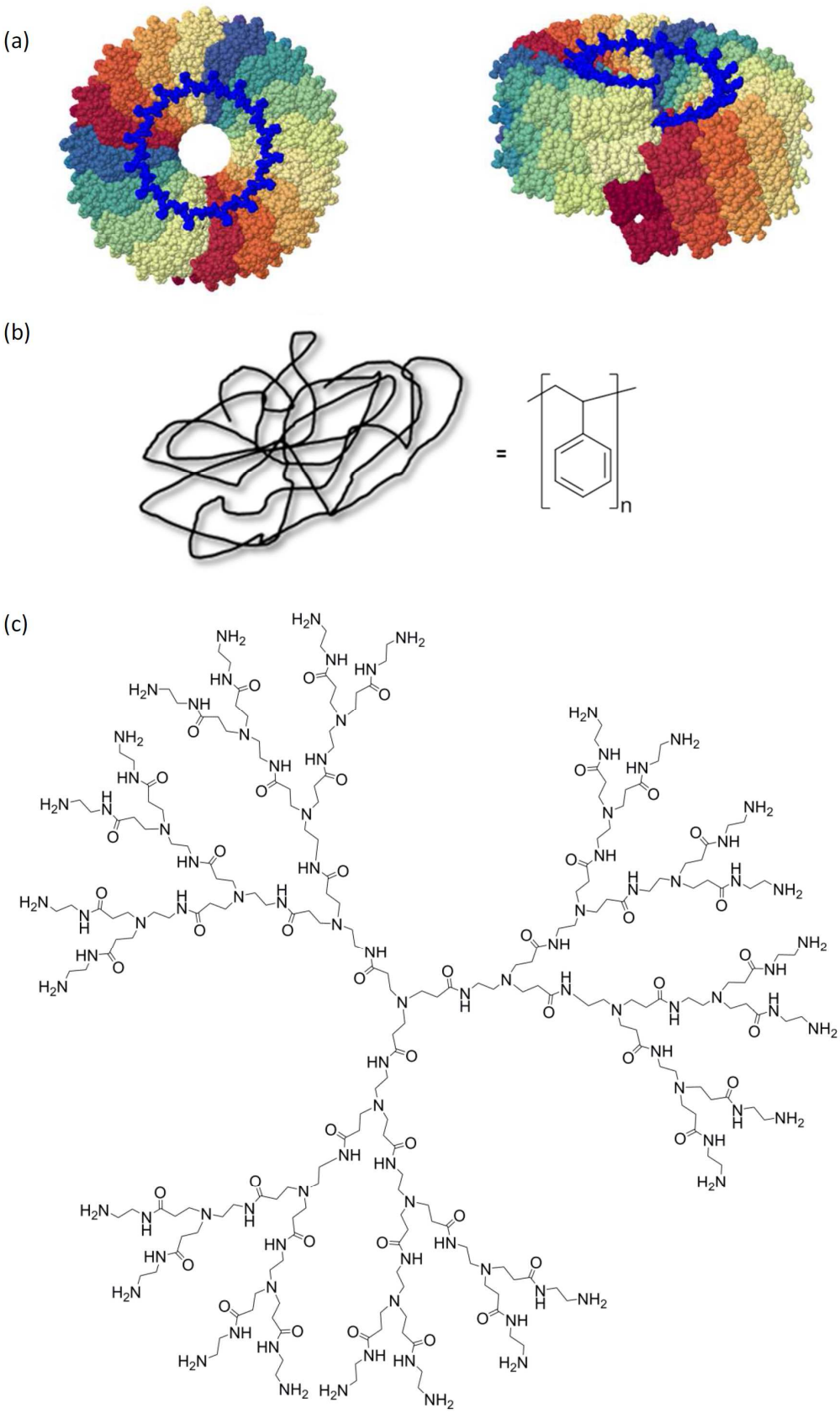

Figure 3 (a) Top and side view of the Tobacco mosaic virus. Each subunit is shown in a different colour and the RNA is shown in blue. Figures generated using PDB entry 2TMV.[21] (b) Random coil of polystyrene. (c) Starburst polymer by Tomalia.[15]

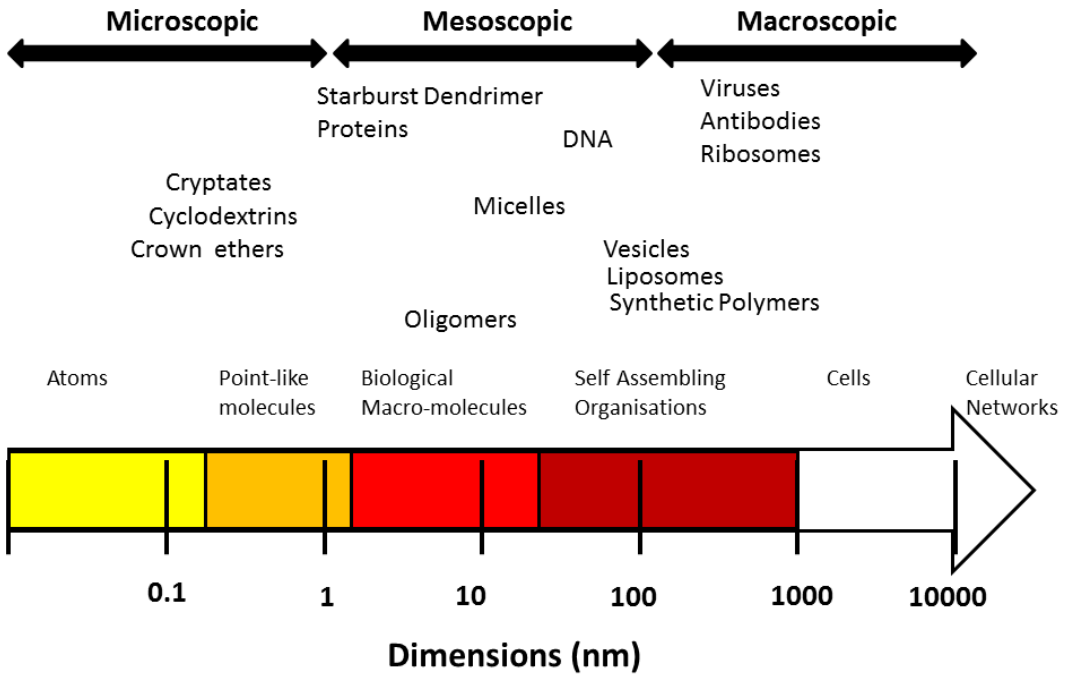

Figure 4 Scale of molecular and submolecular sizes: from atoms to networks.[15]

1.2 Synthesis of dendrimers

Over the years, two basic routes emerged for the synthesis of dendrimers, namely the divergent and convergent pathways (see **Figure 5** for a schematic representation of the two methods). The first method to be developed was the divergent synthesis. In this method the dendrimers are built outwards from the core by the sequential addition of the building blocks through a series of '*shells*', each complete sequence being known as a '*generation*'. In order to obtain a complete generation a number of synthetic steps might be required and by repeating these steps the dendrimer can grow to higher generations. However, this exponential growth in the size of the dendrimer, combined with the large increase in the number of reactive groups, can result in imperfections in the structure and makes dendrimer characterisation harder. On the other hand, in the convergent method the dendrimers are built inwards towards the core from the surface resulting in a wedge shape or '*dendron*', and the target dendrimers are formed by covalently coupling the dendrons to the core. The

convergent method does not have the same problems with structural defects as the divergent method and it is also easier to separate the final product during purification because of the large molecular weight difference compared with the starting materials (dendrons). However, this method suffers from steric complications when coupling the dendrons to the core, resulting in low yields. It is clear that both methods have advantages and disadvantages and both methods are therefore still used to date. The exact synthetic pathway to obtain a dendrimer will thus depend on the specific structure of the desired dendrimer.

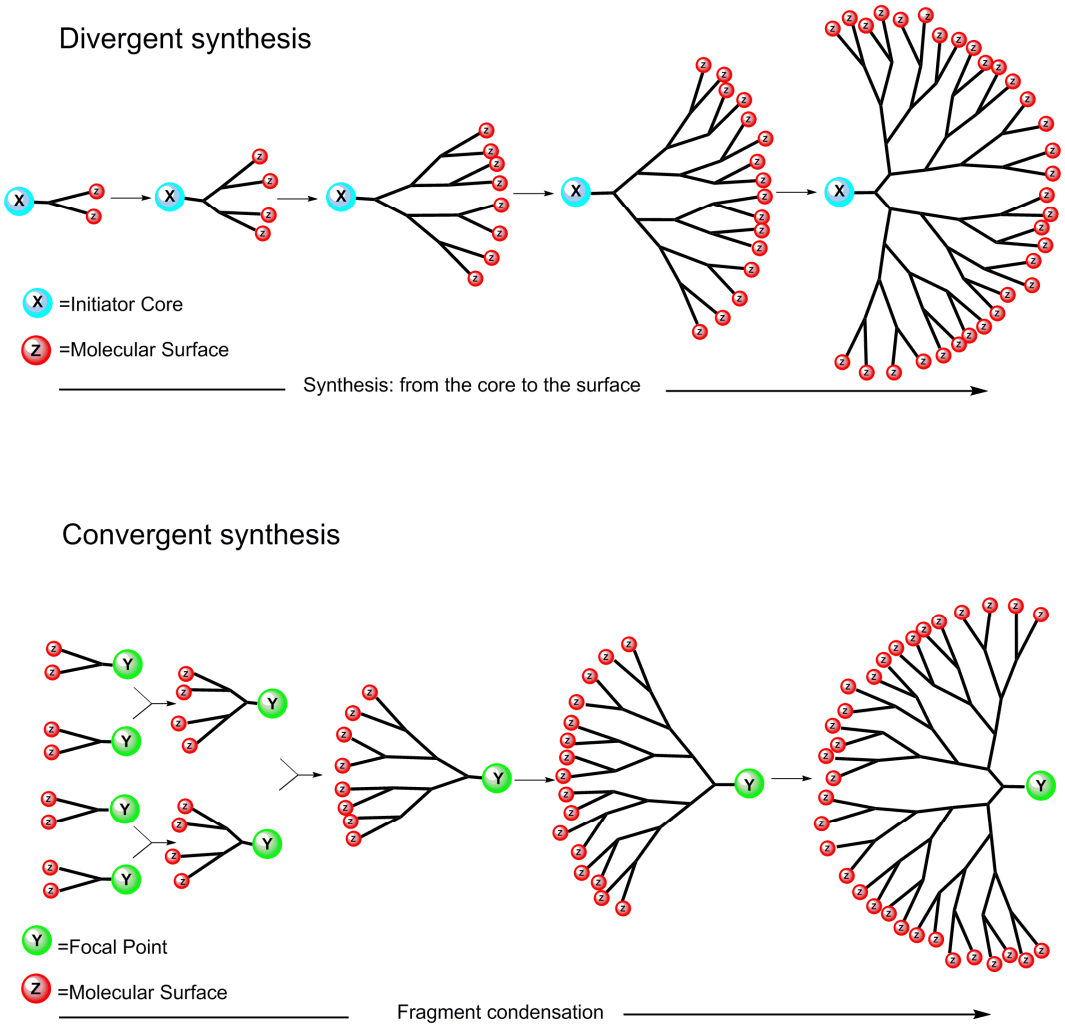

Figure 5 Comparison the between divergent and convergent methods of dendrimers synthesis.

The first dendrimer synthesis by the divergent method was reported in 1978 when Vögtle and co-workers described a synthetic method for what they referred to as '*cascade*' or '*non-skid-chain*' structures. The synthesis was described as *"reaction sequences, which can be carried out repeatingly".* In brief, the synthesis was carried out by reacting primary amines with acrylonitrile in a Michael addition to produce a dinitrile which was reduced to a terminal diamine and after purification the addition sequence were repeated to generate a hepta-amine (see **Scheme 3(a)**). While the final hepta-amine in Vögtle's synthesis is still not a macromolecule, it did demonstrate a repetitive reaction sequence leading to a multiply branched molecule.[14] Subsequently, Denkewalter *et al.* included in a patent the synthesis of a hyperbranched, monodisperse polymer of L-lysine (see **Scheme 3(b)**).[28, 29] Soon after, in late 1979, Tomalia and colleagues had a breakthrough in building highly branched supermolecules, which they referred to as '*starburst polymers*', by alternatingly adding acrylate and diamine monomers to a central molecule (see **Figure 3(c)** for the starburst polymer first developed by Tomalia).[15-17] Around the same time, Newkome *et al.* used a simple mathematical progression that helped them to discover a series of branched polymers that are able to give a cascade-like structure (see **Scheme 3(c)**).[18, 19]

It are these two examples by Tomalia and Newkome that are generally considered to be the first dendrimers synthesised using the 'divergent synthesis' method. However, in 1989 Fréchet and Hawker found a different approach for synthesising dendrimers by raising the possibility of growing the dendrimers from the outside to inwards. They started their synthesis by making wedge shapes or dendrons through a series of ether formations, followed by coupling the dendrons to the core to form the final dendrimer (see **Scheme 4(a)**).[30, 31] Their lead was shortly followed by Miller and Neenan who used this 'convergent synthesis' to develop a polyaromatic dendrimer via a series of Suzuki coupling reactions (see **Scheme 4(b)**).[32]

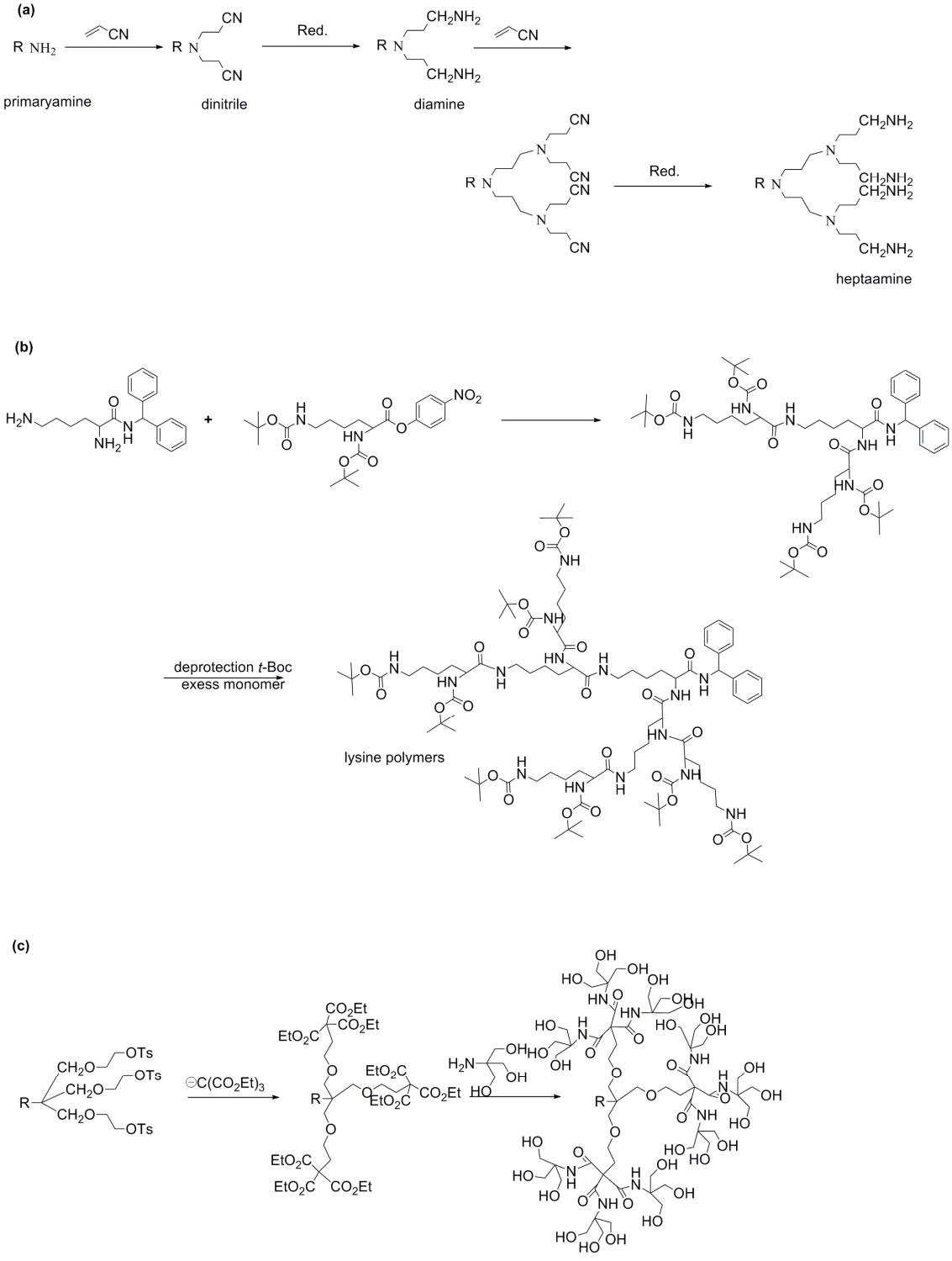

Scheme 3 Divergent pioneering synthesis. (a) Vögtle's approach.[14] (b) Denkewalter's approach.[28] (c) Newkome's *et al* .approach.[18]

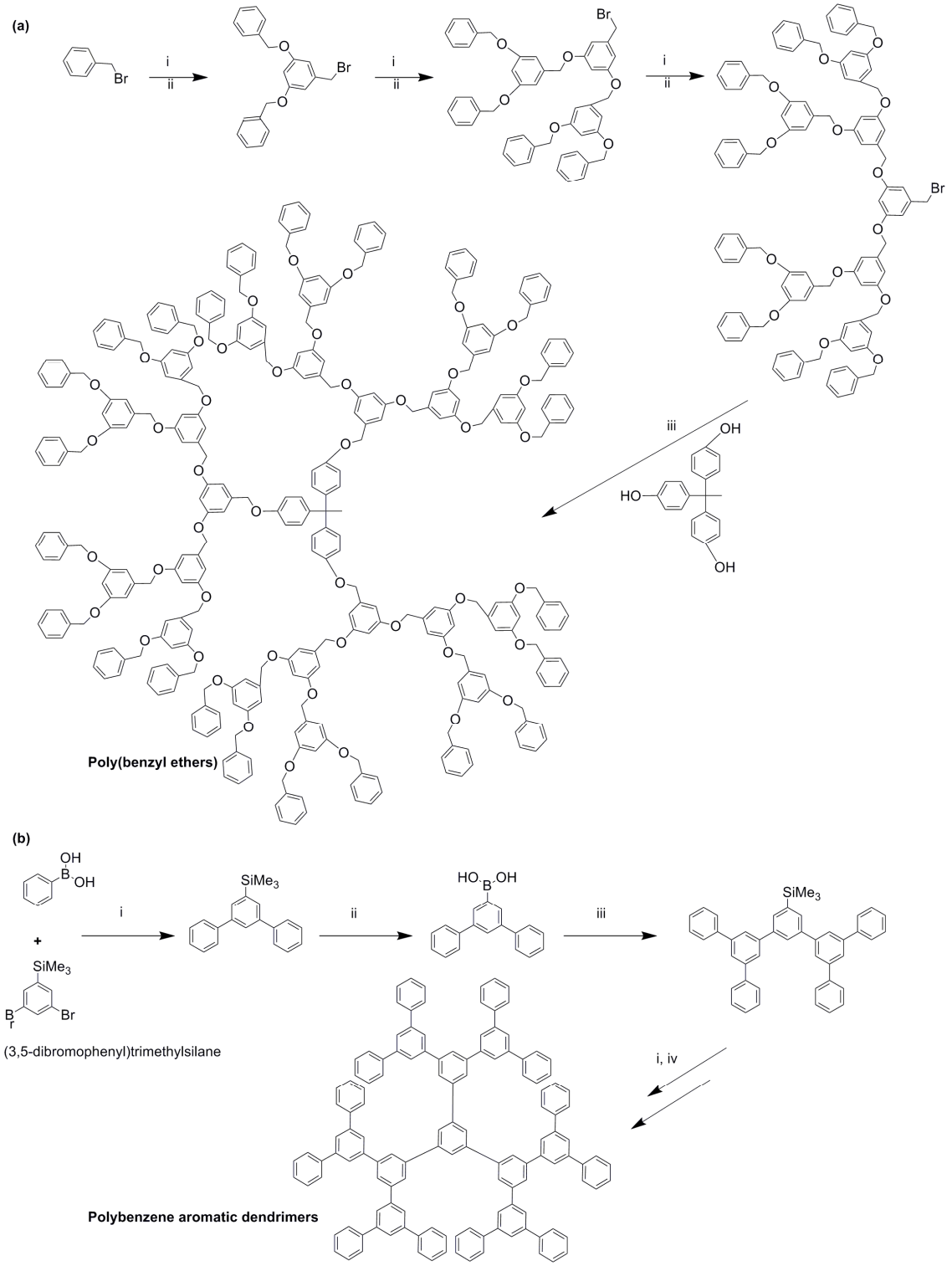

Scheme 4 Convergent pioneering synthesis (a) Fréchet and co-workers developed the synthesis of poly(benzyl ethers): i) 5-(hydroxymethyl)benzene-1,3-diol, K_2CO_3, 18-Crown-6, acetone; ii) CBr_4, PPh_3, THF iii) K_2CO_3, 18-Crown-6, acetone .[30] (b) Polybenzene aromatic dendrimers synthesised by Miller and Neenan: i) $Pd(PPh_3)_4$, Na_2CO_3, EtOH; ii) BBr_3, DCM, KOH, H_2O; iii) (3,5-dibromophenyl)trimethylsilane, $Pd(PPh_3)_4$, Na_2CO_3, DCM/THF; iv) 1,3,5-tribromobenzene, $Pd(PPh_3)_4$, Na_2CO_3, THF[32].

Since the pioneering synthesis in both divergent and convergent methods, a growing numbers of research groups have been utilising these approaches to synthesise novel dendrimers. Ueda *et al.,* for example, used the divergent method to synthesis a poly(arylether) around a calix [4]resorcinarene core in order to obtain a photoresist material (see **Scheme 5**).[33, 34]

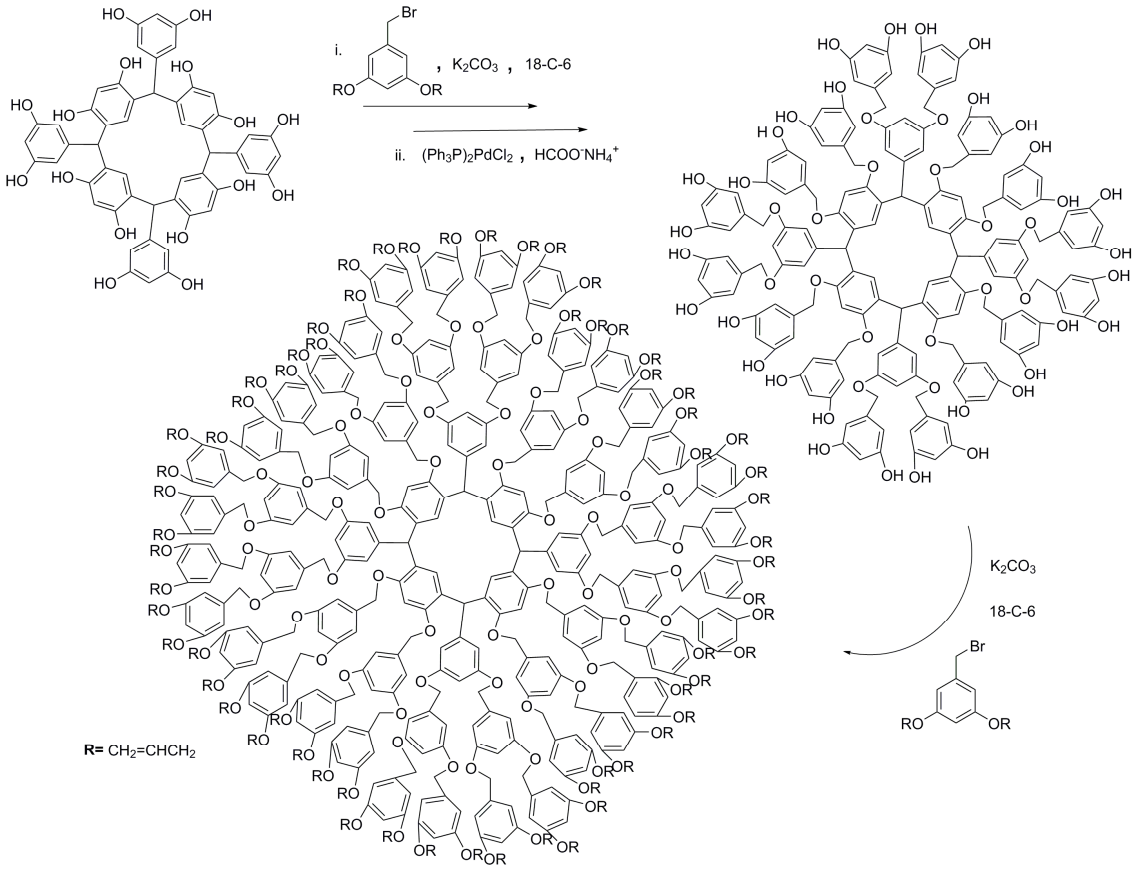

Scheme 5 Synthesis of a poly(arylether) by coating calix[4]resorcinarenes using the divergent method.[33]

In another example, Diederich *et al.* have employed a modified fullerene C_{60} as the core in a convergent synthesis to achieve various dendrimers, including a modified C_{60} with bis(malonate) tetraester core treated with glycine-modified 2nd generation dendrons to give a 36-ester dendrimer (see **Scheme 6**). [35, 36]

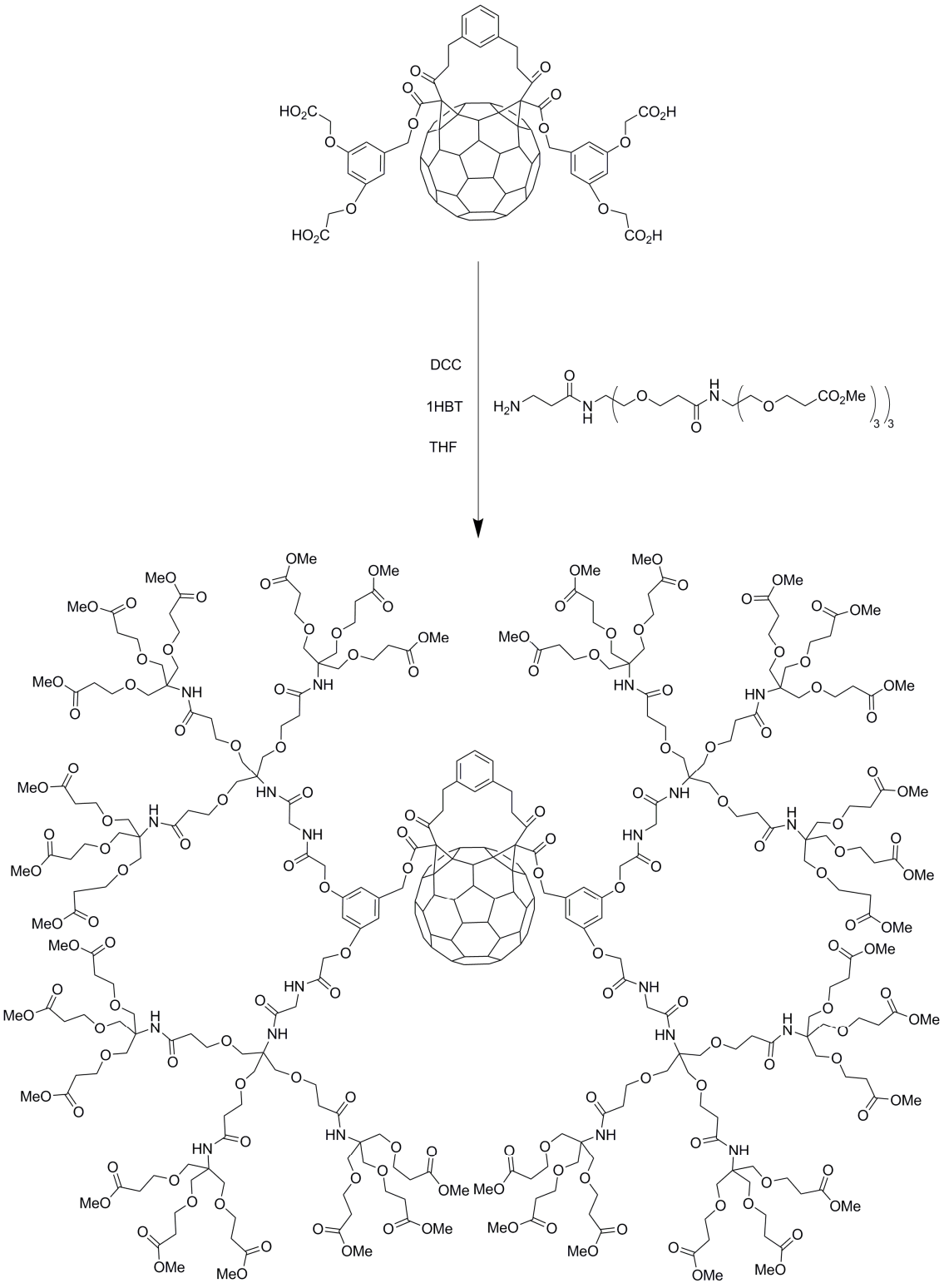

Scheme 6 modified C_{60} macrocycles as a core for dendrimers formation.[35]

Although numerous other examples of dendrimer synthesis can be found in the literature, it is not within the aim of this introduction to give a full overview of synthetic procedures. However, it must be noted that many of the advances in dendrimer synthesis are driven by the desire to built-in new functionalities within the dendrimers in order to achieve potentially useful applications.

1.3 Applications of dendrimers

Since their first discovery, the study of dendrimers has become increasingly popular and dendrimers have now been suggested for a range of applications in the medical sciences, electrochemistry, synthetic chemistry, biology, optics and other research fields.[37-46] Studying all dendrimers in general and their application is beyond the scope of this project and hence this introduction will focus on applications relating to the subject of this thesis: PAMAM (polyamidoamine) dendrimers. PAMAM dendrimers were first developed by Tomalia[15] and form now one of the most well-known examples of dendrimer chemistry. The popularity of PAMAM dendrimers arises from some of their intrinsic properties that render these dendrimers useful for a range of applications. This introduction will therefore give a brief overview of the properties of PAMAM dendrimers before continuing onto the possible applications that have been investigated for this type of dendrimer.

1.3.1 Properties of PAMAM

PAMAM (polyamidoamines) are highly branched spherical organic polymers, first developed by Tomalia and co-workers in 1985.[15] Their synthesis starts with the reaction of an ethylenediamine (EDA) or alternative amine cores with excess methylacrylate by Michael addition, resulting in a branched structure with terminal ester functionalities, followed by reaction of the product with EDA to extend the previously formed branches. By repeating these two reactions in a stepwise manner, PAMAM dendrimers of various sizes

can be obtained (more details regarding the synthetic procedures will be given in **Chapter 2**, see **Figure 6** for an example of a PAMAM dendrimer). PAMAM dendrimers are therefore a variation of the original starburst polymers developed by Tomalia (see **Figure 3(c)**). The PAMAM naming system was developed by Tomalia[15] and it includes the size of the dendrimer (i.e. dendrimer generation *(G)*, the core type *(C)*, the number of surface groups *(N)* and the functional groups on the surface *(F)*, according to the following general formula:

G-[C]-N-F

The core (often ammonia or EDA) is generally considered as generation -1 and is the starting point for deriving the dendrimer generation. When the core or another dendrimer generation are reacted with methyl acrylate the result is a further branched dendrimer with ester groups on the outside that are considered 'half generation' PAMAM dendrimers. On the other hand, adding EDA in the following step will lead to the extension of the branches and the formation of an amine terminated 'full generation' PAMAM dendrimer. Thus, upon each step during the synthesis, the PAMAM dendrimer grows by 0.5 generations. This is illustrated schematically in **Figure 6** for a 3rd generation EDA-core PAMAM dendrimer **3.0-[EDA]-32-amine**. It must be noted that the size of the PAMAM dendrimer and the number of amine functional groups at the surface of the sphere increases upon each generation of dendrimer (see **Table 1** and **Figure 6**) and can thus be easily controlled by the stepwise synthesis employed in the preparation of each generation. It is this facile control of size that has contributed a lot to the popularity of PAMAM dendrimers as the size of the dendrimer can be varied depending on the required application. However, it is important to realise that the surface can reach a point where it is overcrowded with functional groups and the synthesis cannot fully go ahead anymore because not every site can react beyond this point (de Gennes dense packing).[47]

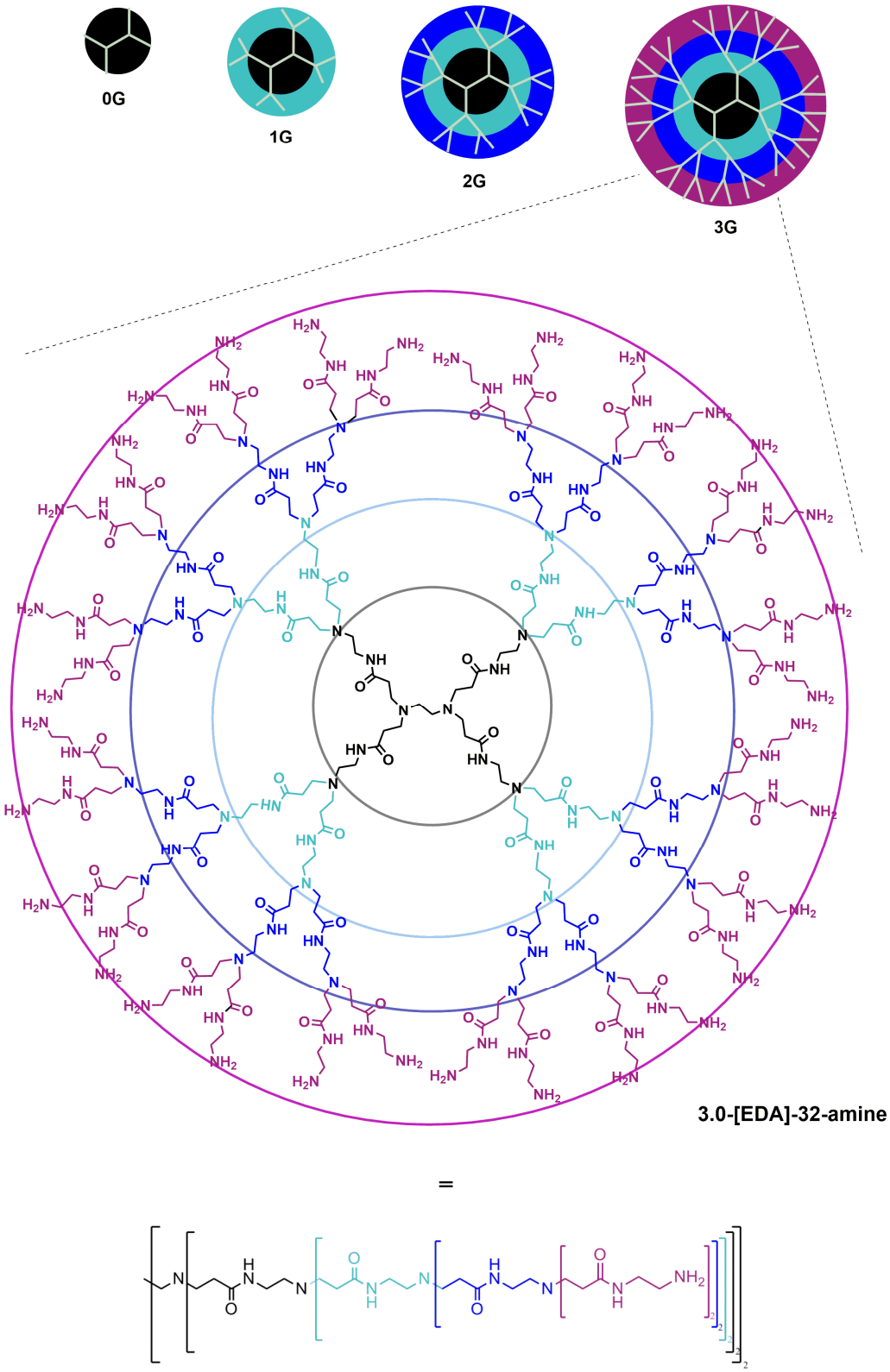

Figure 6 Schematic presentation of the increase in size of PAMAM dendrimers from 0th generation to 3rd generation (top), alongside the structure of the 3rd generation PAMAM (bottom), colour coded for each full generation.

Table 1 Overview of PAMAM dendrimers of varying generations (Gn), with molecular weight (Mw, g/mol), diameter (Ø, Å) and number of surface amine groups (N).

Gn	Mw (g/mol)	Ø (Å)	N
0	517	15	4
1	1430	22	8
2	3256	29	16
3	6909	36	32

Figure 6 also reveals that there are three main domains within a PAMAM dendrimer. The first domain is the *core* from which the dendrimer grows - this core can be changed depending on the desired function or application. The second domain consist of the interior shells and *branches* which surround the core and create spaces and cavities at the branching points - these cavities are important for the encapsulation of guests within the PAMAM dendrimers as will be illustrated below. The third domain is the multivalent *surface groups* (amine groups in the case of full PAMAM generations or ester groups in the case of the half generations) which can be involved in attractive forces and surface bonding or which can be partially or completely functionalised to enhance any required activities of the PAMAM dendrimers. All these properties render PAMAM dendrimers an adaptable platform for a wide range of applications, where the function can be optimised by the facile modification of the size, the core or the surface of the dendrimer.

1.3.2 Optical, catalytic and biological applications of PAMAM

It was mentioned earlier that dendrimers have found applications in the fields of biology, organic synthesis and optics and optoelectronics. The latter is due to the interesting absorbance and fluorescence properties of neat and modified dendrimers (including PAMAMs). One of the main goals of this field is achieving an artificial photosynthesis system by improving the energy transfer efficiency within the so-called 'light-harvesting' dendrimers.[48-53] An example can be found in the work of Georgiev *et al.* who studied the photophysical

behaviour of light-harvesting PAMAM dendrimers synthesised from 0th and 1st generation dendrons attached to a core modified with a single rhodamine dye and functionalised on the surface with a number of 4-alkylamino-1,8-naphthalimide dyes (see **Figure 7**). The light-harvesting properties arise from the fact that the donor fluorophores (4-alkylamino-1,8-naphthalimides) emit yellow-green light and this energy is transferred to the single acceptor dye (rhodamine). Furthermore, the system displays ON-OFF switching of the energy transfer mechanism from acidic to alkaline conditions, according to the rhodamine absorption dependency on pH. They observed an increase in the rhodamine emission intensity in the acidic range and concluded that these novel modified PAMAM dendrons also have the potential of playing a role as a pH dependent switch.[54]

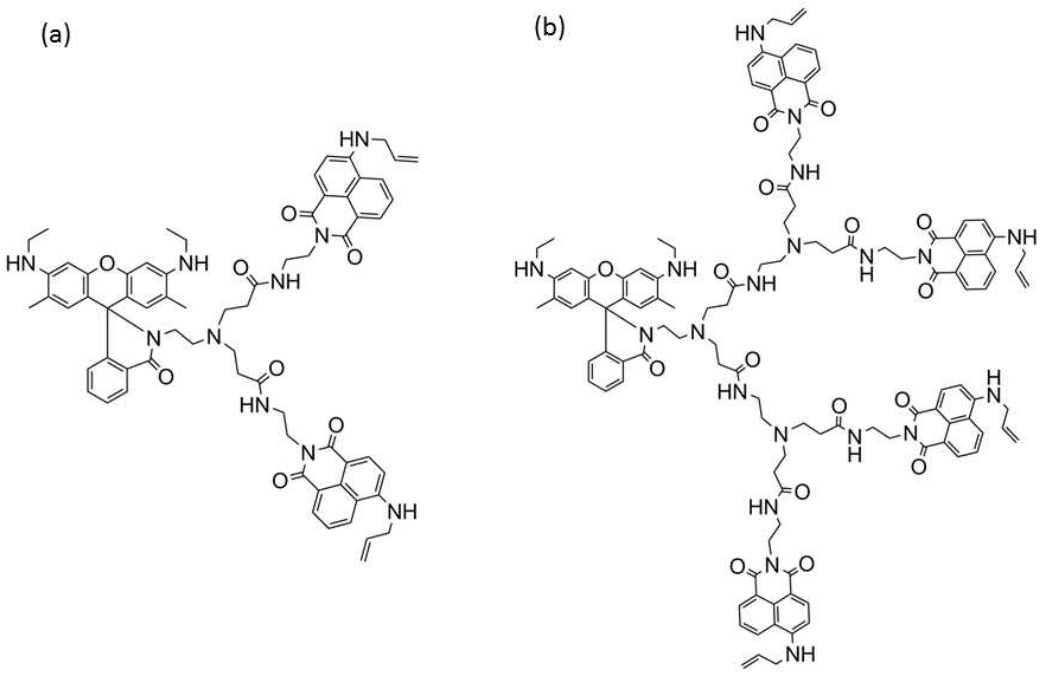

Figure 7 Light-harvesting dendrons containing a modified surface of donors (4-alkylamino-1,8-naphthaimide and a single acceptor dye (rhodamine). (a) Modified 0th generation PAMAM. (b) Modified 1st generation PAMAM dendrimer.

The optical properties of dendrimers can also be employed in the development of highly sensitive sensors. Yamaji and Takaguchi, for example, found 4.5 generation-PAMAM-CO_2Na to be a fluoride sensor in methanol as a decrease in

fluorescence intensity was observed with fluoride ions and not with other halides ions.[55] PAMAM dendrimers can also be utilised for sensing low concentrations of biologically relevant molecules, such as the glucose sensing system developed by Liu *et al.* based on a 3.5 generation PAMAM dendrimer-porphyrin dual luminescence system.[56]

Bioimaging can also be achieved through the employment of the optical properties of dendrimer assemblies. In a recent study Foucault *et al.* synthesised a luminescent complex of eight Sm^{III} ions which was sensitized by thirty two chromophores (2,3-naphthalimide) attached to the surface of a 3rd generation PAMAM dendrimer. Two wavelengths were observed upon exciting the complex in the visible and in the near-infrared (NIR) ranges and the complex penetration into HeLa and NIH3T3 cells was confirmed by confocal microscopy. The complex was validated by epifluorescence microscopy as a versatile probe that emits in the visible and NIR in the living cells and can therefore be useful for bioimaging purposes.[57] Fluorescence spectroscopy is only one way of achieving bioimaging tools, magnetic resonance properties can also be employed for this purpose. In this respect Kobayashi and co-workers have used an 8th generation PAMAM dendrimer functionalised with a Gd^{III} chelating agent, as shown in **Figure 8**, in MRI (magnetic resonance imaging) experiments to visualize and monitor the changes in tumour vessel permeability after one dose of radiation.[58, 59]

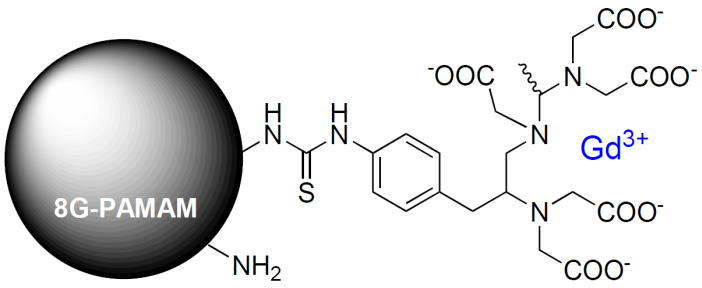

Figure 8 Structure of 8G-PAMAM-Gd^{III} based MRI contrast agent by Kobayashi and co-workers. Only one NH_2 functionalisation is shown for clarity (approximately 35% conversion of the terminal NH_2 functionalities was achieved).

Dendrimers have also been used in the development of liquid crystals,[60] which combined with the optical properties of the dendrimers can result in some interesting new liquid crystals. Jaseer and colleagues have investigated the photophysical properties of PAMAM and PPI (polypropyleneimine) dendrimers by modifying the peripheral surface with decanoic, 4-octyloxybenzoic, and 3,4,5-trioctyloxybenzoic acids generating smectic and columnar phases (see **Figure 9**). They used polarizing optical microscopy (POM) and differential scanning calorimetry (DSC) to examine the dendrimers in both solution and thin solid films. They found that the modified dendrimer based-liquid crystals show blue emission when excited at 370 nm and that the emission intensity is enhanced by an order of magnitude as the generation of dendrimer increases to the 4th generation PAMAM. They therefore concluded that the inherent emission properties of PAMAM and PPI dendrimers are kept in the mesophase. These results imply that luminescence liquid crystals based on dendrimers in the visible region can be obtained without introducing extra fluorophores.[61]

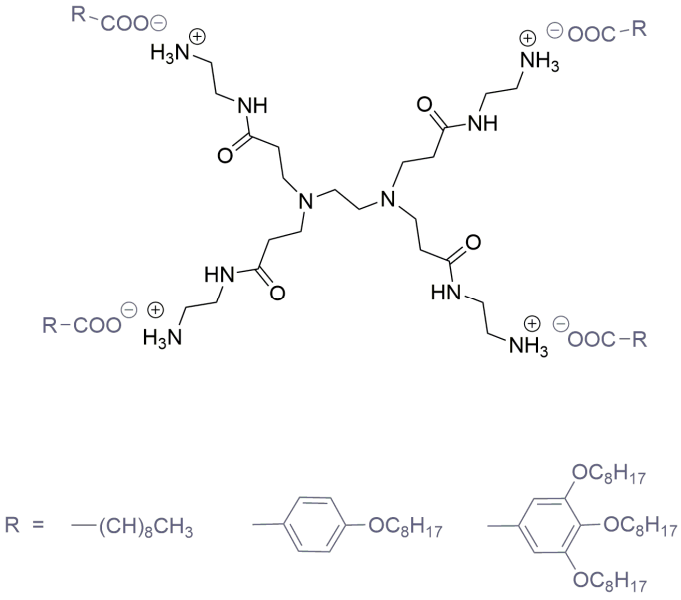

Figure 9 Liquid crystals based on a 0th generation PAMAM dendrimer.

Another useful application of dendrimers is their employment as catalysts in organic and inorganic synthesis. Dendrimer catalysts can be prepared by encapsulating a reactive metal within the dendrimer's cavities. Tomalia and

Balogh were the first to use PAMAM dendrimers as templates and stabilizers of metal ions in an approach that is now known as 'reactive encapsulation'.[62, 63] Since then many studies have demonstrated the encapsulation of transition metal ions such as Cu^{2+}, Ag^{+}, Pt^{2+}, Pd^{+}, Ru^{3+} and Ni^{2+}.[62, 64, 65] Crooks and Zhao encapsulated platinum(II) salts into 4th generation dendrimers terminated with amines or hydroxyls. They subsequently managed to reduce the platinum(II) using BH_4^- resulting in an entrapped clustered spherical platinum nanoparticle containing the same number of platinum atoms $[Pt^0]_n$ and with an approximate diameter of 1.6 nm. The PAMAM dendrimer prevents the metal clusters from agglomeration and the resulting platinum modified dendrimers could thus be used for the electrocatalytic reduction of O_2 (see **Scheme 7**).[66]

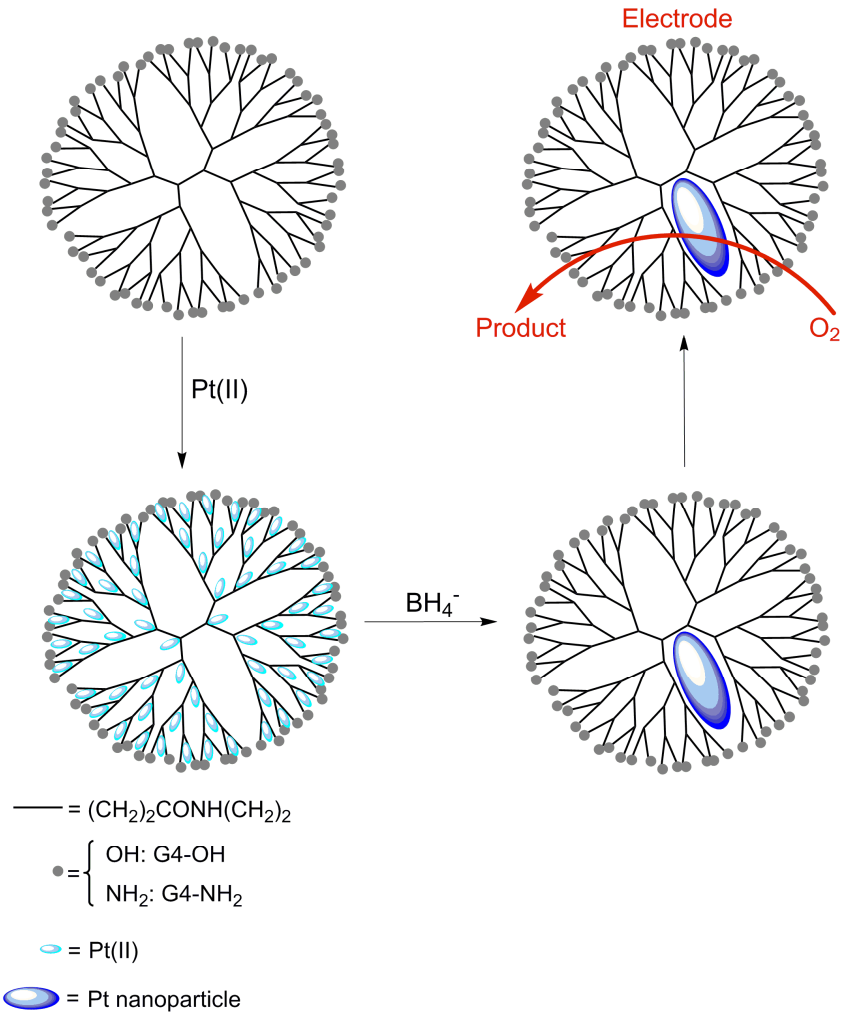

Scheme 7 4th generation PAMAM dendrimer with -OH and -NH_2 terminal groups encapsulating Pt^{2+} ions, followed by reduction with BH_4^- to form Pt nanoparticles with electrocatalytic activities.

In a later study the same group expanded the encapsulation to include Pd^0 and Pt^0 within various hydroxyl-terminated PAMAM dendrimers. They used X-ray photoelectron microscopy (XPS) to support the composition and the oxidation state of the encapsulated nanoparticles. The synthesised modified dendrimers possess catalytic activities for the hydrogenation of alkenes in water with the 4th generation PAMAM dendrimer **4G-OH (Pt_{40})** being the most active. Furthermore they concluded that the catalytic activity can be controlled by the size of the dendrimer and that the dendrimer can act as a 'nanofilter' for substrate molecules.[67]

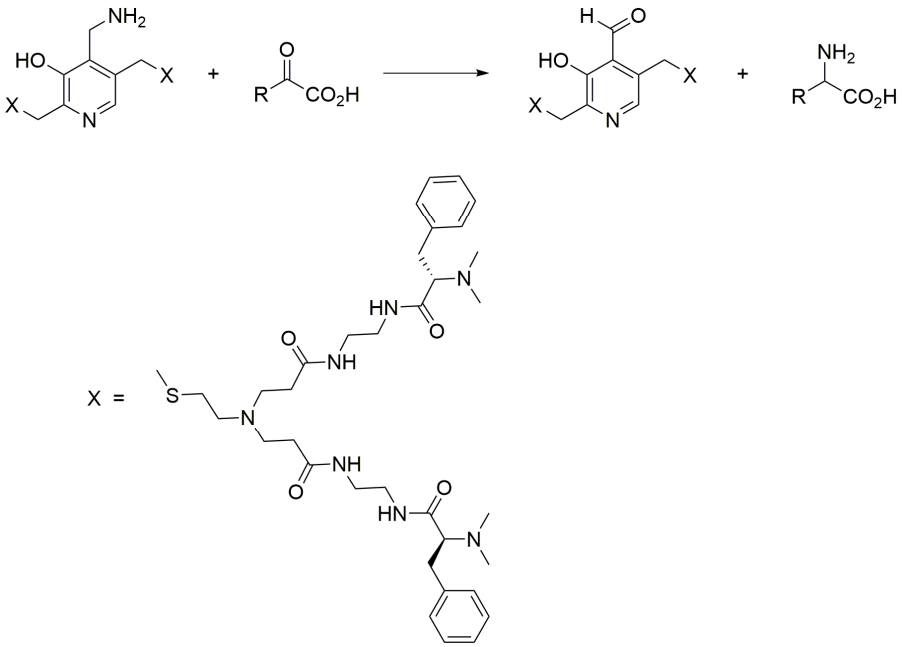

Scheme 8 A PAMAM dendrimer with pyridoxamine core used in transamination reactions mimicking enzymes.

The well-defined and controllable spherical shape of dendrimers, combined with their potential catalytic properties, renders this type of molecule ideal for mimicking enzymes or other proteins. For example, Breslow and co-workers have reported a number of PAMAM dendrimers with pyridoxamine in the core which perform the transamination of pyridoxamine with α-ketoacids (phenylpyruvic and pyruvic acid) to form amino acids and a core pyridoxal (see **Scheme 8**). Due to the observation that the chiral groups on the periphery of the dendrimer can induce enantioselectivity, they concluded that the dendrimer

branches possess a high flexibility and can fold back to the pyridoxamine core, similar to the structure of many enzymes. This proposed folding was also supported by computer modelling. [68, 69] While the reaction shown in **Scheme 8** is not a catalytic reaction, the authors have shown in a separate manuscript that the resulting pyridoxal can be converted back to the initial pyridoxamine using sacrificial 2-amino-2-phenylpropionic acid.[70]

Due to their particular structure, dendrimers have also been proposed for other types of biological mimic. Tomalia and co-workers have shown that the branches of the dendrimers generate internal cavities with controllable sizes and shapes.[15, 71] Furthermore, it was noted that the radius of PAMAM dendrimers is similar to conventional nano-scale micelles[71] which results in similar behaviour for PAMAM dendrimers to traditional micelles and liposomes. Micelles and liposomes have been used for encapsulating small drug molecules and delivering them inside cells[72, 73] and it has therefore been suggested that dendrimers might also function as favourable drug vectors (as will be explained in the next section).[15, 27]

1.3.3 Biomedical applications of PAMAM

While the previous section has shown that dendrimers can find many uses in optical, physical and catalytic applications, one of the most popular uses of dendrimers lies in the field of biomedicine. Some dendrimers, for example, have been shown to function as drugs themselves (e.g. in antitumor treatment),[74-76] while early studies on PAMAM dendrimers have found antiviral activity when the PAMAM surface is modified with naphthyl sulfonate.[77, 78] However, the most well-known biomedical application of dendrimers is their use as a drug or gene delivery system. The reason why dendrimers have become popular as potential delivery systems is due to the fact that small molecules can easily be attached to the surface of dendrimers, as well as the ability of dendrimers to encapsulate small molecules in their interior cavities (see **Figure 10**).

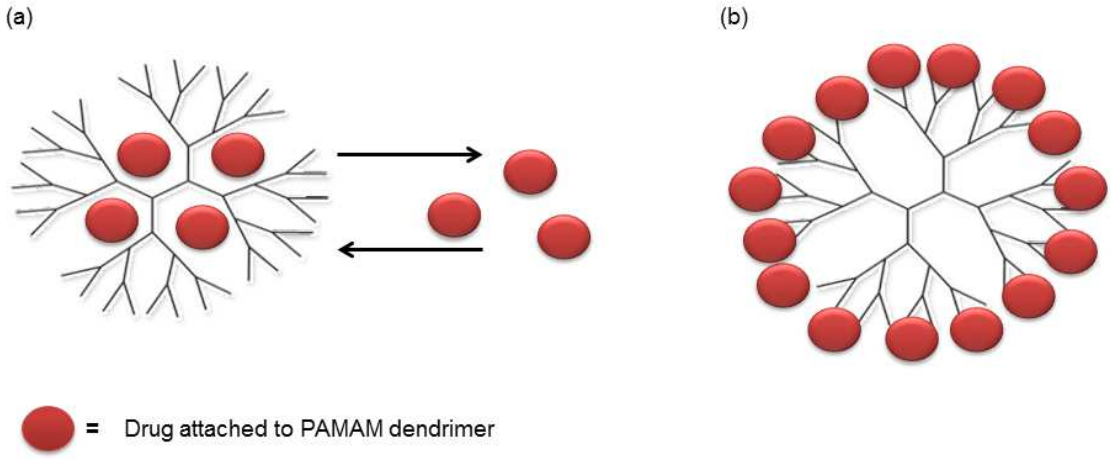

Figure 10 PAMAM dendrimers as drug delivery (a) by encapsulating drug in the interior cavities of the dendrimer, (b) by attaching the drug to surface.

Tomalia and co-workers had already noted this encapsulation phenomenon in their early work and referred to it as *unimolecular encapsulation*,[17, 27] while Meijer *et al.* managed to control the encapsulation and release of a cargo molecule (urea-glycine) in a drug delivery system (a 5th generation poly(propylene imine) dendrimer modified by adamantly and palmityl end groups via a thiourea linkage) which they coined the *dendritic box* approach.[79] Since this pioneering work many researchers have reported the use of various dendrimers, including PAMAM dendrimers, as potential drug delivery systems. Malik and colleagues, for example, encapsulated the anticancer drug cisplatin (see **Figure 6(a)**) within PAMAM dendrimers and reported a slower release and higher accumulation of the drug in solid tumours. Furthermore when compared to non-capsulated cisplatin, the encapsulation in PAMAM dendrimers seemed to have lowered the toxicity of cisplatin.[80] In another study Malik and co-workers observed anti-tumour activities for synthesised complexes of 3.5 generation PAMAM dendrimers with platinum-containing compounds attached to the surface (see **Figure 6(b)**).[81]

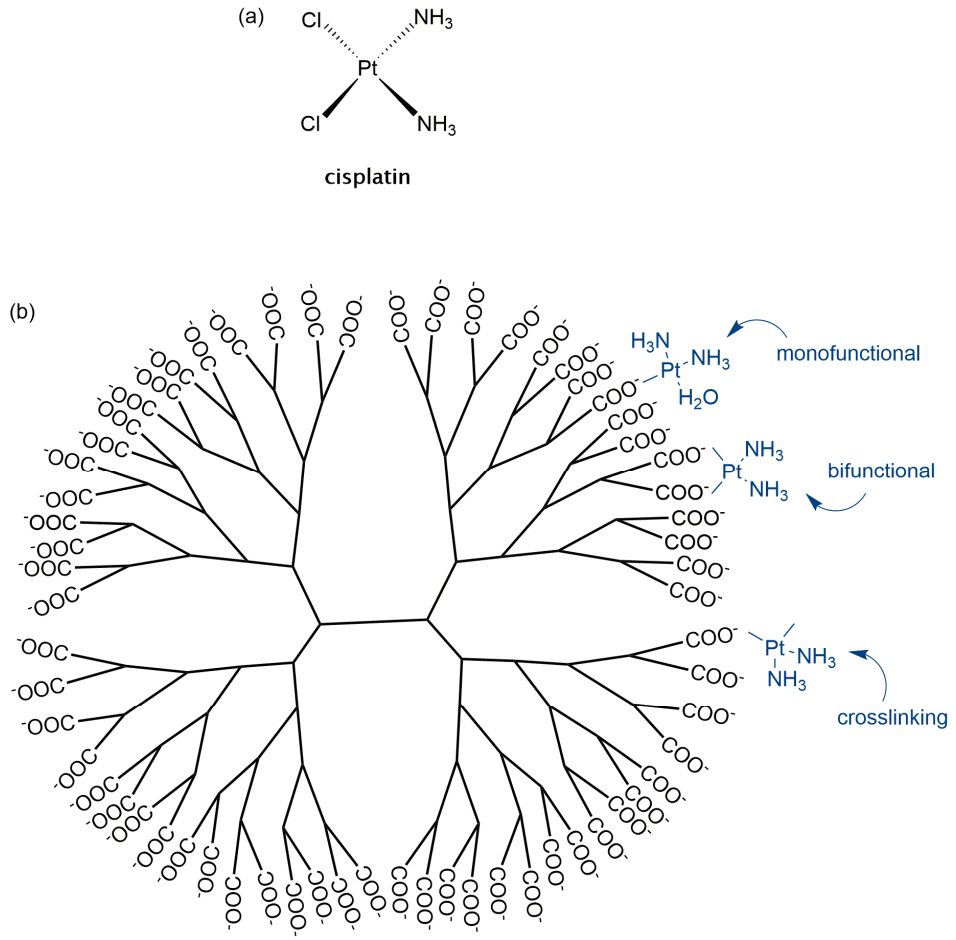

Figure 11 Structures of (a) cisplatin and (b) platinum functionalised 3.5G PAMAM dendrimer by Malik *et al.* with possible variations of platinum binding to the dendrimer.

In another anti-cancer encapsulation approach, Kojima and co-workers investigated the complex formation of the anti-cancer drugs Adriamycin and methotrexate with 3rd and 4th generation PAMAM dendrimers functionalised by attaching poly(ethylene glycol) chains with an average molecular weight of 550 g/mol or 2000 g/mol to every terminus of the dendrimers via a urethane bond (see **Figure 12**). They reported the highest capacity (on average 6.5 Adriamycin molecules or 26 methotrexate molecules) for the 4th generation PAMAM dendrimer terminated with PEG_{2000}. They also reported a slow drug release at low ionic strength and a fast drug release in isotonic solutions.[82] Similarly, Bahadra *et al.* studied the effect of PEGylating the 4th generation dendrimer with PEG_{5000} on the encapsulation and release of the anti-cancer drug 5-fluorouracil. They found that PEGylation increased the drug loading efficiency of the dendrimer and reduced the drug release rate and haemolytic toxicity.[83]

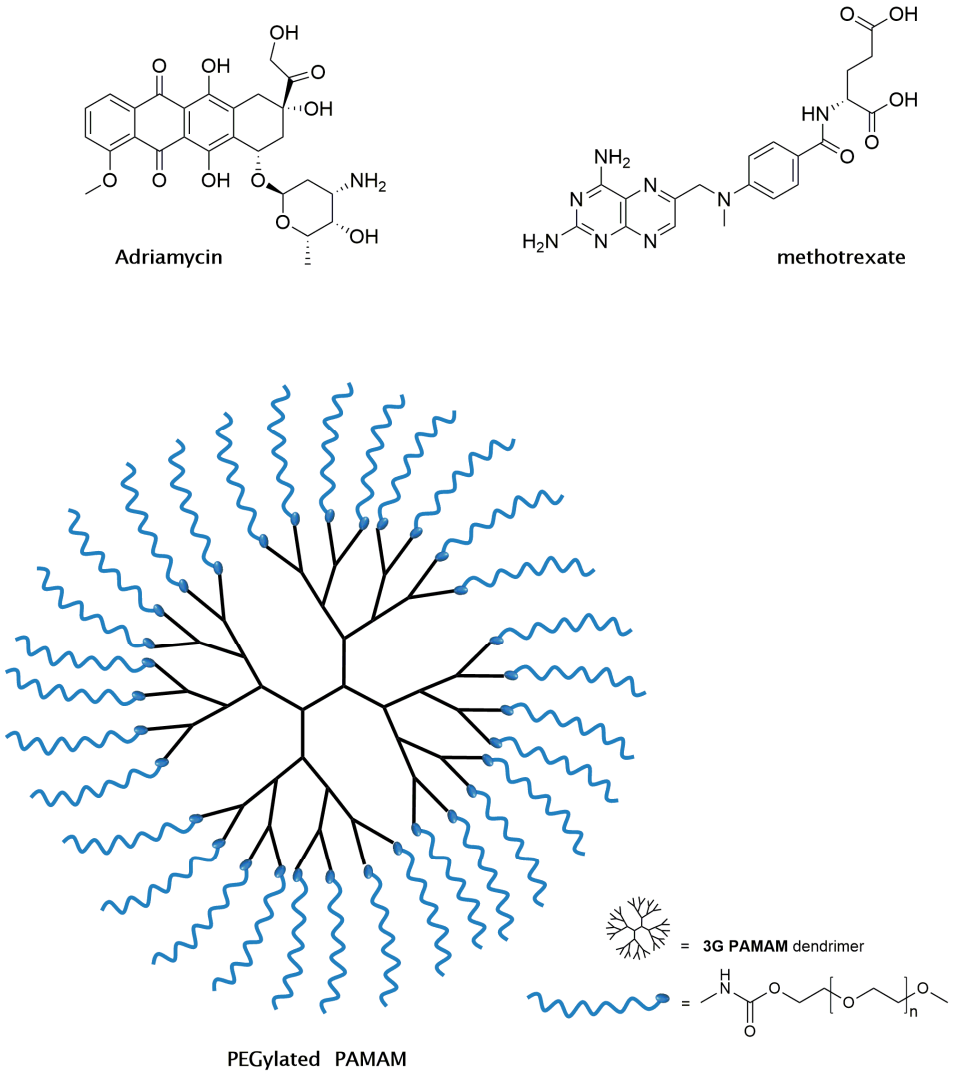

Figure 12 Structures of Adriamycin, methotrexate and 3rd generation PAMAM dendrimers functionalised with PEG_{2000} by Kojima and co-workers.

PAMAM dendrimers have also been studied for the potential delivery of drugs other than anti-cancer drugs. Balogh *et al.*, for example, showed antimicrobial activities for silver complexes of PAMAM dendrimers combined with slow silver release rates.[63] Beezer and colleagues modified the amine surface of first to third generations of PAMAM dendrimers using TRIS (see **Figure 13**), as the replacement of the amine groups is thought to decrease the toxicity of the dendrimers whilst maintaining good water solubility. It was observed that the synthesised dendrimers with the hydroxyl groups in the surface were able to encapsulate small acidic molecules (i.e. benzoic acid, *ortho*-hydroxyl benzoic acid and 2,6-dibromo-4-nitrophenol) due to ion pairing between the guest

molecules and the protonated tertiary amine group in the interior (see **Figure 13**), while non-polar molecules such as tioconazole were not encapsulated by the dendrimers due to the absence of acidic hydrogen atoms.[84]

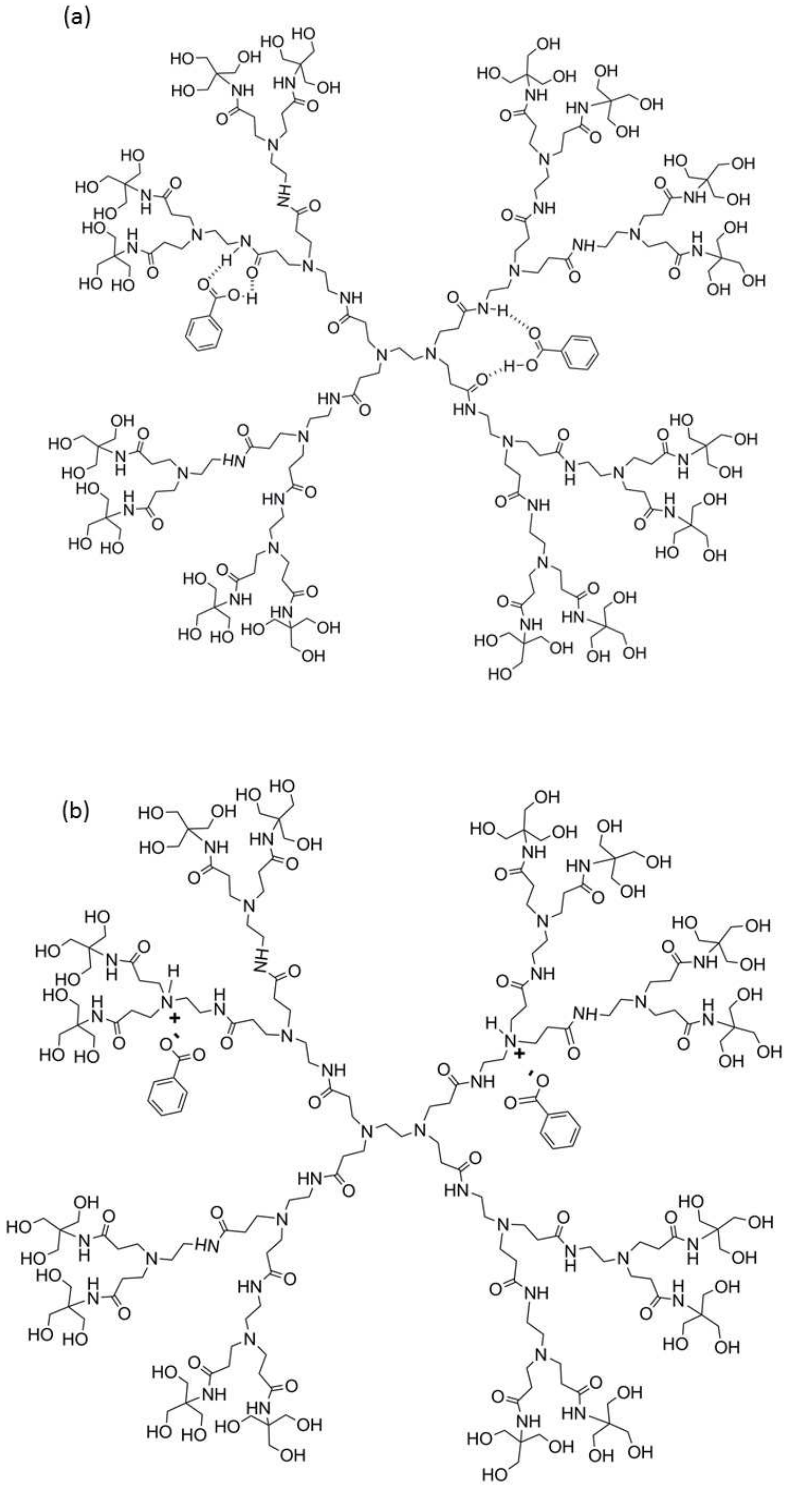

Figure 13 The encapsulation of benzoic acid in the TRIS-modified 2nd generation PAMAM dendrimer caveties by (a) unlikely hydrogen binding interaction, or (b) by ion pairing interaction.

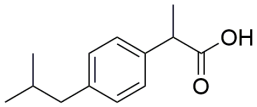

ibuprofen

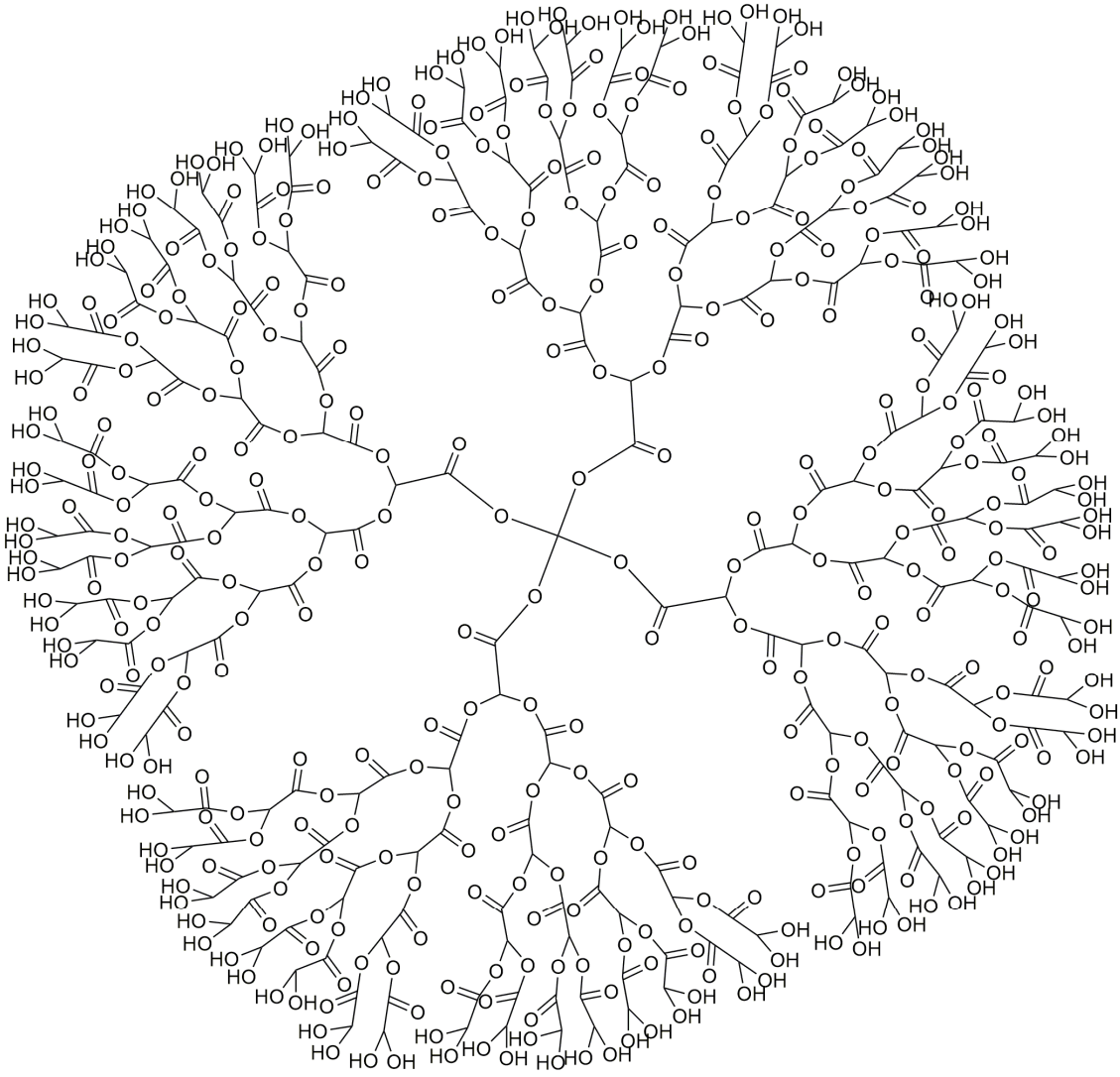

5th generation Perstorp Polyol

Figure 14 Structures of ibuprofen and Perstrop Polyol.

In another drug delivery study, Kolhe and co-workers studied the interaction between ibuprofen and PAMAM dendrimers (3rd and 4th generations) and Perstorp Polyol (5th generation dendritic polyester with OH surface group, see **Figure 14**). They found that ibuprofen forms complexes with PAMAM

dendrimers because of the ionic interaction between the amine end groups and the carboxyl group of the ibuprofen. This was confirmed by the fact that a higher amount of ibuprofen was encapsulated into the PAMAM dendrimer compared to the polyol, presumably due to the absence of ionic interactions between the hydroxyl end groups of the polyol and the carboxyl groups in ibuprofen. Furthermore, the complexes formed with the PAMAM dendrimer were shown to have a good stability in polar solvents (e.g. water and methanol) and showed a slow drug release inside cells, confirming the potential of PAMAM dendrimers as good drug carriers.[85]

In a recent study, Zhou *et al*. investigated the complex formation between carboxyl-terminated PAMAM dendrimers and the anti-bacterial triclosan (see **Figure 15**). This complex can induce the remineralisation of hydroxyapatite (HA) as well as release the encapsulated triclosan over a controllable long period. This study might help to prevent tooth decay by the release of an anti-bacterial and at the same time restore damaged teeth through re-mineralisation.[86]

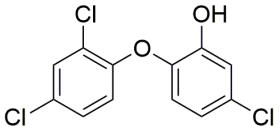

Figure 15 Structure of triclosan.

In another recent study, Winnicka and co-workers have investigated the change in the water solubility and antibacterial activity of the antibiotics erythromycin (EM) and tobramycin (TOB) when encapsulated with 2nd and 3rd generation PAMAM dendrimers with amine or hydroxyl functional terminal groups. They found an increase in the water solubility for EM with both PAMAM-NH_2 and PAMAM-OH and a slight decrease in the antibacterial activity against *Staphylococcus aureus* in the presence of either 3rd or 2nd generation PAMAM-OH or PAMAM-NH_2 dendrimers. On the other hand, TOB is already a water soluble drug and therefore PAMAM dendrimers did not have any effect on the

water solubility and antibacterial activity of this drug.[87] A similar observation was made by Devarakonda *et al.* who observed an increase in the aqueous solubility of the calcium channel blocker nifedipine when it formed complexes with low generation PAMAM dendrimers.[88]

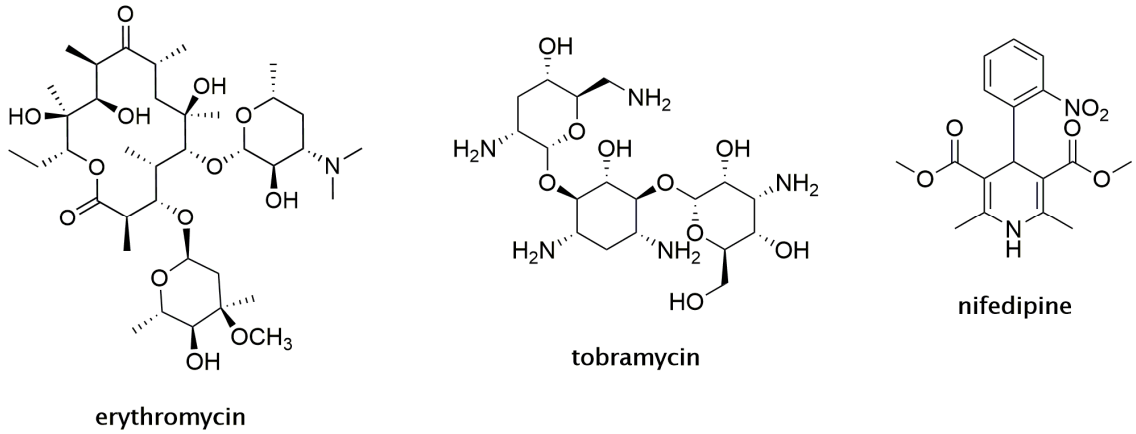

Figure 16 Structures of erythromycin, tobramycin and nifedipine.

Dendrimers have not only been suggested for the delivery of low molecular weight drug molecules, but many studies have also reported the usage of dendrimers as gene delivery vehicles into the cells and subsequently into the cell nucleus.[89-97] It is generally believed that the interaction between cationic polymers or dendrimers and DNA which is required for a gene delivery system is driven by electrostatic forces,[98] as shown in **Figure 17**. Tang *et al.*, for example, compared the complexes formed between DNA and various cationic polymers (polylysine, intact PAMAM dendrimer, fractured PAMAM and polyethylenimine) and found that the cationic polymers bind to DNA in an almost 1:1 ratio primary amines to DNA phosphates. Using electron microscopy (EM) dynamic light scattering (DLS) and the determination of the zeta potential of the complexes formed in solutions, it was also observed that all cationic polymers are able to form toroidal structures with diameters around 55 nm. However, the authors noted that the complexes formed from fractured PAMAM and polyethylenimine were in single units, whereas the unit toroidal complexes formed from polylysine and intact PAMAM dendrimer aggregated in larger clusters with diameters around 1000 nm. Interestingly,

the polymers that formed these larger aggregates were shown to have lower transfection activities than the polymers that did not form the aggregates.[99, 100]

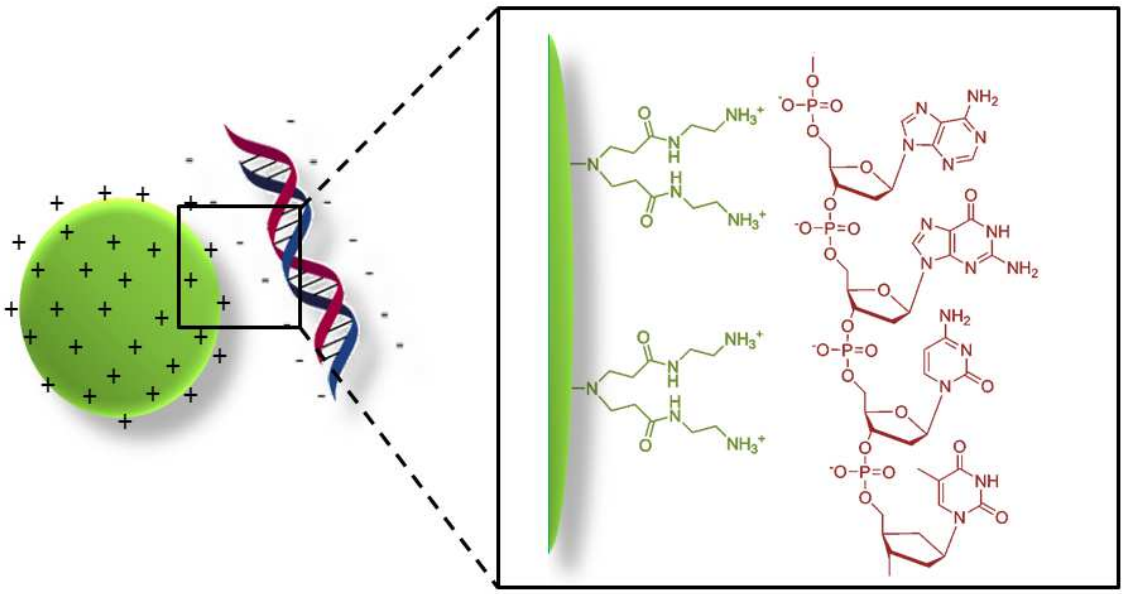

Figure 17 The electrostatic interaction between the protonated primary amines in the cationic polymers and the DNA phosphates; the green sphere represents the cationic polymer.

Hidetoshi and colleagues synthesised 2nd generation PAMAM dendrimers conjugated with α-, β- or γ-cyclodextrins attached to the surface (see **Figure 18(a)**) and reported that these modified PAMAM dendrimers have improved transfection efficiency. An optimal improvement of 100 times in transfection efficiency was observed by using α-cyclodextrin in a 2.4:1 ratio covalently bound to the 3rd generation PAMAM dendrimer or as physical mixture between the PAMAM dendrimer and the α-cyclodextrins (compared to the dendrimer alone).[101] A similar enhancement of gene transfection efficiency was reported by Hoon Yoo and R. L. Juliano when they attached fluorescent dye Oregon green 488 to the surface of 5th generation PAMAM dendrimers set to deliver 2'-*O*-methyl antisense oligonucleotides (see **Figure 18(b)**).[102]

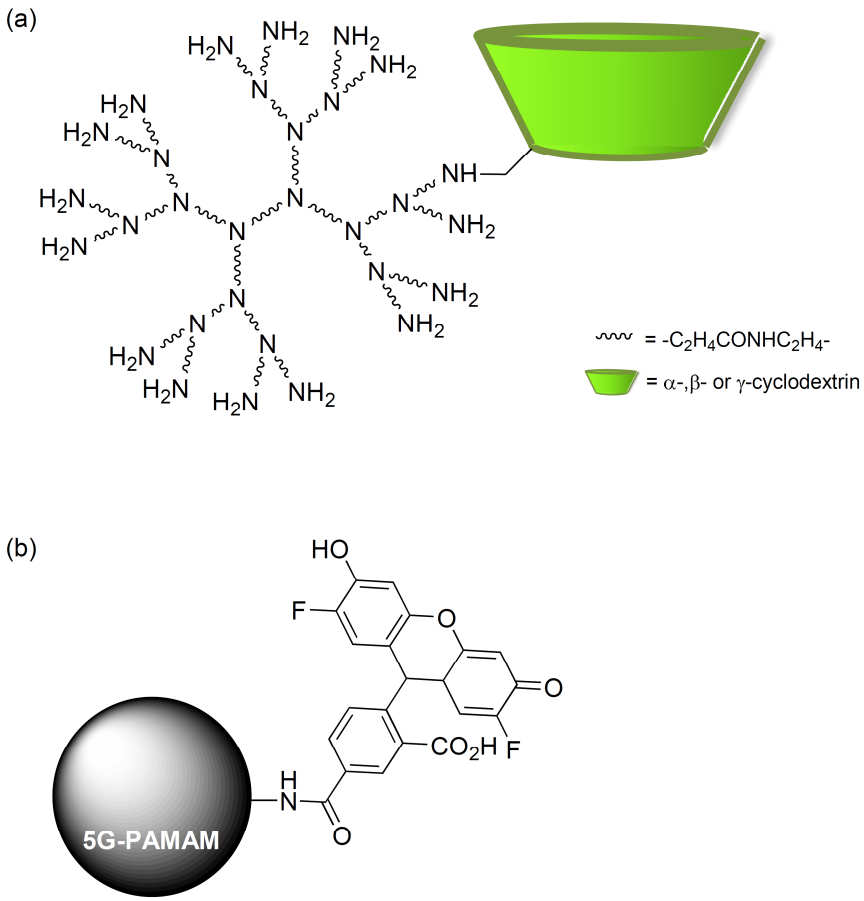

Figure 18 (a) Structure of 2nd generation PAMAM dendrimers conjugated with cyclodextrins reported by Hidetoshi and co-workers; (b) Structure of Oregon green 488 attached to the surface of 5th generation PAMAM dendrimers by Hoon Yoo and R. L. Juliano.

Maksimenko *et al.* reported an improvement in the transfection efficiency of PAMAM dendrimers and phosphorus-containing dendrimers in the presence of linear anionic oligonucleotides (length 6-55 bases) or dextran sulphate. They found an optimum transfection efficiency for 36-mer oligonucleotides or for dextran sulphate with a matching molecular weight. They concluded that the increase in transfection efficiency is due to the formation of less condensed dendrimer-DNA complexes in the presence of negatively charged macro-molecules.[103]

Takahashi and colleagues synthesised a series of PAMAM dendrimers generations 1-4 with di-*n*-dodecylamine as the core. It was evident that the

hydrophobic core mimicked the membrane transfection ability of natural phospholipids and improved the transfection efficiency through the membrane when forming complexes with DNA.[104]

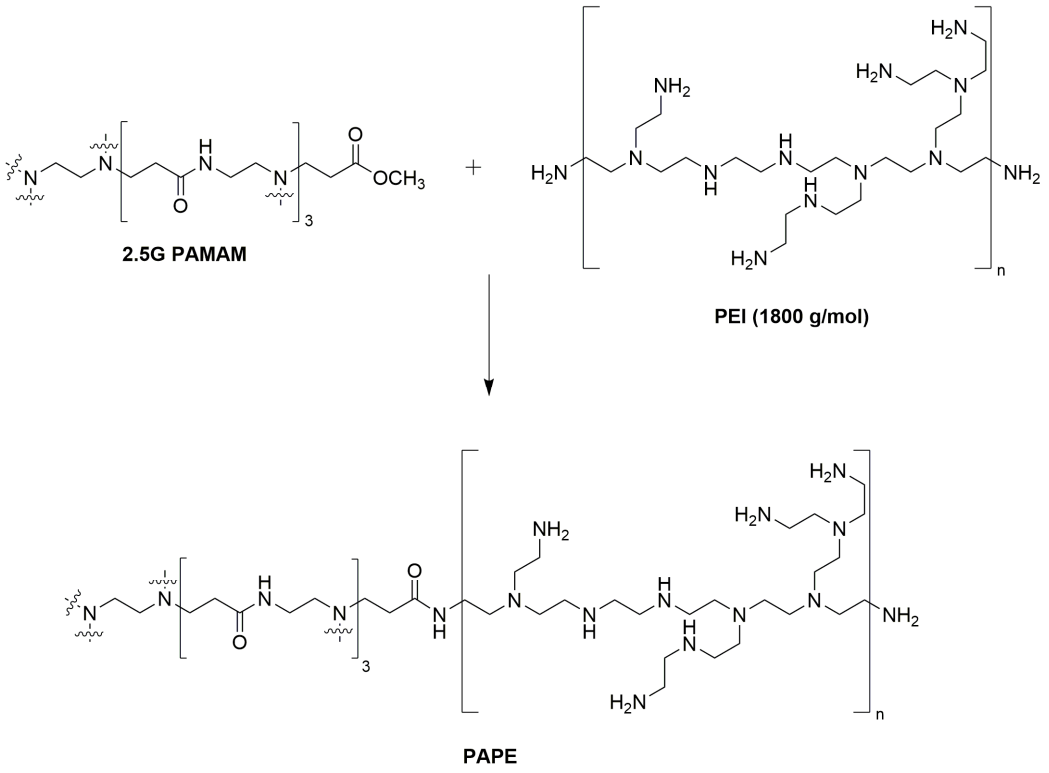

Scheme 9 Synthesis of PAPE from 2.5G PAMAM and PEI as reported by Duanwen Cao.

In a recent study, Figuero *et al.* developed various gold nanoparticle-PAMAM dendrimer conjugates that can be used in gene transfection. They reported that the conjugate with the highest colloidal stability also displayed the highest DNA condensation ability and gene transfection efficiency.[105] Hybrid cationic polymers were synthesised by Duanwen Cao and colleagues from a low generation PAMAM dendrimer in the core and PEI (polyethyleneimine) as outer layer branches (see **Scheme 9**) and the synthesised hybrid polymer, coined PAPE, was characterised by FTIR, ^{1}H NMR and gel permeation chromatography. They found that the PAPEs self-assemble with pDNA (plasmid DNA) forming PAPE-pDNA complexes with spherical shape, size of 70-204 nm and zeta potentials of 13-33 mV. Furthermore the complexes showed lower cytotoxicity and higher transfection efficiency when compared with PEI with an average

moleculer weight of 25000 g/mol in a variety of cell lines. The authors suggest that the high levels of gene transfection mediated by these complexes are due to caveolae-mediated cellular uptake, reduced entry into lysosomes and entry into nuclei during the cell division mitosis.[106]

1.4 Aims and objectives

The aim of this MPhil project has been to investigate the interactions between PAMAM dendrimers and biological membranes in order to gain a better understanding of how PAMAM dendrimers can permeate through lipid bilayers, which in the long term can be beneficial for the development of PAMAM dendrimers as drug delivery systems.

During the present study POPC (1-palmitoyl-2-oleoyl-*sn*-glycero-3-phospho-choline) and POPG (1-palmitoyl-2-oleoyl-*sn*-glycero-3-phospho-(1'-rac-glycerol) (sodium salt)) mixtures have been used as a model for biological membranes. The interactions between PAMAM dendrimers and biological membranes (POPC and POPG) have been explored using solid state NMR, fluorescence spectroscopy studies and molecular dynamics modelling under buffered and non-buffered conditions. The project has involved the synthesis and characterisation of several different generations of PAMAM dendrimers and their surface functionalization in order to introduce suitable dye markers. Finally preliminary modelling studies were carried out to investigate the effect of differently charged PAMAM dendrimers on the lipid-dendrimer interactions.

Chapter 2: Results and Discussion

As has already been mentioned in **Chapter 1** dendrimers can be used for drug or gene delivery to cells and tissues. This implies that the dendrimers need to be able to interact with the lipid bilayer surrounding these cells in order to help the cargo crossing the membrane. However, the nature of this dendrimer-lipid interaction is not yet fully understood. Based on experimental data collected by atomic force microscopy (AFM),[107-113] isothermal titration calorimetry (ITC),[112] fluorescence correlated spectroscopy (FCS),[112] *in vitro* experiments[113, 114] and molecular dynamics simulations (MD)[110, 112, 115] it is widely believed that cationic dendrimers can disrupt lipid bilayers and form holes in the membrane, but the exact mechanism of this pore formation is unknown. In recent years a number of different mechanisms for pore formation by dendrimers have been suggested, *e.g.* the formation of dendrimer-filled vesicles,[109, 116] the formation of dendrimer-lipid micelles,[109, 117] the formation of toroidal pores by dendrimer-induced curvatures[118] and the insertion of dendrimers within the bilayer.[119] An overview of these mechanisms is given in **Figure 19**.

One of the most intuitive mechanisms is the formation of lipid vesicles around the dendrimer (see **Figure 19(a)**), as this maximizes the number of contacts between the positively charged dendrimer surface and the charged lipid headgroups. In this process lipid molecules are removed from the membrane to form the vesicle and as a consequence a pore is formed in the remaining membrane. This mechanism has been suggested by Mecke *et al*. based on AFM, DLS (dynamic light scattering) and ^{31}P NMR studies of the interaction between a series of functionalised 7th generation PAMAM dendrimers and DMPC

lipid bilayers.[109, 116] However; the authors noted that these observations could also be explained by the formation of hybrid dendrimer-lipid micelles, whereby the lipids intercalate inside the dendrimer's branches (see **Figure 19(b)**). In this mechanism there is both an interaction between the dendrimer headgroups and the lipid headgroups, and an interaction between the hydrophobic lipid tails and the hydrophobic core of the dendrimer. Both the mechanism shown in **Figure 19(a)** and that shown in **Figure 19(b)** involve the removal of lipids from the bilayer to form either vesicles or micelles and are thus related mechanisms. It is possible that the exact pathway depends on the size of the dendrimer. For example, Mecke and co-workers calculated that a vesicle filled with a single dendrimer molecule can only be formed for PAMAM dendrimers of generation 5 or higher, based on AFM, thermodynamics, interaction free energy and geometry of the formed vesicles.[109] However, it is also possible that multiple smaller generation PAMAMs can be combined into a dendrimer-filled vesicle.

A third possible mechanism that has been proposed is shown in **Figure 19(c)**. This mechanism suggests that the dendrimer reaches the membrane leaflets and then binds to the surface causing the membrane to curve and this eventually results in formation of a toroidal pore or wormhole structure (see **Figure 19(c)**). Akesson and co-workers studied the effect of 6th Generation PAMAM dendrimer on unilamellar liposomes with dynamic light scattering, cryo-TEM and small-angle X-ray scattering (SAXS) and concluded that dendrimers will attach to the vesicle's surface, thereby joining the vesicles together which eventually leads to the collapse of the liposomes into a lamellar phase where dendrimer molecules are located between the layers.[120] They also found that dendrimers encourage the permeation of small molecules into the membrane in GUVs (giant unilamellar vesicles) without forming holes or passive translocation across the membrane and they concluded that the lipid bilayer changes its curvature to follow the dendrimer's shape. Pore formation is thought to occur on a nanoscale when PAMAM dendrimers come into contact with lipid bilayers. The formation of deep pores in the lipid can eventually result in the release of the cargo of the delivering dendrimer and might lead to the complete translocation of the dendrimer through the lipid bilayer via the pore.

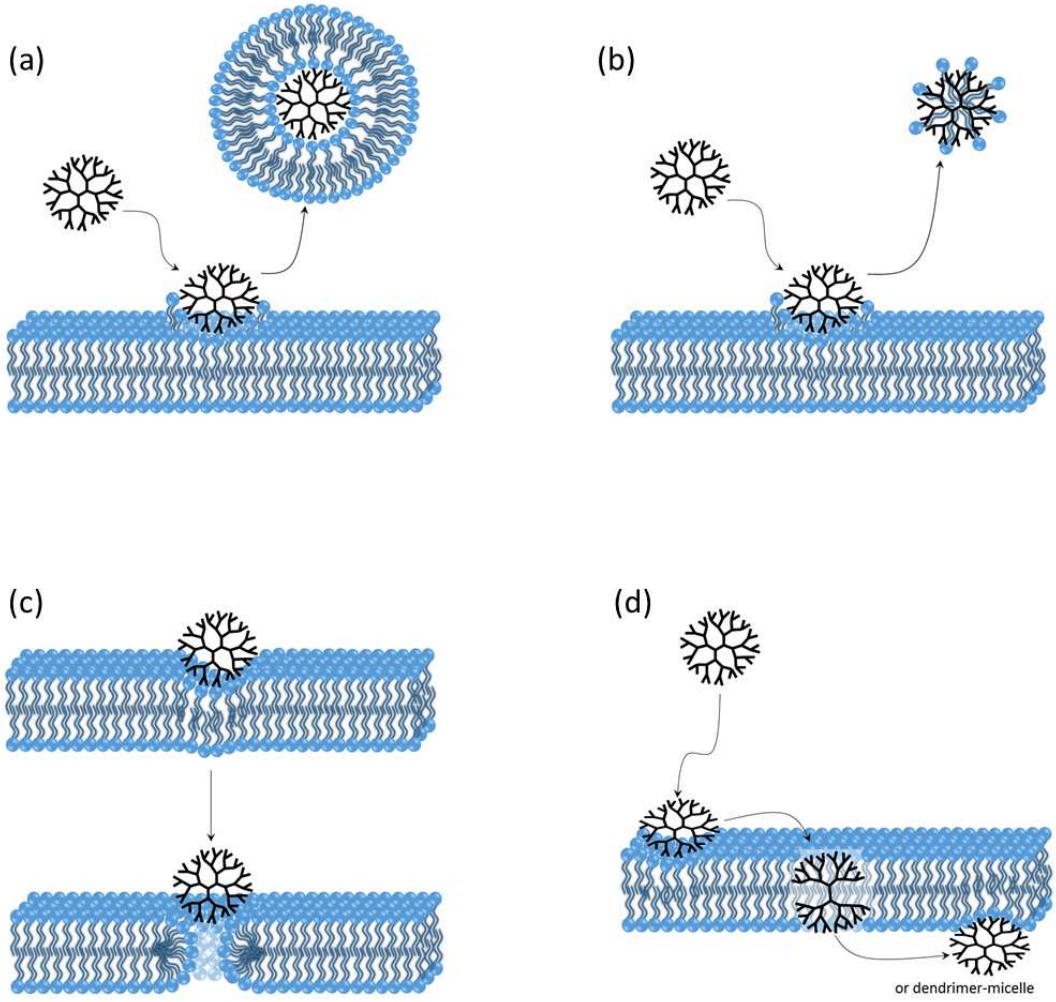

Figure 19 Various suggested mechanisms of PAMAM dendrimer and lipids bilayer interactions: (a) The formation of vesicles surrounding the dendrimer; (b) Micelle formation by intercalation of the lipids inside the dendrimer branches; (c) Toroidal pore formation due to membrane curvature; (d) The full insertion of the dendrimer into the membrane, whereby the dendrimer can leave the bilayer as such or as a hybrid dendrimer-lipid micelle.

Another mechanism has been suggested by Smith *et al.* (see **Figure 19(d)**). They concluded that 5th and 7th generations PAMAM dendrimers were localized deep within the interior of the zwitterionic lipid bilayer made of 1,2-ditetradecanoyl-*sn*-glycero-3-phosphocholine (DMPC), as ^{31}P NMR and ^{1}H-^{1}H MAS-NOESY NMR experiments did not show a strong electrostatic interaction between the dendrimers and the phosphate head groups of the lipid and instead suggested interactions between the dendrimer and lipid tails. They noted that since the experiments were run on samples of dendrimer and lipid bilayers premixed in organic solvents, there is a possibility of a kinetic barrier preventing the dendrimer insertion from the water phase into the hydrophobic

core of the preformed bilayer when the dendrimer was added to pre-formed vesicles or cells. They also suggested that at high concentrations the dendrimers tend to flatten out on the membrane surface to maximise the binding to lipids as much as possible.[119] This has also been suggested by Kelly *et al.*[121, 122] who found that, as dendrimers flatten on the surface of the membrane, they release the entrapped water molecules and replace the hydrogen bonds with water for hydrogen bonding with the lipid. This exposes the dendrimer interior to the lipid and allows the dendrimer branches to penetrate into the membrane and eventually contact the opposite leaflet of the bilayer. Coarse-grained molecular dynamics simulations by Lee *et al.* have also provided evidence for the full penetration of dendrimers into lipid bilayers.[115, 123] As the contact between dendrimer branches and the lipid bilayer increases, lipid-lipid interactions are replaced with dendrimer-lipid interactions which weaken the bilayer leading either to the collapse of the membrane at high dendrimer concentrations or to membrane disturbance at lower concentrations (see **Figure 19(d)**). Similar behaviour was noted when dendrimers were added to the amphipathic surfactant sodium dodecyl sulphate (SDS).[117] The full insertion of dendrimers into lipid bilayers has been supported by various studies; for example EPR experiments on samples where dendrimers and zwitterionic lipids were incubated separately showed restricted motions for the lipid's tail which suggest an insertion of the dendrimer into the lipid bilayer vesicles.[65] Klajnert *et al.* have used DSC to show a transition from gel phase to liquid crystalline phase in lipids upon the addition of 3rd generation PAMAM and have linked the transition to 3rd generation insertion into the lipid bilayer.[124] Based on DSC and Raman spectroscopy Konstantinos *et al.* concluded that 4th generation and 3.5th generation PAMAM dendrimers insert into dipalmytoylphosphatidylcholine (DPPC) membranes without major damage to the membrane integrity.[125] It was observed from ITC studies that the interaction between PAMAM dendrimer and zwitterionic lipid bilayers is entropy driven while the interactions with a charged lipid bilayer are driven by the enthalpic electrostatic contribution to the binding energy.[112, 124]

The previous discussion has shown that the exact mechanism by which dendrimers can interact with membranes has not yet been fully elucidated. Furthermore, it is quite possible that the mechanism depends on the size and

nature of the dendrimer and on the exact nature and composition of the membrane. Kelly *et al.*, for example, suggested that an unfunctionalised 3rd generation PAMAM dendrimer would penetrate deeper into lipid bilayer than if it was terminated with acetamide or carboxylate.[121] Similarly, Karoonuthaisiri *et al.* found that PAMAM dendrimers highly disrupt lipid bilayer membranes containing non-bilayer forming lipids (e.g. dioleylphosphoethanolamine/DOPE) but did not have any significant effect on membranes containing only phosphocholine lipids.[126] The aim of this project is therefore to investigate the interaction of different generations of PAMAM dendrimers with both zwitter-ionic and anionic lipids in order to establish which factors can influence the nature of the dendrimer-lipid interaction. Low generation PAMAM dendrimers were chosen (0th and 3rd generation) because higher generation dendrimers are known to show cell toxicity.[127, 128]

2.1 Synthesis

Prior to investigating the interaction between dendrimers and phospholipids, PAMAM dendrimers up to generation 3 were synthesised according to the procedures established by Tomalia *et al.*[15, 129, 130] and optimised by Amabilino[131]. It is important that before all the reactions were carried out all reagents were distilled under dry conditions and that the reactions were carried out under nitrogen. The synthesis starts with a Michael addition over a period of 48 hours at room temperature between an excess of methyl acrylate (MA) and ethylene diamine (-**1G**, EDA) to afford a branched -**0.5-[EDA]-4-Ester (-0.5G)** after column chromatography using 1:9 methanol:DCM as eluent. The use of excess methyl acrylate allows each $-NH_2$ group to react with 2 equivalents methyl acrylate and cause branching of the dendrimer. In the next step -**0.5G** PAMAM is reacted with ethylene diamine for 4 days at 5°C to extend the branches of the -0.5 generation PAMAM dendrimer and to form zero generation PAMAM **0-[EDA]-4-Amine (0G)** (see **Scheme 10**).

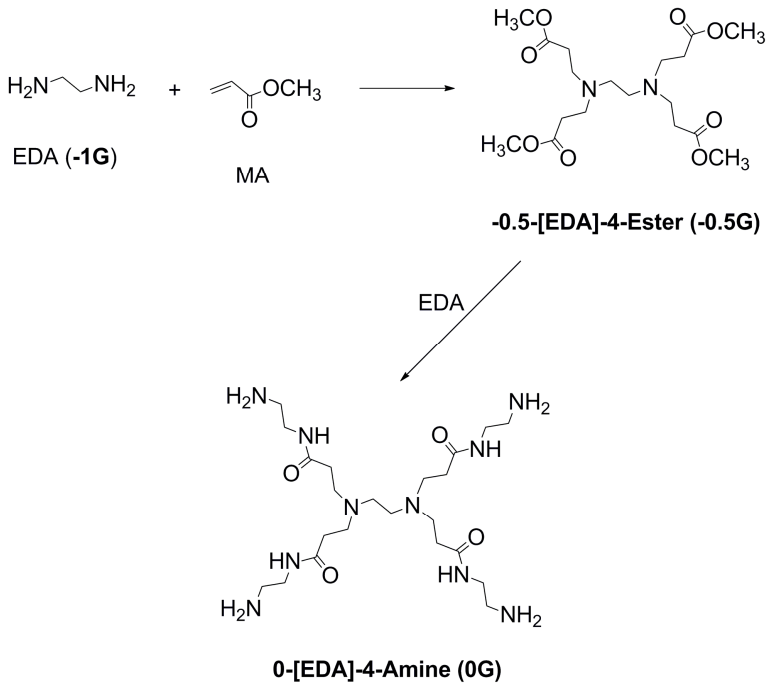

Scheme 10 Synthesis of **0-[EDA]-4-Amine** (0th generation PAMAM dendrimer).

The zero generation PAMAM dendrimer **0-[EDA]-4-Amine (0G)** (10% in methanol) is then further branched *via* a Michael addition with excess methyl acrylate to produce **0.5-[EDA]-8-Ester (0.5G)** after stirring for 7 days at room temperature and then purified by column chromatography using 1:9 methanol:DCM as eluent. This is subsequently converted into first generation PAMAM dendrimer **1-[EDA]-8-Amine (1G)** by reacting EDA with the synthesised 0.5G ester for 7 days at 5°C (see **Scheme 11**).

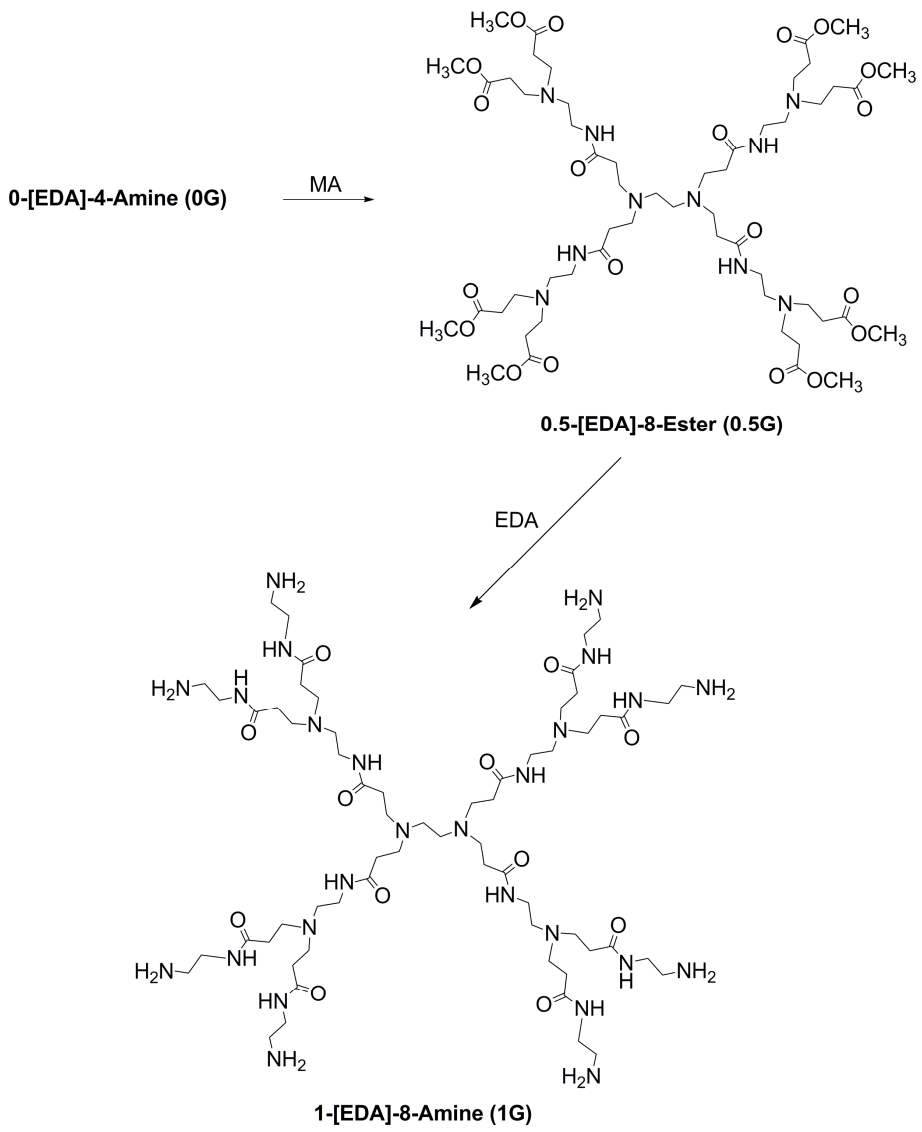

Scheme 11 Synthesis of **1-[EDA]-8-Amine** (1st generation PAMAM dendrimer).

Higher generation PAMAM dendrimers are then synthesised using the same sequence of reactions i.e. successive treatment with methyl acrylate and ethylene diamine. Thus, **2-[EDA]-16-Amine** (**2G**) (second generation PAMAM dendrimer) was synthesised by branching 1st generation PAMAM dendrimer **1-[EDA]-8-Amine (1G)** (10% in methanol) *via* a Michael addition reaction with excess methyl acrylate to produce **1.5-[EDA]-16-Ester (1.5G)** after stirring for 8 days at room temperature and purification by column chromatography using 1:4 methanol:DCM as eluent, followed by extending the newly formed branches with ethylene diamine for 14 days at 5˚C to form second generation

PAMAM dendrimer **2-[EDA]-16-Amine** after purification by dialysis for 7 days in de-ionised water with changing the water after 2 days (see **Scheme 12**). Second generation PAMAM dendrimer **2-[EDA]-16-Amine (2G)** (10% in methanol) was then further branched *via* a Michael addition with excess methyl acrylate to produce **2.5-[EDA]-32-Ester (2.5G)** after stirring for 6 days at room temperature. Third generation PAMAM dendrimer **3-[EDA]-32-Amine (3G)** was synthesised by repeating the previous steps starting from **2-[EDA]-16-Amine (2G)** after purification by dialysis for 10 days in de-ionised water changing water after 2 days and 7 days (see **Scheme 13**). Additional synthetic details and characterisation of the dendrimers can be found in the Experimental Section (**Chapter 4**).

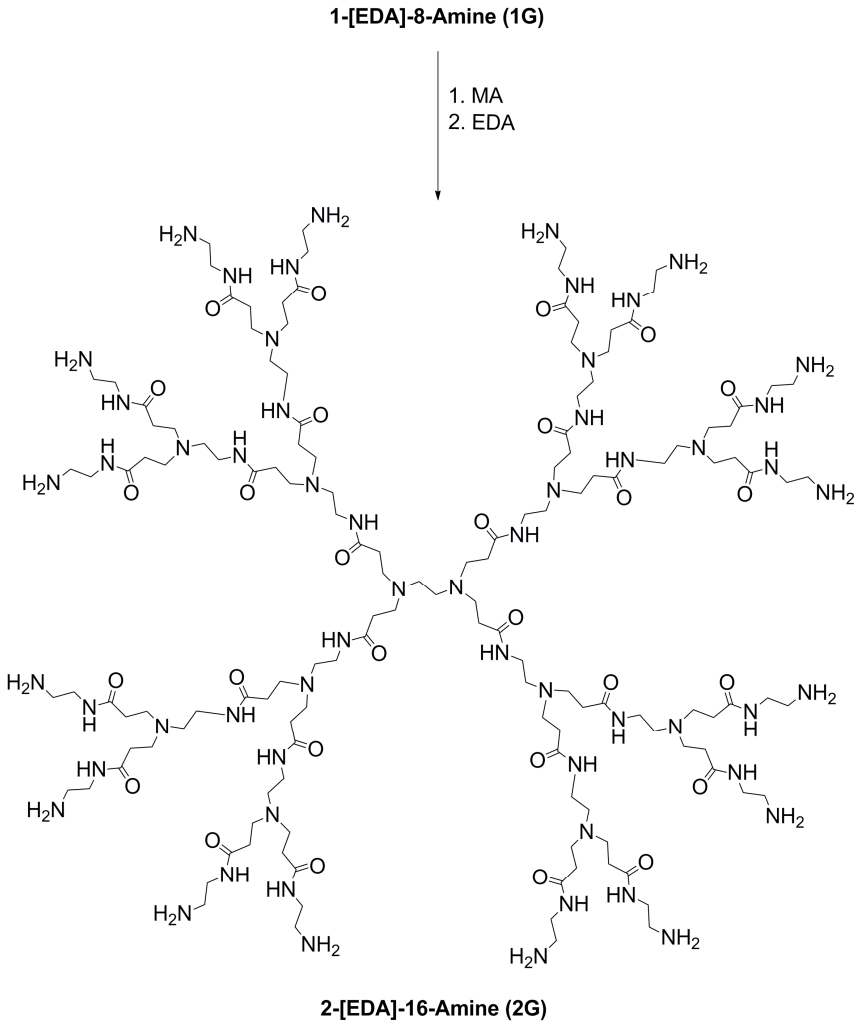

Scheme 12 Synthesis of **2-[EDA]-16-Amine** (2nd generation PAMAM dendrimer).

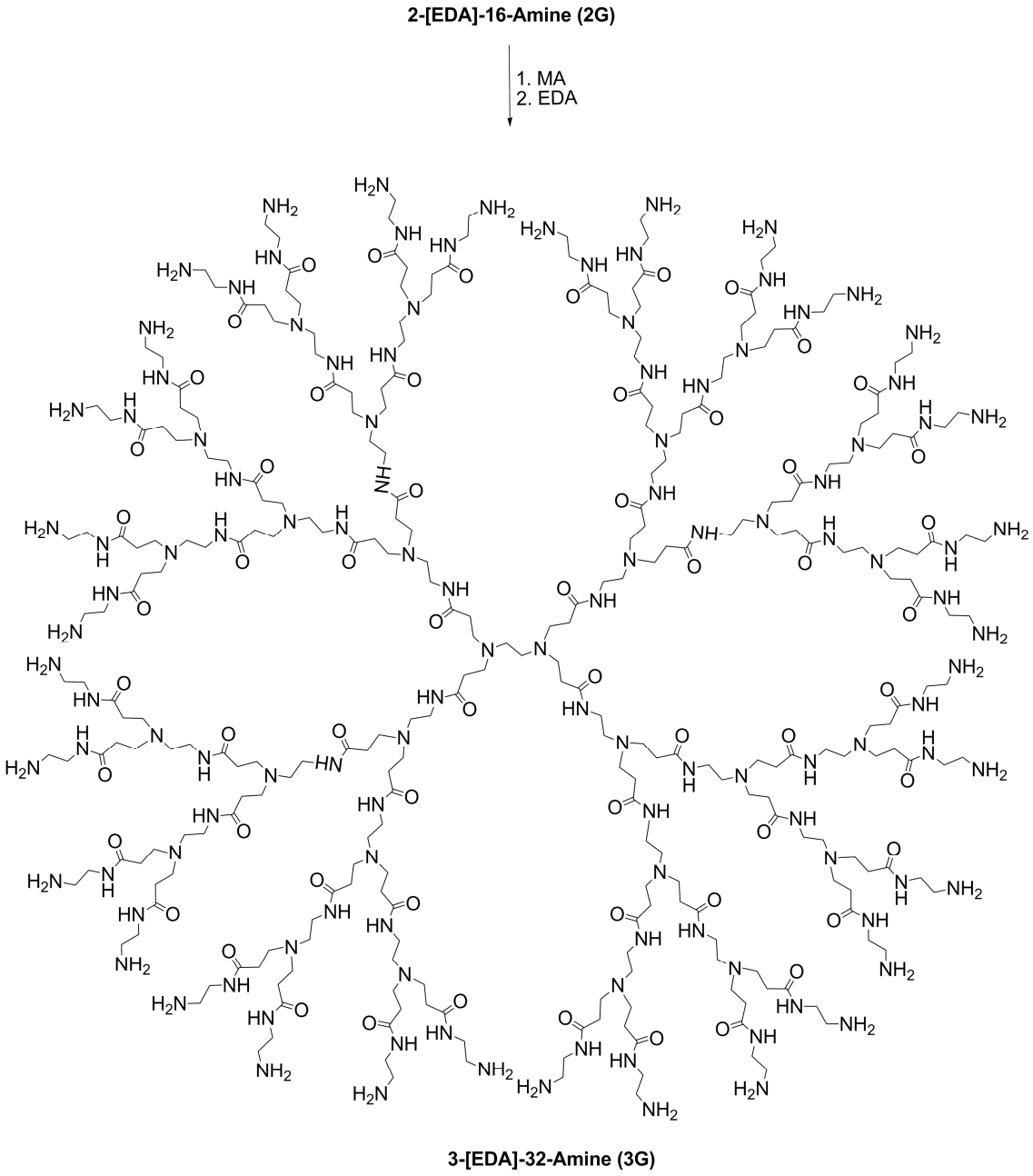

Scheme 13 Synthesis of **3-[EDA]-32-Amine** (3rd generation PAMAM dendrimer).

In order to check whether the synthesis described in **Scheme 10** - **Scheme 13** was successful, the ^{1}H NMR spectra in D_2O of the synthesised full generation PAMAM dendrimers (**0G**, **1G**, **2G**, **3G**) were compared with those of full generation PAMAM dendrimer standards purchased from *Sigma-Aldrich*. The results are shown in **Figure 20**-**Figure 23** and show good agreement between the spectra of the newly synthesised PAMAM dendrimers and the commercially

available samples. In general, five different proton environments are expected for full generation PAMAM dendrimers based on various degrees of (de)shielding by neighbouring functional groups: (a) CH_2 next to amide carbonyl, (b) CH_2 next to branching nitrogen atoms and close to amide NH, (c) CH_2 next to terminal $-NH_2$, (d) CH_2 next to branching nitrogen atom and close to amide carbonyl, (e) CH_2 next to amide NH (exchangeable NH or NH_2 protons are usually not visible in ^{1}H NMR spectra in D_2O). The variation between the different generations PAMAM lies in the relative intensities of these five peaks and the number of protons they correspond to. As can be seen from the compared figures between the synthesised PAMAM dendrimers and the dendrimers bought from *Sigma-Aldrich* (see **Figure 20**-**Figure 23**), there is a good agreement between the theoretically calculated number of protons that should be present in the dendrimers and the observed number of protons in the ^{1}H NMR spectra. This indicates that the PAMAM dendrimers synthesised during this project are of high quality and can be used for studying the interactions between PAMAM dendrimers and phospholipids.

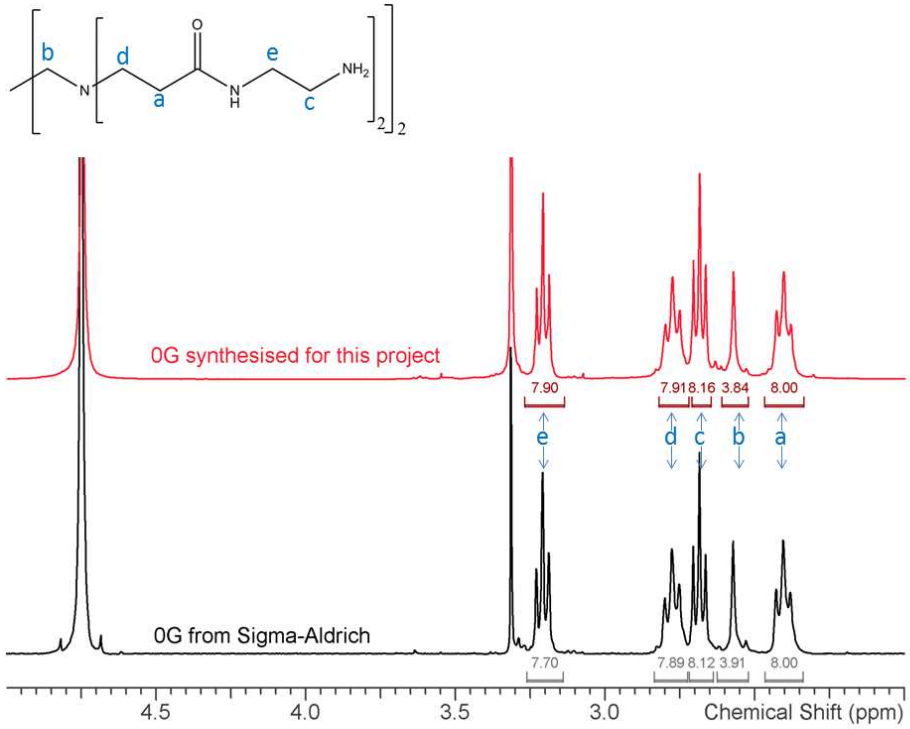

Figure 20 Comparison between ^{1}H NMR spectra in D_2O at 298 K for the 0th generation PAMAM dendrimer synthesised during this project (red) and bought from *Sigma-Aldrich* (black). Theoretical number of protons are: a=8, b=4, c=8, d=8, e=8.

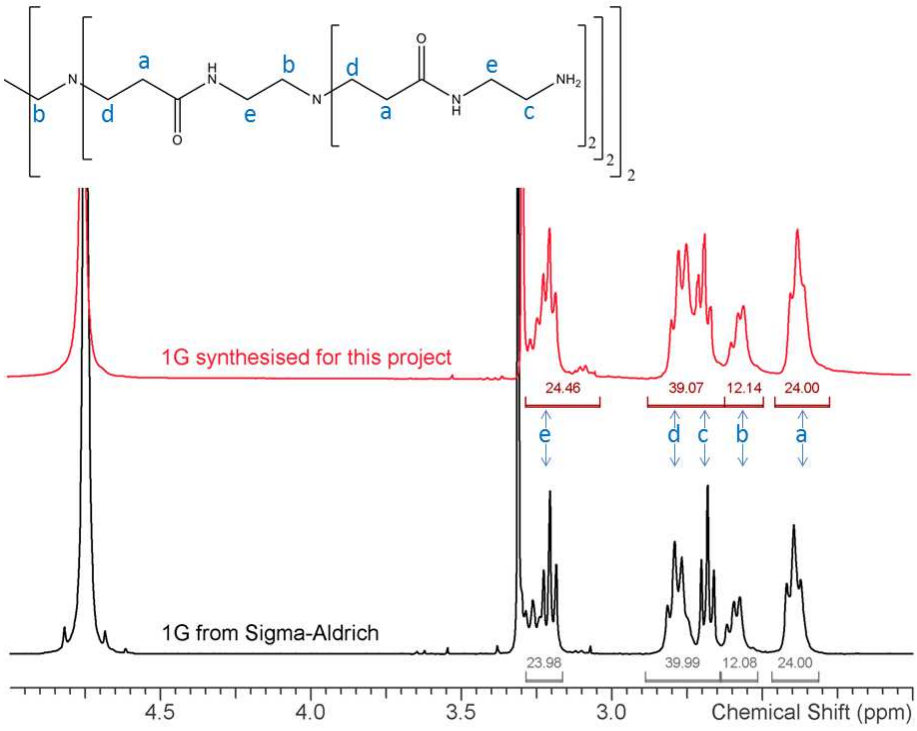

Figure 21 Comparison between ^{1}H NMR spectra in D_2O at 298 K for the 1st generation PAMAM dendrimer synthesised during this project (red) and bought from *Sigma-Aldrich* (black). Theoretical number of protons are: a=24, b=12, c=16, d=24, e=24.

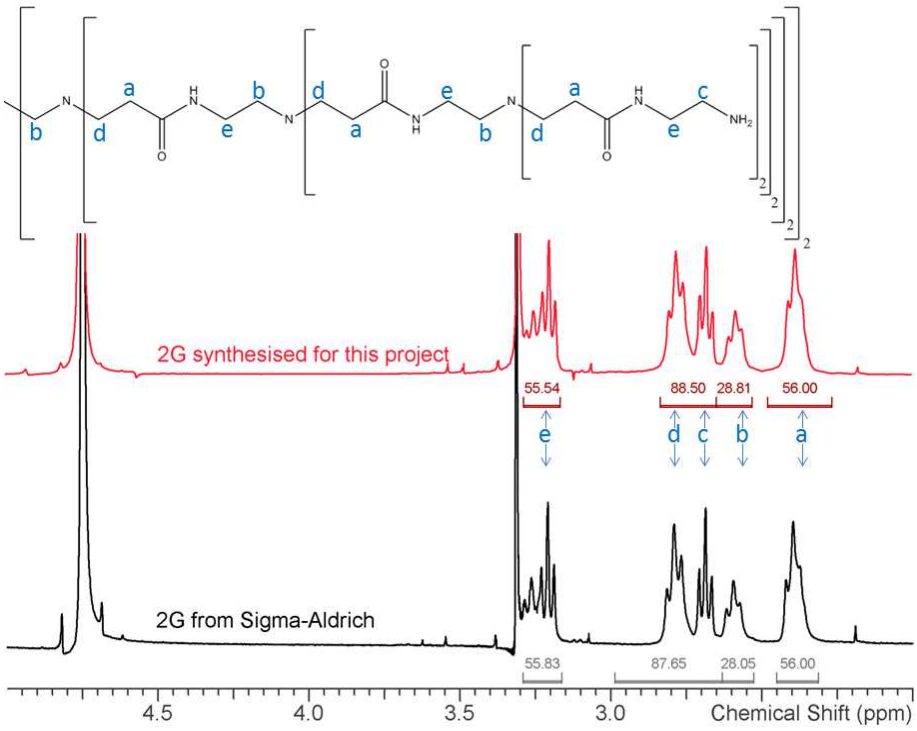

Figure 22 Comparison between ^{1}H NMR spectra in D_2O at 298 K for the 2nd generation PAMAM dendrimer synthesised during this project (red) and bought from *Sigma-Aldrich* (black). Theoretical number of protons are: a=56, b=28, c=32, d=56, e=56.

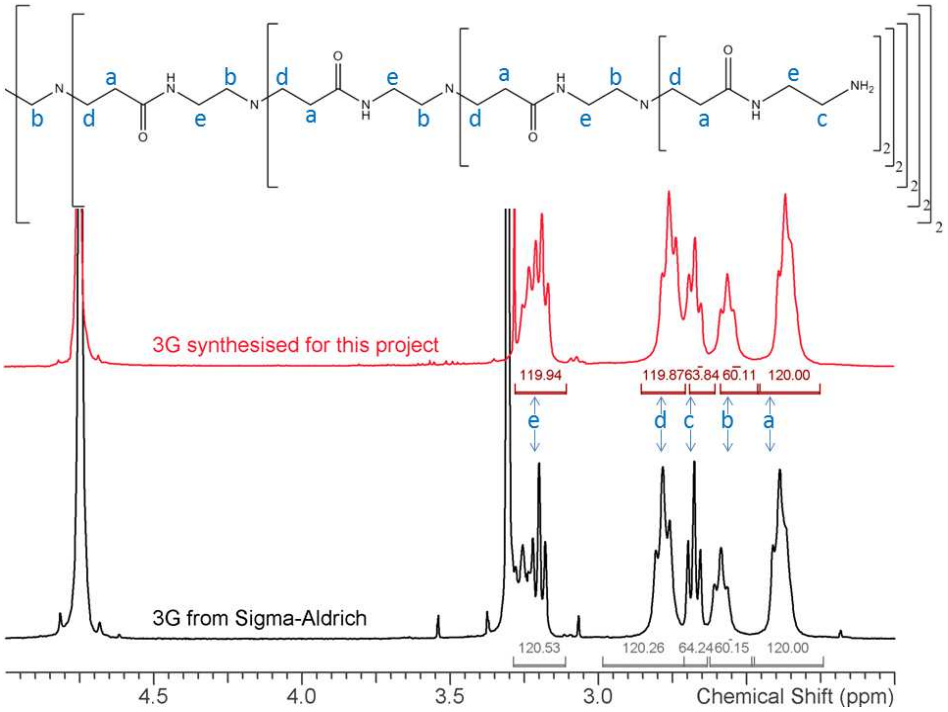

Figure 23 Comparison between ^{1}H NMR spectra in D_2O at 298 K for the 3rd generation PAMAM dendrimer synthesised during this project (red) and bought from *Sigma-Aldrich* (black). Theoretical number of protons are: a=120, b=60, c=64, d=120, e=120.

During dendrimer synthesis potential defects may occur as a result of dendrimer bridging between two end groups (see **Figure 24**) or incomplete reactions (not all functional groups have reacted), resulting in asymmetrical growth of the dendrimer. Normally, dendrimers are highly symmetrical molecules which results in simple ^{1}H NMR spectra due to overlapping peaks corresponding to symmetrically equivalent protons. When defects are present, the dendrimer is not fully symmetrical anymore and the defects can thus be detected by peak broading and more complex ^{1}H NMR spectra and the appearance of small extra peaks in ^{13}C NMR at δ 47.8, 45.1 and 36.0, as reported by Tomalia *et al.* [15] It is clear from ^{1}H NMR spectra shown in **Figure 20**-**Figure 23** that no major defects are present in the dendrimers synthesised during this project. Furthermore, the ^{13}C NMR spectra of the 3rd generation dendrimer synthesised in this project did not show obvious peaks at the mentioned chemical shifts, consistent with only very low levels of any such defects in the sample (see **Figure 25**).

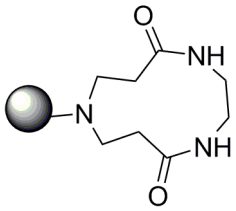

Figure 24 Potential defect in PAMAM dendrimers due to bridging of the branches.

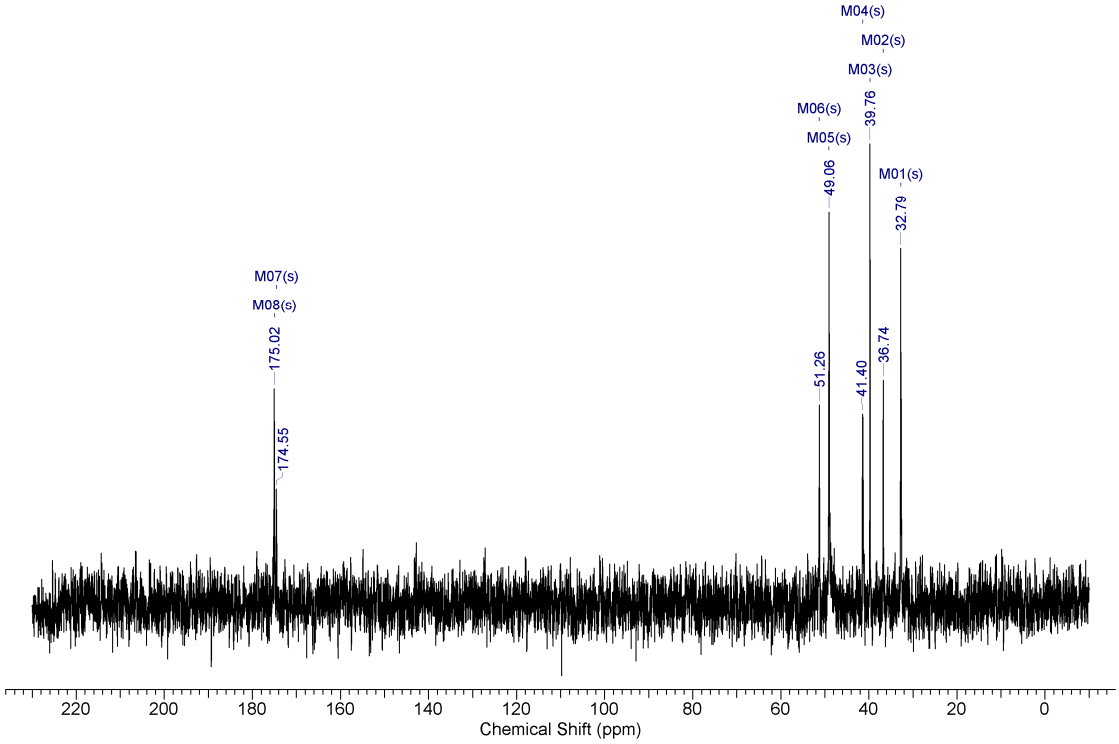

Figure 25 ^{13}C NMR in D_2O for the 3rd generation PAMAM dendrimer synthesised and used in this project, no extra peaks related to defects in the structure were observed.

2.2 Solid state NMR

Nuclear magnetic resonance (NMR) has been widely used in organic chemistry and biochemistry[132] because it can provide information on various levels depending on the applied technique. When measuring ^{1}H NMR data, for example, the different signals can be analysed to gain insight into the ratio of protons (based on the integral) and the local chemical environment.[133] Similar types of information can be gathered when studying ^{13}C NMR spectra.[133] Further knowledge regarding the flexibility/rigidity of the proton or other environments along a chain in a molecule can be gathered by measuring T_1 (spin-lattice relaxation time) and T_2 (spin-spin relaxation time).[134] Newer techniques such as NOESY (Nuclear Overhauser Effect SpectroscopY), COSY (COrrelation SpectroscopY), TOCSY (TOtal Correlation SpectroscopY) have also been increasingly used to gain a better understanding of the interactions in three dimensional space.[133] In compounds containing phosphorus atoms, ^{31}P NMR measurements can be useful due to the high NMR sensitivity of the ^{31}P nucleus, the comparative simplicity of its proton decoupled spectrum and the low chance of interference from other compounds that do not contain phosphorus atoms.[133]

When investigating the interaction of a given (macro)molecule with phospholipids ^{31}P or ^{1}H-^{1}H NOESY NMR can be insightful. However, due to the liquid-crystalline or gel-like phase of phospholipid membranes, classical solution-based NMR techniques can be problematic and solid state NMR techniques are therefore more useful when studying lipid bilayers. For example, various solid state NMR studies have proved to be a powerful tool for investigating the disruption of lipid bilayers by membrane-active peptides,[135] while solid state NOESY NMR has proven effective for investigating the association between lipid head groups and hydrocarbon chains.[136] However, solid state NMR is usually hindered by broad NMR signals and special techniques, such as magic angle spinning (MAS), are often needed to obtain easily interpretable spectra. Various solid state NMR techniques under MAS conditions were therefore explored in this study to build an idea of the way PAMAM dendrimers interact with POPC (1-palmitoyl-2-oleoyl-*sn*-glycero-3-phosphocholine) or POPG (1-palmitoyl-2-oleoyl-*sn*-glycero-3-phosphoglycerol) lipid bilayers. As POPC/POPG lipid bilayers

contain a phosphorous head group, the changes in the ^{31}P powder pattern upon the addition of 0th and 3rd PAMAM dendrimers were investigated, as well as the changes in the ^{31}P relaxation times (T_1 and T_2). Additionally, ^{1}H-^{1}H NOESY NMR measurements were collected to show the proton environments involved in the interaction between 0th generation or 3rd generation PAMAM and pure POPC membranes or mixed POPC/POPG membranes. The experiments in this section were performed in association with Andrew Hutchin (project student), Dr. Ian Stuart Findlow and Dr. Philip T. F. Williamson, all members of the centre for Biological Sciences/Institute for Life Sciences, University of Southampton.

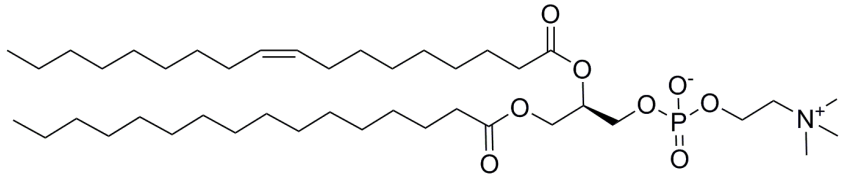

POPC

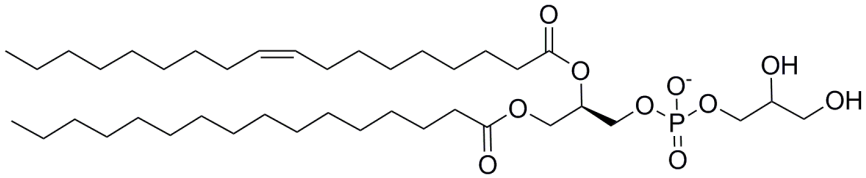

POPG

2.2.1 ^{31}P NMR: powder pattern

^{31}P NMR spectroscopy is a useful technique when studying phospholipids such as POPC and POPG because of the presence of a phosphate head group in these lipids. Most phospholipid membranes can exist in different phases depending on the temperature of the bilayer. Some of the most important phases are the rigid gel phase at lower temperature (L_β) and the more fluid liquid-crystalline phase at higher temperature (L_α), as shown in **Figure 26**.[105] Each of these phases shows a distinct powder pattern (line shape) in solid state ^{31}P NMR experiments and ^{31}P NMR can therefore be used to study the effect of the addition of (macro)molecules on the phase of the membrane and to find the exact phase transition temperature of a specific phospholipid bilayer.[137] For

this reason, ^{31}P NMR was used to compare the effect of introducing 0th and 3rd generation PAMAM dendrimers on the ^{31}P powder patterns and the phase transition temperature of POPC and POPC/POPG membranes.

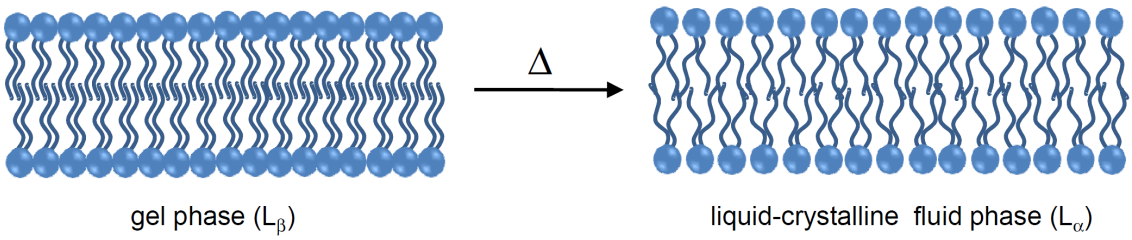

Figure 26 Depiction of the gel phase (L_β) and liquid-crystalline phase (L_α) that can be present in phospholipids. The gel phase has more ordered lipids and is therefore more rigid, while the lipid tails in the liquid-crystalline is less ordered and the membrane is more fluid-like.

Initially, ^{31}P NMR spectra of POPC in D_2O were obtained at a range of temperatures in the presence and absence of PAMAM dendrimers. The second moments of these spectra were calculated and plotted against temperature, as the second moments are a measure of the strength of dipole-dipole interactions[138] and thus allow an estimation of the phase transition temperature. The results for POPC in the presence and absence of **0G** PAMAM are shown in **Figure 28**. Pure POPC vesicles are known to have a phase transition temperature from L_α liquid crystalline phase to L_β gel phase between -4˚C to -2˚C.[139] The ^{31}P NMR experiments presented here showed a similar phase transition temperature for pure POPC (see blue line in **Figure 27**, the sudden change in the slope of the blue line indicates a phase transition temperature), revealing the usefulness and sensitivity of the ^{31}P NMR experiments. In the presence of the 0th generation PAMAM the transition temperature from the liquid crystalline phase to the gel phase decreased from around -2˚C to below -20˚C (see **Figure 27**). Furthermore, at -4˚C the ^{31}P NMR spectra of the POPC lipid changed from a powder pattern suggesting an L_β gel phase for POPC alone to a powder pattern suggesting an L_α liquid-crystalline phase in the presence of **0G** PAMAM dendrimer (see **Figure 28**). These observations indicate that **0G** PAMAM interacts with the POPC lipid bilayer at -4˚C, preventing it from forming the ordered L_β gel phase by keeping some distance between the lipid

molecules (presumably as a result of binding of the dendrimer to the surface of the membrane or due to intercalation of the dendrimer into the lipid bilayer).

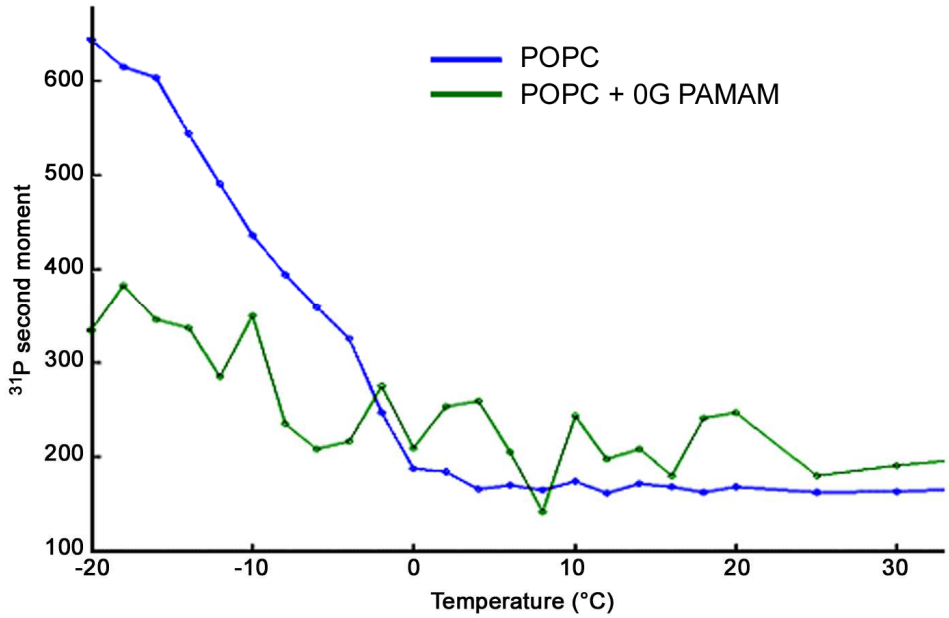

Figure 27 The changes in the phase transition temperature for POPC in the presence (green) and absence (blue) of **0G** PAMAM dendrimer based on the ^{31}P second moments. A molar ratio of 1:75 dendrimer:lipid was used and the total lipid concentration was 30% (w/w) in D_2O.

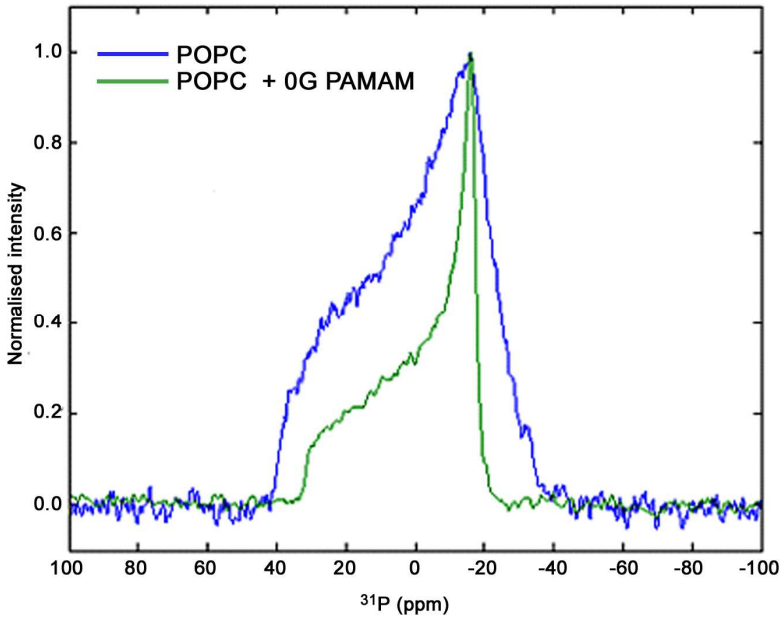

Figure 28 ^{31}P NMR spectra of POPC in the absence (blue) and in the presence (green) of the 0th generation PAMAM dendrimer at -4˚C. A molar ratio of 1:75 dendrimer:lipid was used and the total lipid concentration was 30% (w/w) in D_2O.

When the solid state ^{31}P NMR experiments were repeated for pure POPC vesicles in the presence of 3rd generation PAMAM dendrimers, similar observations could be made. Again, the transition temperature from the liquid crystalline phase to the gel phase decreased from the range (-4˚C to -2˚C) to below -20˚C (see **Figure 29**). Once again, for the 3th generation PAMAM, the ^{31}P NMR powder pattern of the POPC lipid at -4˚C indicated a change from the L_β gel phase for POPC alone to the L_α liquid crystalline phase in the presence of **3G** PAMAM dendrimer (see **Figure 30**). These results suggest that at -4˚C both the 0th generation and the 3rd generation PAMAM dendrimer can interact with neat POPC lipid bilayers, thereby preventing them from forming the rigid L_β gel phase. In other words, the results indicate that low generation PAMAM dendrimers cause disruption in the POPC bilayer that hinders the lipid tails from creating an ordered, densely packed phase and instead keeps the bilayer in the more fluid-like L_α phase.

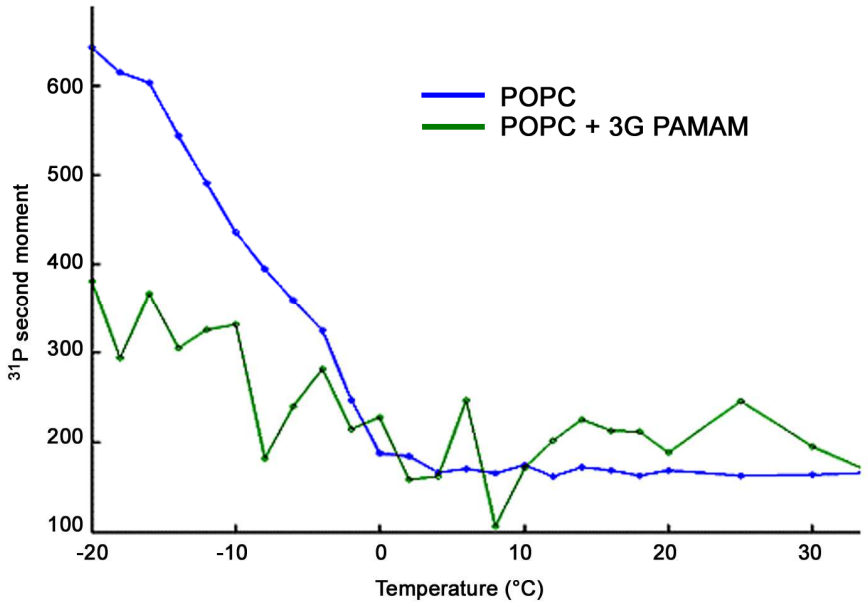

Figure 29 The changes in the phase transition temperature for POPC in the presence (green) and absence (blue) of **3G** PAMAM dendrimer based on the ^{31}P second moments. A molar ratio of 1:75 dendrimer:lipid was used and the total lipid concentration was 30% (w/w) in D_2O.

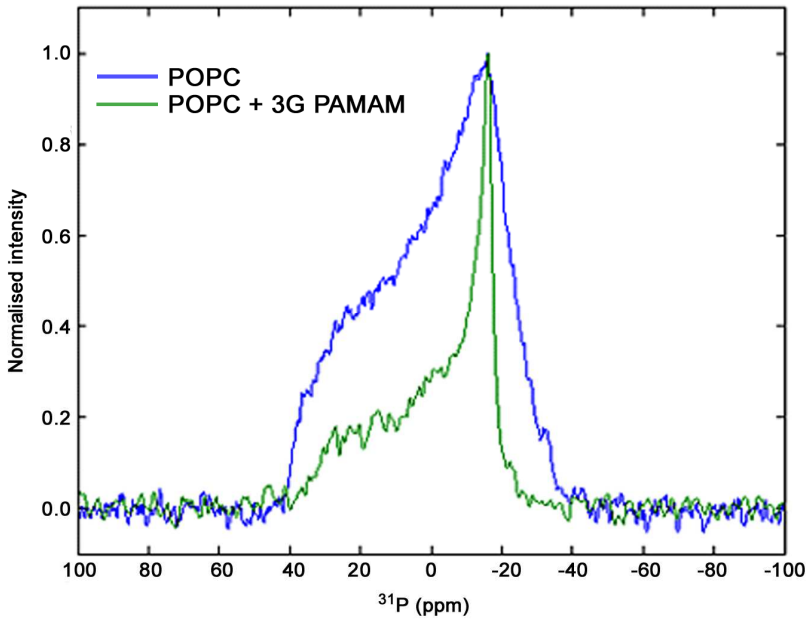

Figure 30 ^{31}P NMR spectra of POPC in the absence (blue) and in the presence (green) of the 3rd generation PAMAM dendrimer at -4˚C. A molar ratio of 1:75 dendrimer:lipid was used and the total lipid concentration was 30% (w/w) in D_2O.

Unmodified PAMAM dendrimers have free –NH_2 groups at their surface which can be protonated and previous studies have shown that PAMAM dendrimers are positively charged at neutral pH because of protonation of the terminal amines.[140] It is thus expected that PAMAM dendrimers will interact more strongly with negatively charged phospholipids such as POPG than with zwitterionic phospholipids such as POPC. The experiments discussed above were therefore repeated with membranes consisting of 2:1 POPC:POPG (see **Figure 31** and **Figure 32**). In the presence of the 0th generation PAMAM an alteration in the slope of the ^{31}P second moment versus temperature plot was observed (see **Figure 31**). However, unlike the results for neat POPC, it is not completely clear whether the addition of **0G** PAMAM has resulted in a change in transition temperature, as the exact transition temperature cannot be easily derived from the plotted data shown in **Figure 31**. Nevertheless, the difference between the two curves in **Figure 31** indicates that there is indeed an interaction between **0G** PAMAM and the 2:1 POPC:POPG bilayer. Furthermore, at -2˚C a change in the powder pattern of the ^{31}P NMR spectra of the POPC/POPG lipid mixture was observed when **0G** PAMAM dendrimer was added, suggesting that the lipid mixture has a different ratio of L_α liquid-

crystalline phase and L_β gel phase in the presence and absence of **0G** PAMAM dendrimer at this temperature (see **Figure 32**).

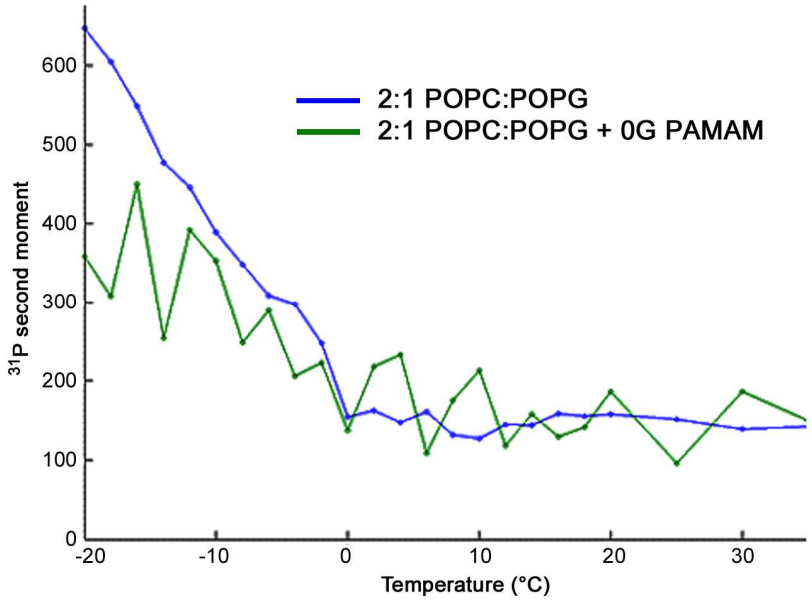

Figure 31 The changes in the phase transition temperature for the mixture 2:1 POPC:POPG before and after introducing **0G** PAMAM dendrimer. A molar ratio of 1:75 dendrimer:lipid was used and the total lipid concentration was 30% (w/w) in D_2O.

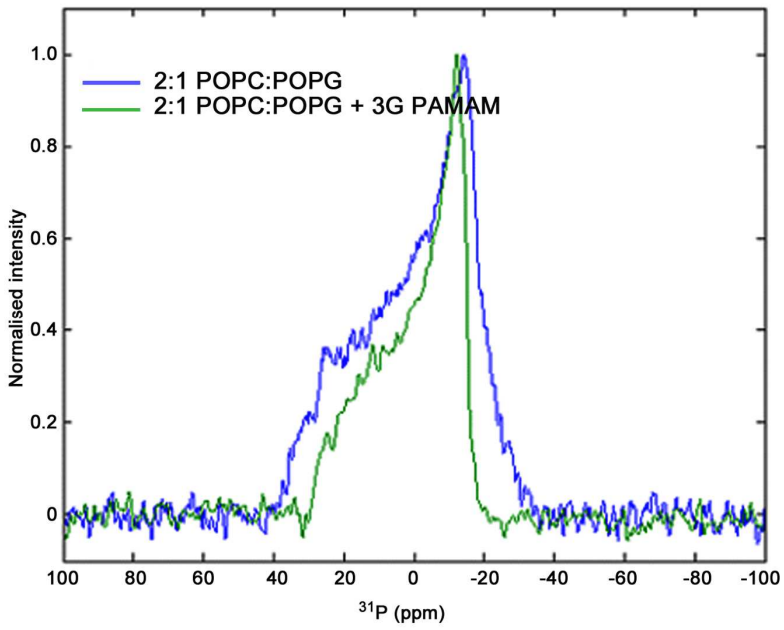

Figure 32 ^{31}P Spectra of POPC/POPG lipids mixture (blue) in the absence and in the presence (green) of the both generation PAMAM dendrimer at -2°C. A molar ratio of 1:75 dendrimer:lipid was used and the total lipid concentration was 30% (w/w) in D_2O.

Similar observations were reported when 3rd generation PAMAM dendrimers were introduced to 2:1 POPC:POPG membranes. Once again, there is a change in the ^{31}P second moment versus temperature plot, but this change does not seem to correspond with a large alteration of the transition temperature from the liquid-crystalline phase to the gel phase (see **Figure 33**). On the other hand, at -2˚C the ^{31}P spectra of the POPC/POPG mixture lipids changed from a powder pattern suggesting mainly the presence of L_β gel phase for the lipid mixture alone, to a powder pattern suggesting a higher fraction of L_α liquid crystalline phase when **3G** PAMAM dendrimer was added (See **Figure 34**). This could suggest that at -2˚C the **3G** PAMAM interacts with POPC/POPG lipid bilayers and prevents them from forming the L_β gel phase by keeping some distance between the lipid molecules.

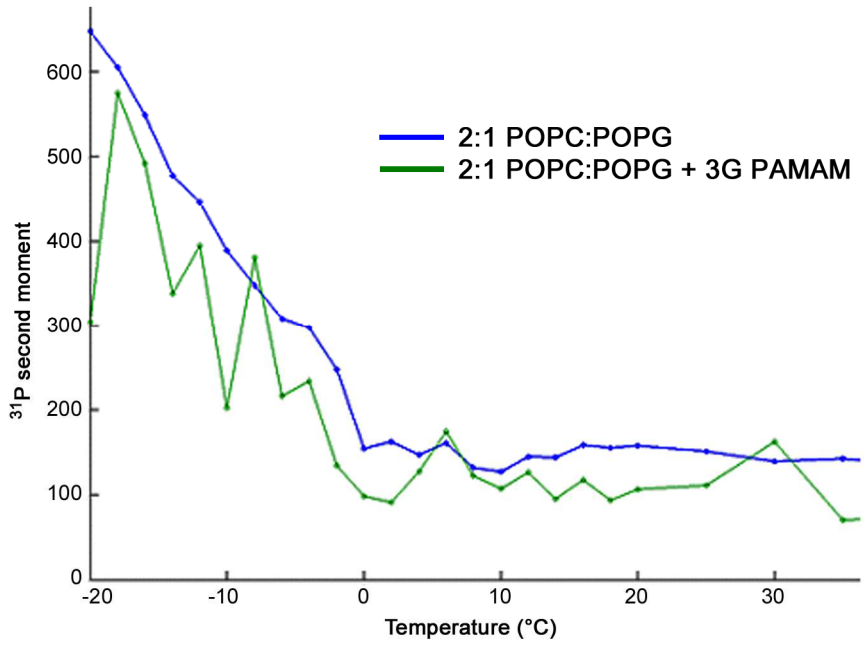

Figure 33 Phase transition temperature for the mixture POPC/POPG before and after introducing 3rd Generation PAMAM dendrimer. A molar ratio of 1:75 dendrimer:lipid was used and the total lipid concentration was 30% (w/w) in D_2O.

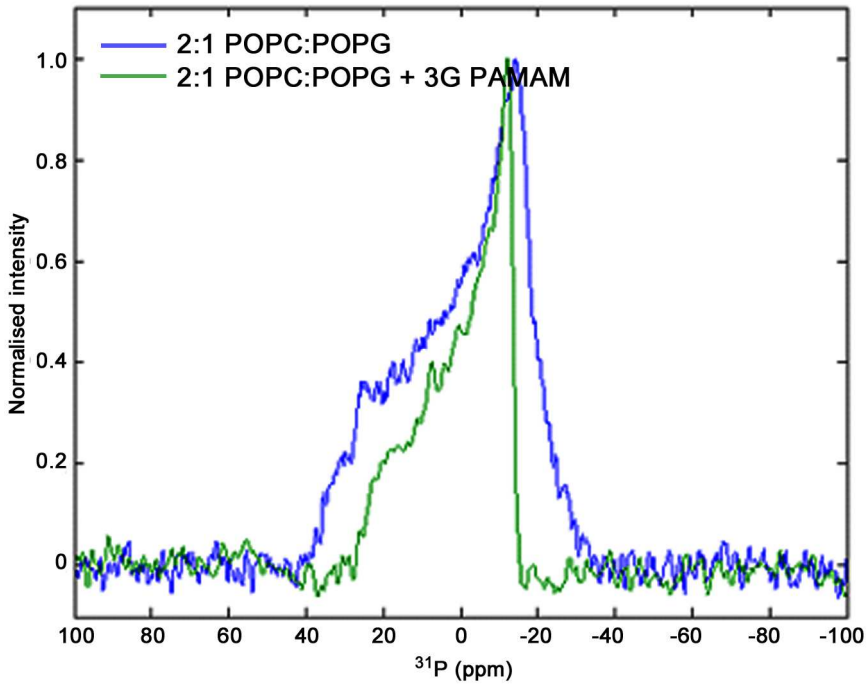

Figure 34 ^{31}P Spectra of POPC/POPG lipids mixture (blue) in the absence and (green) in the presence 3rd generation PAMAM dendrimer at -2°. A molar ratio of 1:75 dendrimer:lipid was used and the total lipid concentration was 30% (w/w) in D_2O

The results discussed in this section have revealed that 0th and 3rd generation PAMAM dendrimers are able to interact with POPC and POPC:POPG membranes. While the changes in the ^{31}P NMR spectra appeared to be larger upon the addition of PAMAM dendrimers to neat POPC than to POPC:POPG bilayers, these type of experiments do not give an indication of the magnitude of the interaction. Additional experiments were therefore performed in order to gain a better understanding of the nature and strength of the interaction between PAMAM dendrimers and phospholipids.

2.2.2 ^{31}P NMR: relaxation times

In order to study the effect of PAMAM on the POPC and POPC/POPG head group dynamics in more detail, the spin-lattice relaxation time (T_1) and spin-spin relaxation time (T_2) of the phosphorus nucleus in POPC and POPC/POPG were measured. The results showed a small increase of the POPC ^{31}P T_1 relaxation rates upon the addition of 3rd generation PAMAM dendrimer and an even smaller increase in the case of 0th generation PAMAM dendrimer. In the case of POPC/POPG the largest change in T_1 was seen upon the addition of the 0th generation PAMAM dendrimer, while hardly any change was observed upon the addition of the 3rd generation PAMAM dendrimer (see **Figure 35**). These changes in spin-lattice relaxation time suggest a significant change in head group dynamics on the nanosecond time scale. [132, 136]

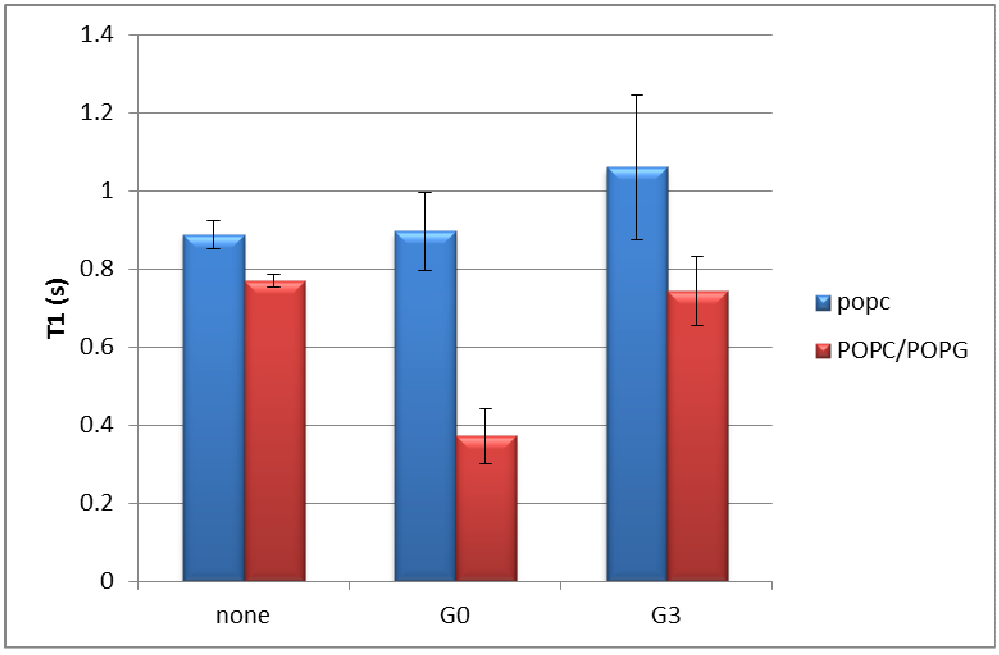

Figure 35 ^{31}P T_1 relaxation rates for POPC (blue) and POPC/POPG in 2:1 ratio (red) in the absence and in the presence of 0th and 3rd generation PAMAM dendrimers. A molar ratio of 1:75 dendrimer:lipid was used and the total lipid concentration was 30% (w/w) in D_2O.

Changes in the spin-spin relaxation times of the phosphorus nucleus in POPC and POPC/POPG membranes were also observed in the presence of PAMAM dendrimers (see **Figure 36**). POPC showed a major change in ^{31}P T_2 relaxation

rates upon the addition of 3rd generation PAMAM dendrimer, while no changes were seen upon the addition of 0th generation PAMAM dendrimer. In the case of POPC/POPG, both the 0th and the 3rd generation PAMAM resulted in an increase in T_2, with the largest increase observed in the presence of **3G** PAMAM. The changes in T_2 indicate alterations in motion on the microsecond time scale and confirm that PAMAM dendrimers can interact with phospholipid bilayers and thereby alter the dynamics of the headgroup of the lipids.

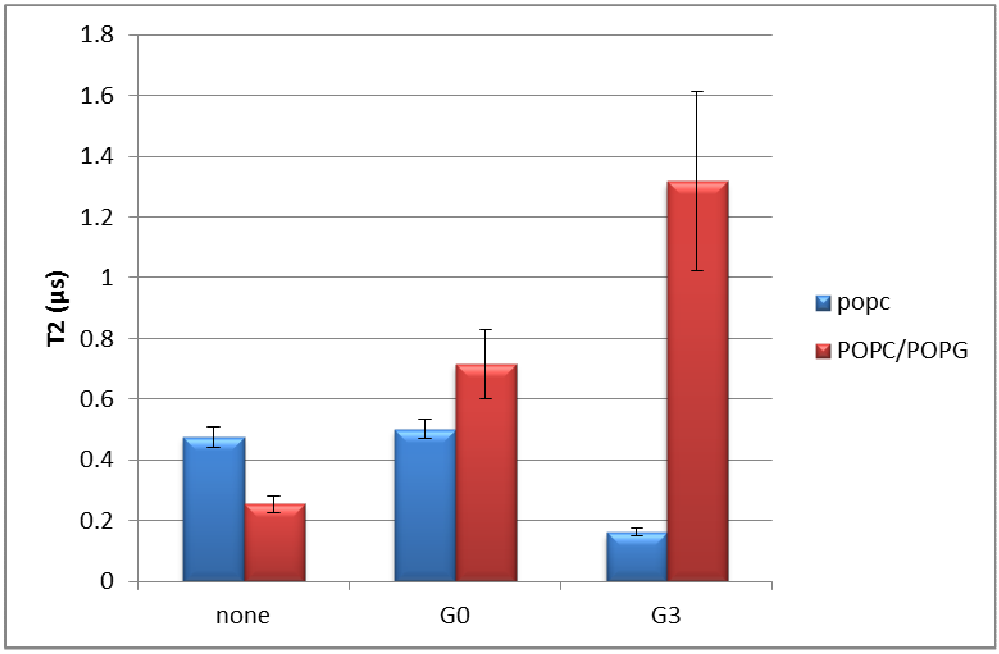

Figure 36 ^{31}P T_2 relaxation rates for POPC (blue) and POPC/POPG in 2:1 ratio (red) in the absence and in the presence of 0th and 3rd generation PAMAM dendrimers. A molar ratio of 1:75 dendrimer:lipid was used and the total lipid concentration was 30% (w/w) in D_2O.

2.2.3 NOESY (Nuclear Overhauser Effect SpectroscopY)

As mentioned previously, the liquid-crystalline or gel like phase of phospholipid membranes requires that solid state NMR techniques should be employed rather than classical solution based NMR techniques. While ^{31}P NMR experiments can give a good idea about the effect of dendrimers on the

headgroup of phospholipids, NOESY NMR is better suited to investigate if the dendrimer is in close proximity to the headgroup or to the tail (or both) of the phospholipids. Smith *et al*., for example, have employed solid state NOESY NMR to investigate the interaction between 5th and 7th generation PAMAM dendrimers and zwitterionic DMPC lipids and concluded that these dendrimers can be localised inside the hydrophobic core of the membrane (see above).[119] However, they did not investigate the effect of the presumably positively charged PAMAM dendrimers on negatively charged lipids. Furthermore, as POPC is the most abundant phopsholipid in mammalian cells[141] it might be useful to investigate the interaction between PAMAM dendrimers and POPC as well.

Solid state ^{1}H-^{1}H NOESY NMR spectra under magic angle spinning (MAS) conditions were run initially in unbuffered deuterium oxide at 500 ms mixing. The localisation of the dendrimer within the lipid bilayer could then be identified by the existence of cross peaks between dendrimer protons and lipid protons. Previous NOESY NMR studies on POPC membranes have shown that the chemical shifts for the protons in the lipid tail are found in the region of δ 1.0-2.5 ppm (except for the double bond, which is shifted more downfield towards δ 5.3 ppm), while the ^{1}H NMR signals corresponding to the headgroup are in the range of δ 3.5-5.5 ppm.[142] The NOESY NMR spectrum indicating an interaction between **0G** PAMAM and POPC bilayers is shown in **Figure 37(a)**, whereby the amber band indicates the region of possible cross peaks between PAMAM dendrimer protons and lipid protons (the signals inside the blue square box of around δ 2.5-3.0 ppm correspond to dendrimer-dendrimer cross peaks). **Figure 37(a)** clearly shows cross peaks of the PAMAM dendrimer with the POPC lipid tail (including with the double bond in the tail at δ 5.3 ppm), indicating an interaction between the tail of the POPC lipids and 0th generation PAMAM in the unbuffered condition. A similar effect was observed when **0G** PAMAM was introduced to membranes consisting of POPC:POPG in a 2:1 ratio (see **Figure 37(b)**), suggesting that **0G** PAMAM dendrimers are located close to the lipid tails in both POPC and POPC:POPG bilayers.

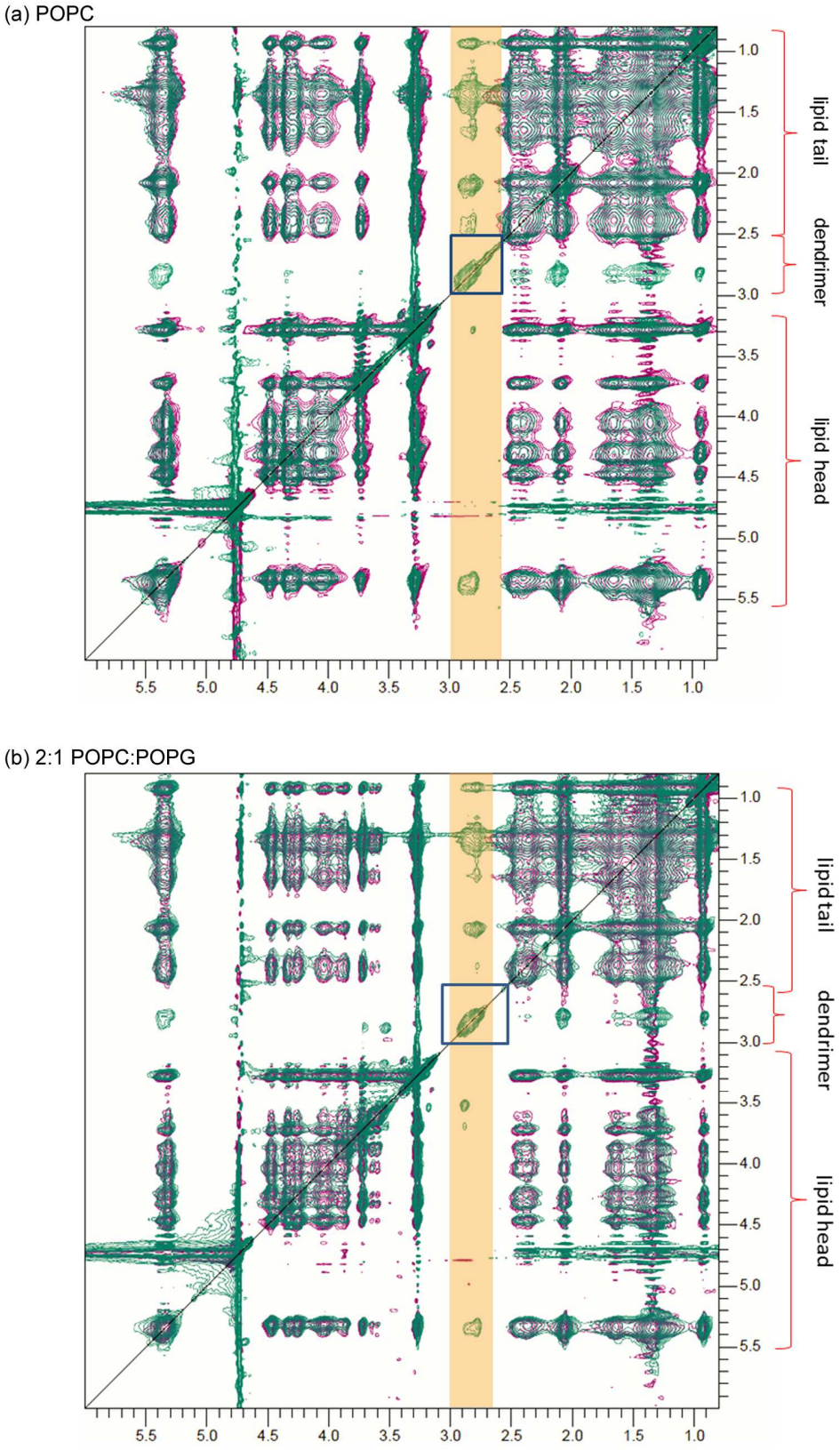

Figure 37 ^{1}H-^{1}H MAS NOESY NMR spectra of (a) POPC and (b) 2:1 POPC:POPG, with and without (green and purple repectively) 0th generation PAMAM (blue square) in unbuffered D_2O. Areas of potential dendrimer/lipid interactions are highlighted by an amber band. A molar ratio of 1:75 dendrimer:lipid was used and the total lipid concentration was 30% (w/w) in D_2O.

The experiments were repeated with **3G** PAMAM. Similar to the results obtained for **0G** PAMAM, an interaction between the tail of the POPC and 3rd generation PAMAM dendrimer was evident in unbuffered conditions, as indicated by the dendrimer-lipid cross peaks that can be observed in the amber band in **Figure 38**. However, the situation was different when 3rd generation PAMAM dendrimer was added to a 2:1 POPC:POPG mixture in unbuffered D_2O. In this case very few cross peaks were observed in the solid state ^1H-^1H MAS NOESY NMR spectrum (see **Figure 39**). There could be several reasons for the lack of signals in the NOESY spectra, such as the possibility that the lipid vesicles had not formed, the sample was contaminated, or an effect of the surrounding uncontrolled pH. In order to exclude the possibility that unbuffered conditions affect the experiments, the ^1H-^1H MAS NOESY NMR studies were repeated in D_2O controlled to pH = 7.2 with Tris buffer (this pH was chosen as it is more physiologically relevant).

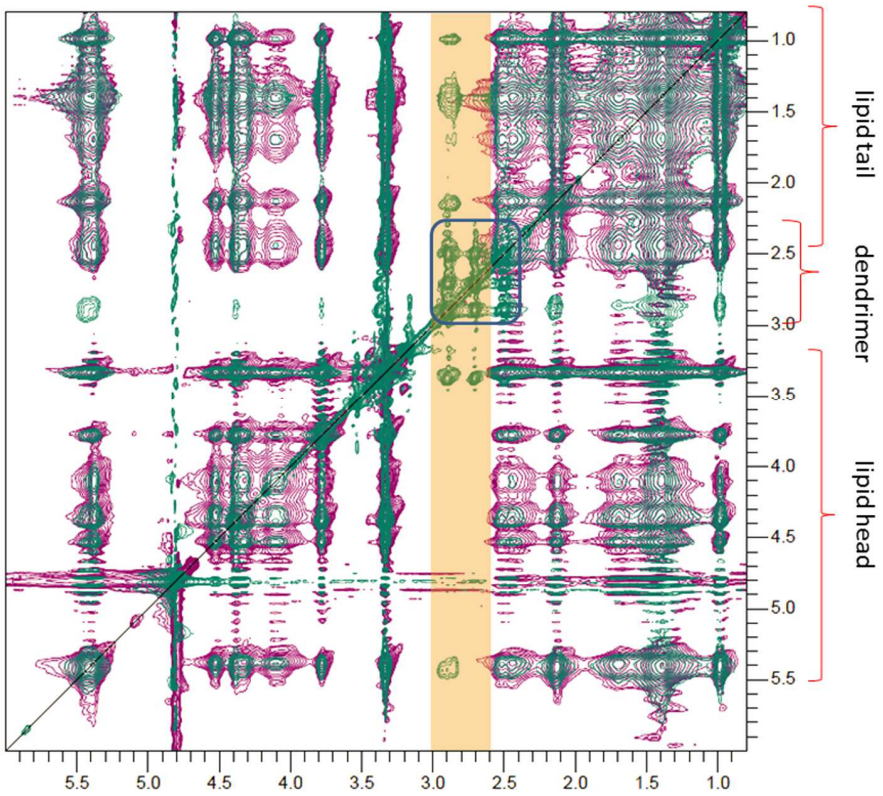

Figure 38 ^1H-^1H MAS NOESY NMR spectra of POPC with and without (green and purple repectively) 3rd generation PAMAM (blue square) in unbuffered D_2O. Areas of potential dendrimer/lipid interactions are highlighted by an amber band. A molar ratio of 1:75 dendrimer:lipid was used and the total lipid concentration was 30% (w/w) in D_2O.

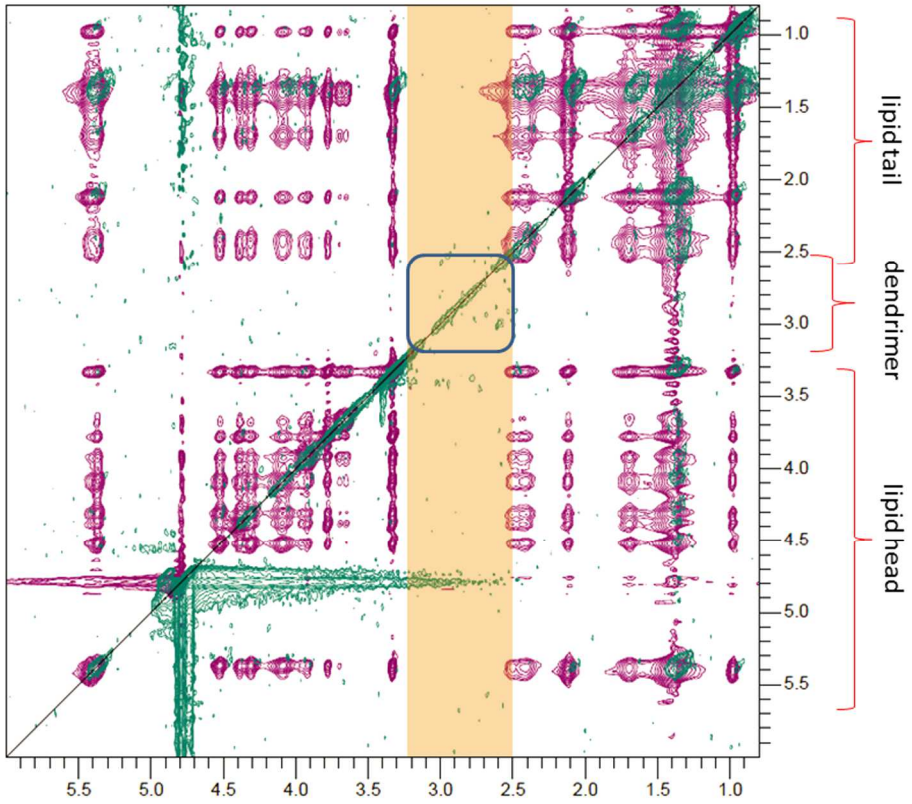

Figure 39 ^{1}H-^{1}H MAS NOESY NMR spectra of 2:1 POPC:POPG with and without (green and purple repectively) 3rd generation PAMAM (blue square) in unbuffered D_2O. Areas of potential dendrimer/lipid interactions are highlighted by an amber band. A molar ratio of 1:75 dendrimer:lipid was used and the total lipid concentration was 30% (w/w) in D_2O.

When the ^{1}H-^{1}H MAS NOESY NMR experiments were repeated at controlled pH, no interaction between the 0th generation PAMAM dendrimer and POPC alone or 2:1 POPC:POPG could be observed (see **Figure 40**). On the other hand, the solid state NOESY spectra in the presence of **3G** PAMAM controlled to pH 7.2 showed a small number of lipid-dendrimer cross peaks for pure POPC bilayers (see **Figure 41(a)**) and a much larger number of cross peaks for membranes consisting of 2:1 POPC:POPG (see **Figure 41(b)**). The results in buffered conditions therefore indicated that 3rd generation PAMAM dendrimers can interact with phospholipid bilayers, and interact more strongly with negatively charged lipids such as POPG than with zwitterionic lipids such as POPC, while 0th generation PAMAM dendrimer does not interact as strongly.

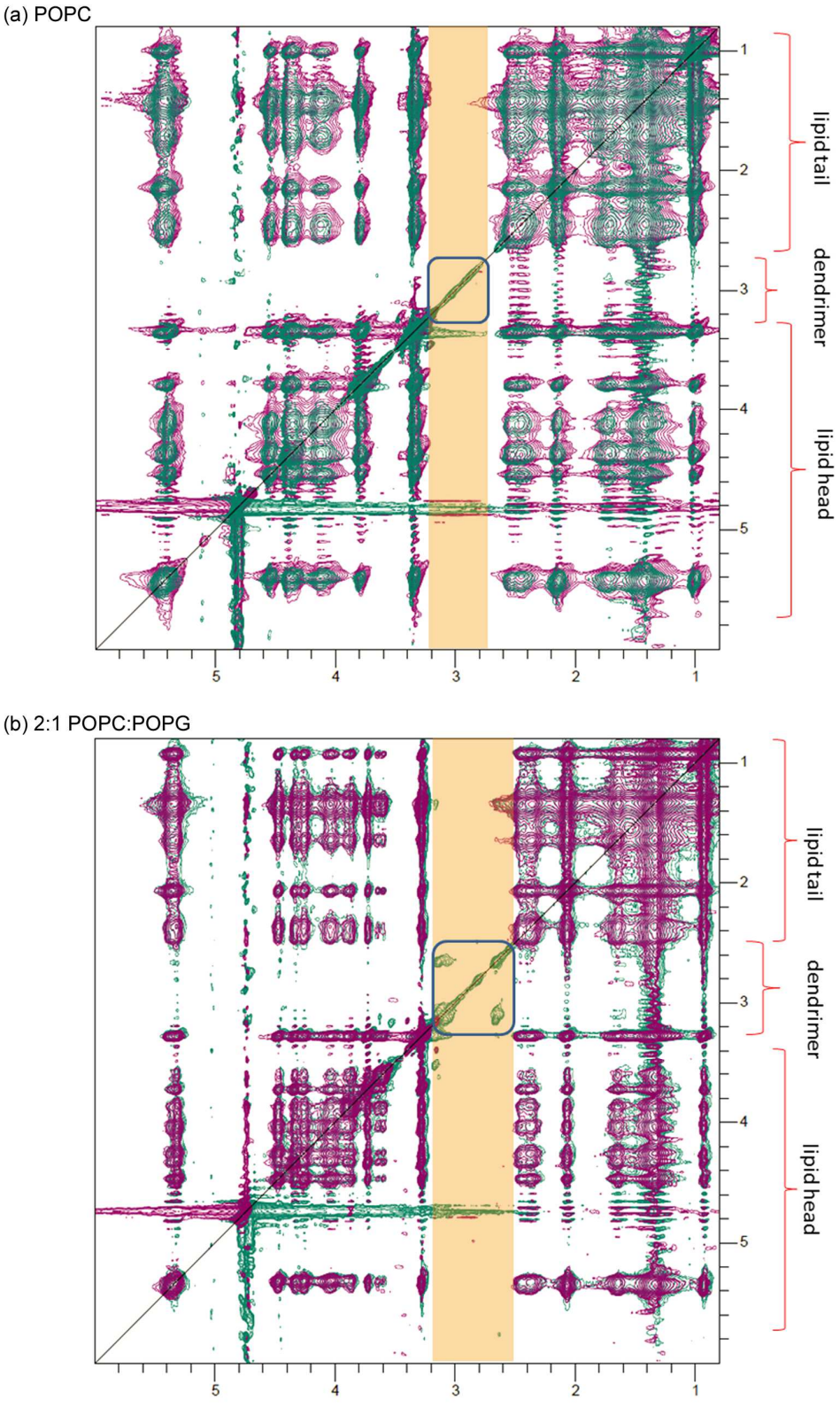

Figure 40 ^{1}H-^{1}H MAS NOESY NMR spectra of (a) POPC and (b) 2:1 POPC:POPG, with and without (green and purple repectively) 0th generation PAMAM (blue square) in D_2O buffered to pH 7.2. Areas of potential dendrimer/lipid interactions are highlighted by an amber band. A molar ratio of 1:75 dendrimer:lipid was used and the total lipid concentration was 30% (w/w) in D_2O.

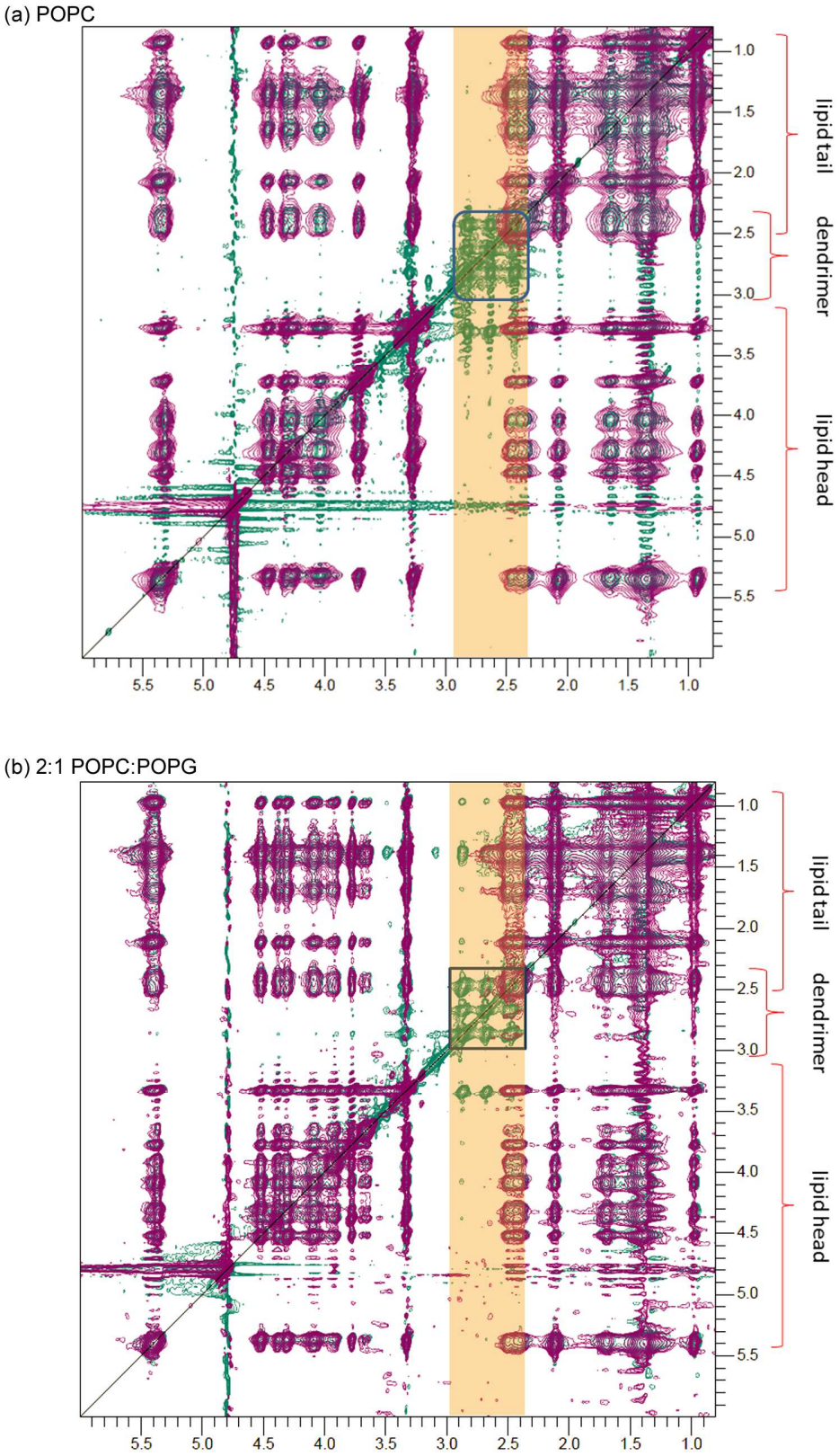

Figure 41 ^{1}H-^{1}H MAS NOESY NMR spectra of (a) POPC and (b) 2:1 POPC:POPG, with and without (green and purple repectively) 3rd generation PAMAM (blue square) in D_2O buffered to pH 7.2. Areas of potential dendrimer/lipid interactions are highlighted by an amber band. A molar ratio of 1:75 dendrimer:lipid was used and the total lipid concentration was 30% (w/w) in D_2O.

A summary of the various ^{1}H-^{1}H NOESY NMR experiments for lipid/dendrimer interactions is given in **Table 2**. It can be seen that in buffered conditions (pH=7.2), which are a better mimic to the real biological conditions, the 3rd generation PAMAM dendrimer has clearly shown interaction with lipid chains. This agrees with the observations made by Smith *et al.* on the interaction of 5th and 7th generation PAMAM dendrimers and DMPC lipids.[119] The results imply that mechanism B or D (see **Figure 19**) provide a suitable explanation for the interaction between 3rd generation PAMAM dendrimers and POPC and 2:1 POPC:POPG membranes, since mechanisms A and C do not suggest an interaction between the dendrimer and the lipid chains but only between the dendrimer and the lipid headgroups. The fact that the 0th generation did not show any interaction with the lipid chains in buffered conditions can be due to its relative small size, rendering the 0th generation dendrimer too small to span the membrane (mechanism D) or to have insertion of lipids in the dendrimer (mechanism B). The evidence for dendrimer-lipid interaction for 0th generation PAMAM observed by the ^{31}P NMR experiments (**Section 2.2.1**) is therefore most likely the result of some electrostatic interaction of the dendrimer with the phospholipid headgroups whereby the dendrimer is probably situated on the surface of the bilayer. In conclusion, the solid state NMR experiments have shown that low generation PAMAM dendrimers can interact with phospholipid bilayers, whereby the 3rd generation PAMAM can insert into the bilayer (or form micelles) but the 0th generation cannot. Furthermore, the interaction with the lipid tails seems to be more pronounced in the presence of negatively charged lipids (such as POPG) than in pure zwitterionic (POPC) membranes.

Table 2 Overview of lipid/dendrimer interactions as determined by NOESY NMR experiments.

		Area of lipid interacting with dendrimer	
pH condition	**Lipid[a]**	**0G PAMAM**	**3G PAMAM**
Non-controlled	POPC	Chain	Chain
	POPC/POPG[b]	Chain	n.a.[c]
Controlled pH=7.2	POPC	None	Chain
	POPC/POPG[b]	None	Chain

[a] A molar ratio of 1:75 dendrimer:lipid was used and the total lipid concentration was 30% (w/w) in D_2O. [b] POPC:POPG mixed in 2:1 ratio; [c] Interaction could not be determined due to low number of signals (see main text for details).

2.3 Fluorescence studies

In the previous section, solid state ^{1}H-^{1}H MAS NOESY NMR studies identified that no association was present between 0th generation PAMAM and either POPC or POPC/POPG lipid bilayers. On the other hand, limited interaction between the 3rd generation PAMAM and POPC was observed and this interaction was significantly increased in the presence of POPG due to its negatively charged head group which can associate with the positively charged PAMAM surface amines. In order to gain additional insight of the nature of the interaction between 3rd generation PAMAM and both POPC and POPC/POPG lipid bilayers, a series of preliminary fluorescence spectroscopy studies were performed on 3rd generation PAMAM dendrimers tagged with a fluorophore.

Marking polymers with pyrene or dansyl dyes is an effective technique used for characterising polymers as the changes of the fluorescence intensity reflect the variation of the polarity around the chromophore.[143, 144] While the influence of the polarity of the local environment on the fluorescence spectrum of pyrene is well established, this label has a high ability for exciplex formation in water at low concentration.[145] Therefore dansyl was chosen to label the 3rd generation PAMAM, as it has been shown that its fluorescence intensity and emission maximum (λ_{em}) depend on the polarity of the environment.[144] Furthermore the high reactivity of dansyl chloride towards amines renders it the ideal candidate to be used for labelling dendrimers. 3rd Generation PAMAM dendrimer was prepared according to literature procedures[15] (see **Section 2.1**) and subsequently labelled with dansyl by reacting it with dansyl chloride in a 2:1 ratio of dansyl chloride to dendrimer, as shown in **Scheme 14** (full experimental details can be found in **Chapter 4**). It has previously been shown that the molar extinction coefficient of a dansyl-labelled PAMAM dendrimer increases linearly with the number of dansyl groups attached.[146] For compound **3G-dansyl** it was found that the molar extinction coefficient in water at 330 nm is ε_{330nm} = 10,969 $M^{-1}cm^{-1}$ (see **Chapter 4**). As the molar extinction coefficient of a single dansyl unit is around 4,000 $M^{-1}cm^{-1}$ in water,[146] this result suggests that on average two to three dansyl units were attached to the PAMAM dendrimer in compound **3G-dansyl**.

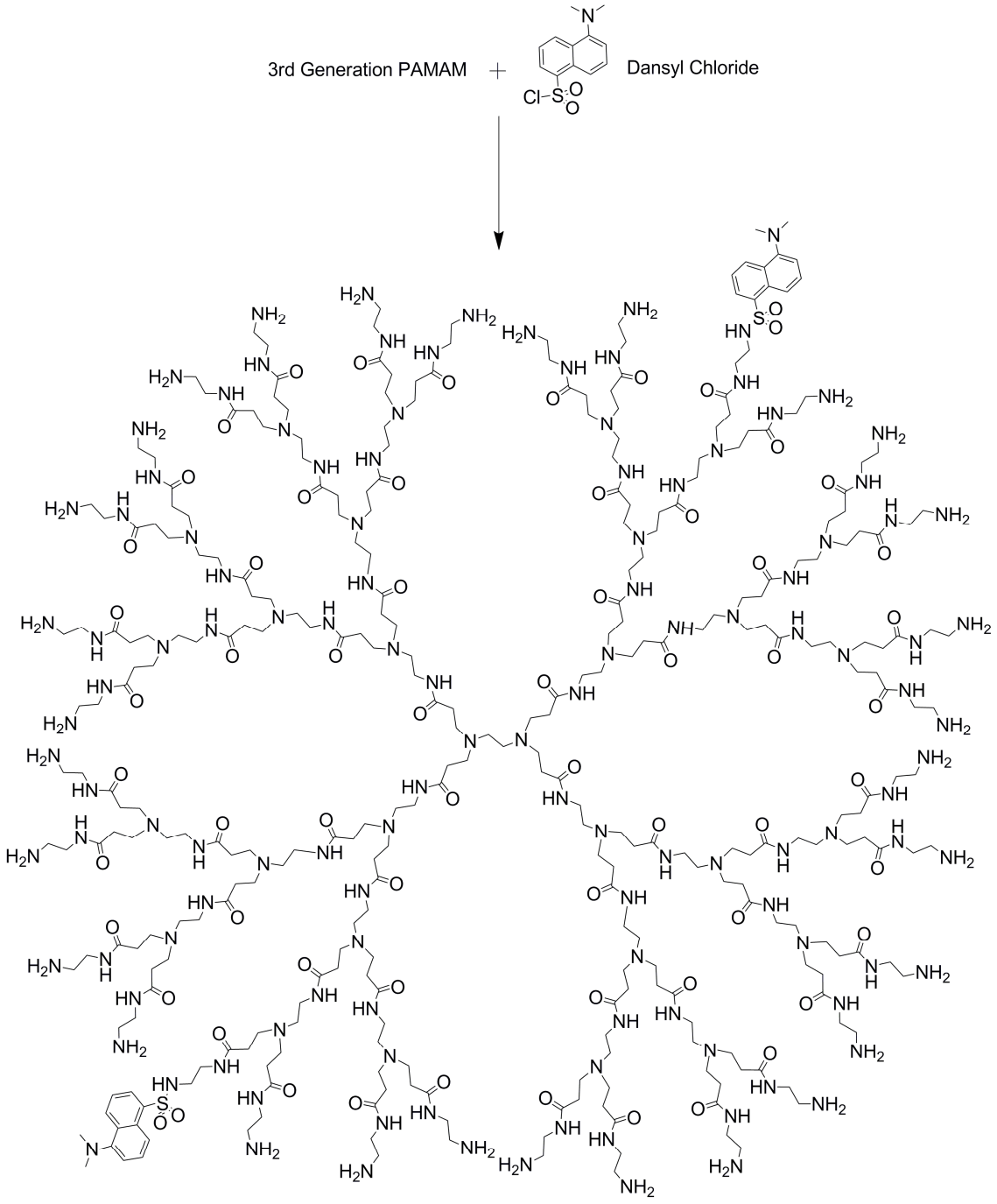

Scheme 14 Synthesis of compound **3G-dansyl** (3rd generation PAMAM dendrimer tagged with dansyl) from the reaction of dansyl chloride with 3rd generation PAMAM dendrimer in a 2:1 ratio dansyl:dendrimer

When a dansyl tag is surrounded by a polar environment, reorientation of the dipoles of the solvent molecules around the excited state of the fluorophore lowers the energy of the excited state and shifts the emission wavelength to

higher values (red shifted). Additionally, in a polar environment the fluorescence intensity of the dansyl is significantly lower in comparison to a nonpolar environment due to the relaxation mechanism offered by the solvent molecules. Therefore when changing the polarity of the environment surrounding the dansyl from an aqueous solvent to a less polar environment there will be shifting in the emission wavelength towards blue and a higher fluorescence intensity.[144, 147] This makes the dansyl dye an ideal candidate for measuring interactions with lipids, as the association of the water-soluble PAMAM with a lipid bilayer will change the polarity around the dansyl tag.

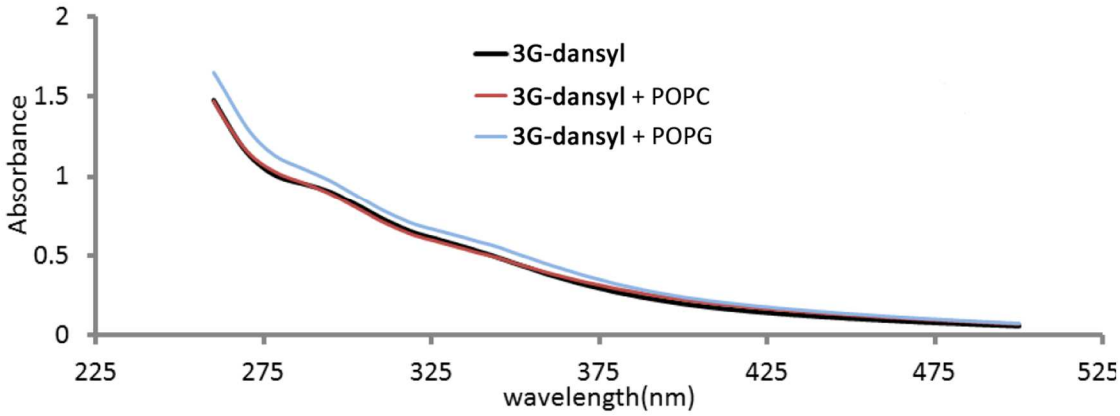

Figure 42. No significant changes were observed in the absorbance and wavelength (nm) when introducing POPC or POPG lipids vesicles to **3G-dansyl** (40 μM in water). Mixing ratio 1:75 dendrimer:lipid.

The absorbance spectrum for compound **3G-dansyl** did not show any significant changes when POPC or POPG were introduced (see **Figure 42**). Introducing only POPC did not cause any major change in the fluorescence intensity either. However, a large increase in the fluorescence intensity was observed when POPG was introduced to an aqueous solution of compound **3G-dansyl,** either neat or mixed in a 1:2 ratio with POPC (see **Figure 43**). Furthermore, a comparison of the wavelength for the emission maximum shows that a blue shift occurs when POPG is added (alone or as a 2:1 POPC:POPG mix), while only a minor shift in the wavelength occurred upon the addition of POPC alone (see **Table 3**).

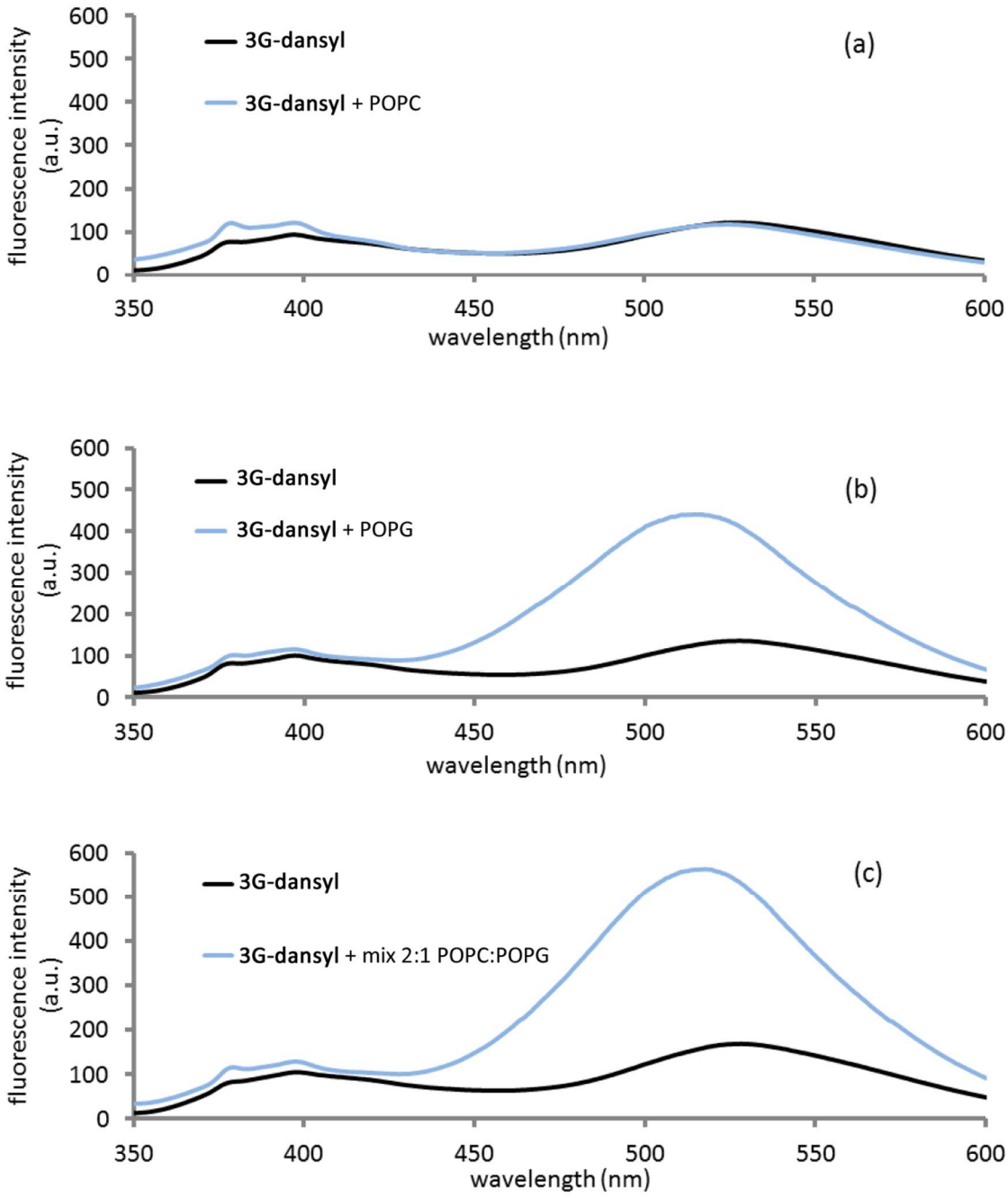

Figure 43 Changes in the fluorescence intensity (a.u.) and wavelength (nm) when introducing various lipid vesicles to the 3rd generation PAMAM dendrimers marked with dansyl (40 μM in water). Mixing ratio 1:75 dendrimer:lipid. (a) Introducing POPC did not show a significant change; (b) An increase on the fluorescence intensity observed when introducing POPG; (c) Introducing 1:2 POPG:POPC vesicles results in an increase of the fluorescence intensity.

Table 3 Comparison of the I_{rel} (relative intensity) and the change in wavelength of the emission maximum ($\Delta\lambda_{em}$) for an aqueous solution of **3G-dansyl** (40 μM) upon introducing different lipid vesicles. I_{rel} relative intensity calculated I_{rel} = fluorescence intensity with added lipid to **3G-dansyl** divided on fluorescence intensity of **3G-dansyl** only. Values for fluorescence intensities calculated according to emission maximum (λ_{em})).

3G-dansyl environment	I_{rel}	$\Delta\lambda_{em}$ (nm)
POPC	0.96	-3.5
POPG	3.25	-13
2:1 POPG:POPC	3.34	-11

The increase in the fluorescence intensity after introducing POPG indicates a decrease in the polarity of the environment surrounding the dansyl-tag in compound **3G-dansyl**. This decrease in the polarity happens as the aqueous solvent molecules get forced away from the nearby area around the labelled dendrimer by POPG. It is reasonable to assume that this interaction occurs between POPG and **3G-dansyl** due to the association between the negatively charged lipid polar headgroups and the positively charged amine terminal groups on the dendrimer (Tomalia and co-workers have previously established that PAMAM dendrimers are positively charged in water)[16]. A similar interaction does not occur when introducing POPC, as the negative charge is not dominant in the polar head group of POPC (it is a zwitterionic head group containing both a negative and a positive charge) and therefore it shows a lower affinity towards 3rd generation dansyl-labelled dendrimer. These results are in good agreement with the solid state NMR measurements discussed in **Section 2.2** (see above).

To have a better idea of the effect of the charge of the polar head groups on the dendrimer/vesicle interactions, the above experiments were repeated using a positively charged head group surfactant CTAB (cetyltrimethylammonium bromide), a negatively charged head group surfactant SDS (sodium dodecyl sulphate) and a neutral analogue 1,2-dodecyldiol. CTAB was selected based on the fact that the cationic polar head mimics the positively charged quaternary amine present in POPC, while SDS was chosen because the anionic sulphate headgroup mimics the polar phosphate headgroup in POPG and POPC in both

negative charge and tetrahedral geometry. Finally, 1,2-dodecyldiol was selected to mimic the two hydroxyl groups present in POPG but without the mimicking the negative phosphate group in order to isolate any role played by the two hydroxyl groups in the interaction of POPG with compound **3G-dansyl**.

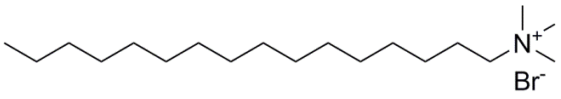

CTAB

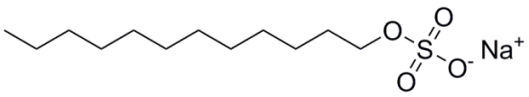

SDS

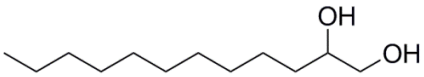

1,2dodecyldiol

Once again, the absorbance spectrum for compound **3G-dansyl** did not show any significant changes when any of the surfactants were introduced (see **Figure 44**). However, when comparing the wavelength for the emission maximum (**Table 4**), a blue shift in the wavelength towards lower values occurred in all cases, with the highest shift seen for the addition of SDS and smaller shifts seen in the case of CTAB and 1,2-dodecyldiol. By considering the similar shift effect found with POPC and POPG it is noted that the shift difference increases as the negative charge of the polar head group increases for both the lipids and the surfactants. Introducing CTAB or 1,2-dodecyldiol did also not cause as big a change in the fluorescence intensity and the changes that are observed may be attributed to additional light scattering (CTAB) or dilution effects (1,2-dodecyldiol). However, a significant increase in the fluorescence intensity was observed when SDS was introduced to the solvent environment surrounding compound **3G-dansyl** (see **Figure 45**).

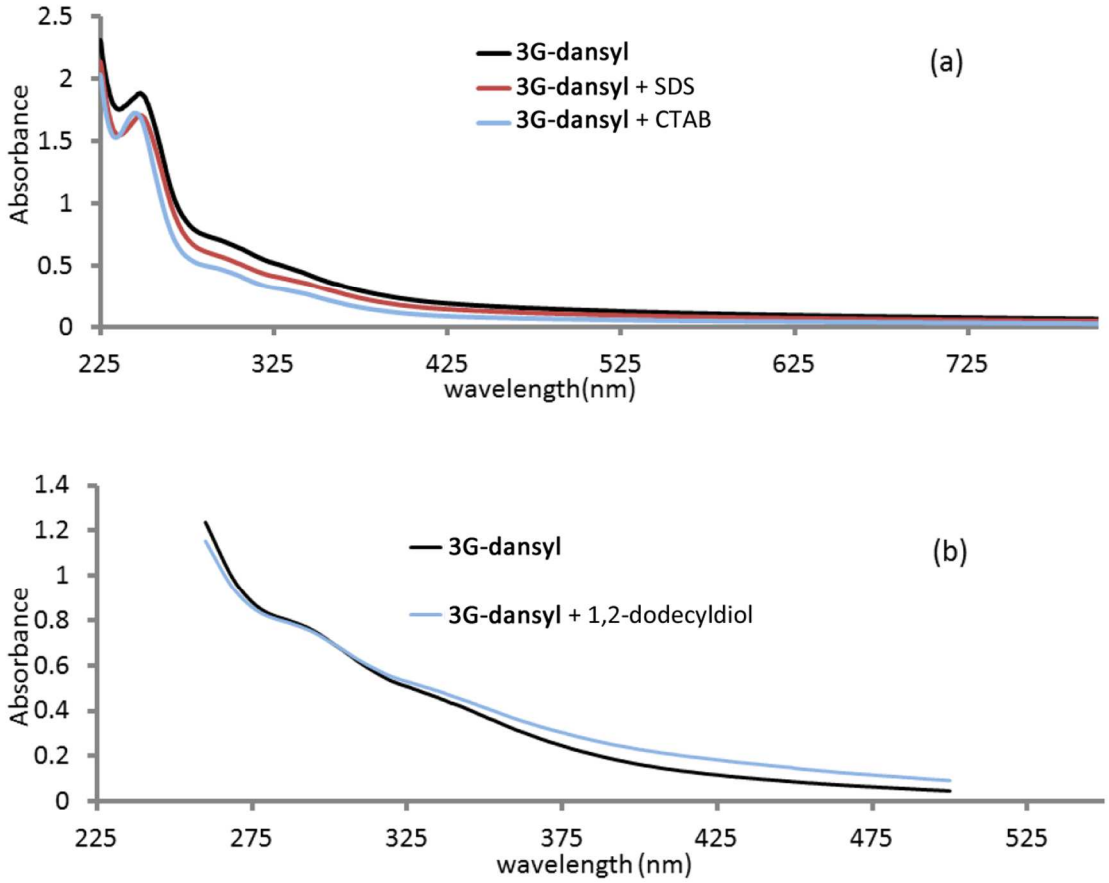

Figure 44. No significant changes were observed in the absorbance (a.u.) and wavelength (nm) when introducing various surfactants to the 3rd generation PAMAM dendrimer marked with dansyl (40 μM in water). Mixing ratio 1:75 dendrimer:surfactant. (a) Introducing SDS/CTAB; (b) Introducing 1,2-dodecyldiol.

Table 4 Comparison of the I_{rel} (relative intensity) and the change in wavelength of the emission maximum ($\Delta\lambda_{em}$) for an aqueous solution of **3G-dansyl** (40 μM) upon the addition of various surfactants. I_{rel} relative intensity calculated I_{rel}= fluorescence intensity with added lipid to **3G-dansyl** divided on fluorescence intensity of **3G-dansyl** only. Values for fluorescence intensities calculated according to emission maximum (λ_{em})).

3G-dansyl environment	I_{rel}	$\Delta\lambda_{em}$ **(nm)**
CTAB	1.25	-6
SDS	2.40	-15
1,2-dodecyldiol	0.75	0.5

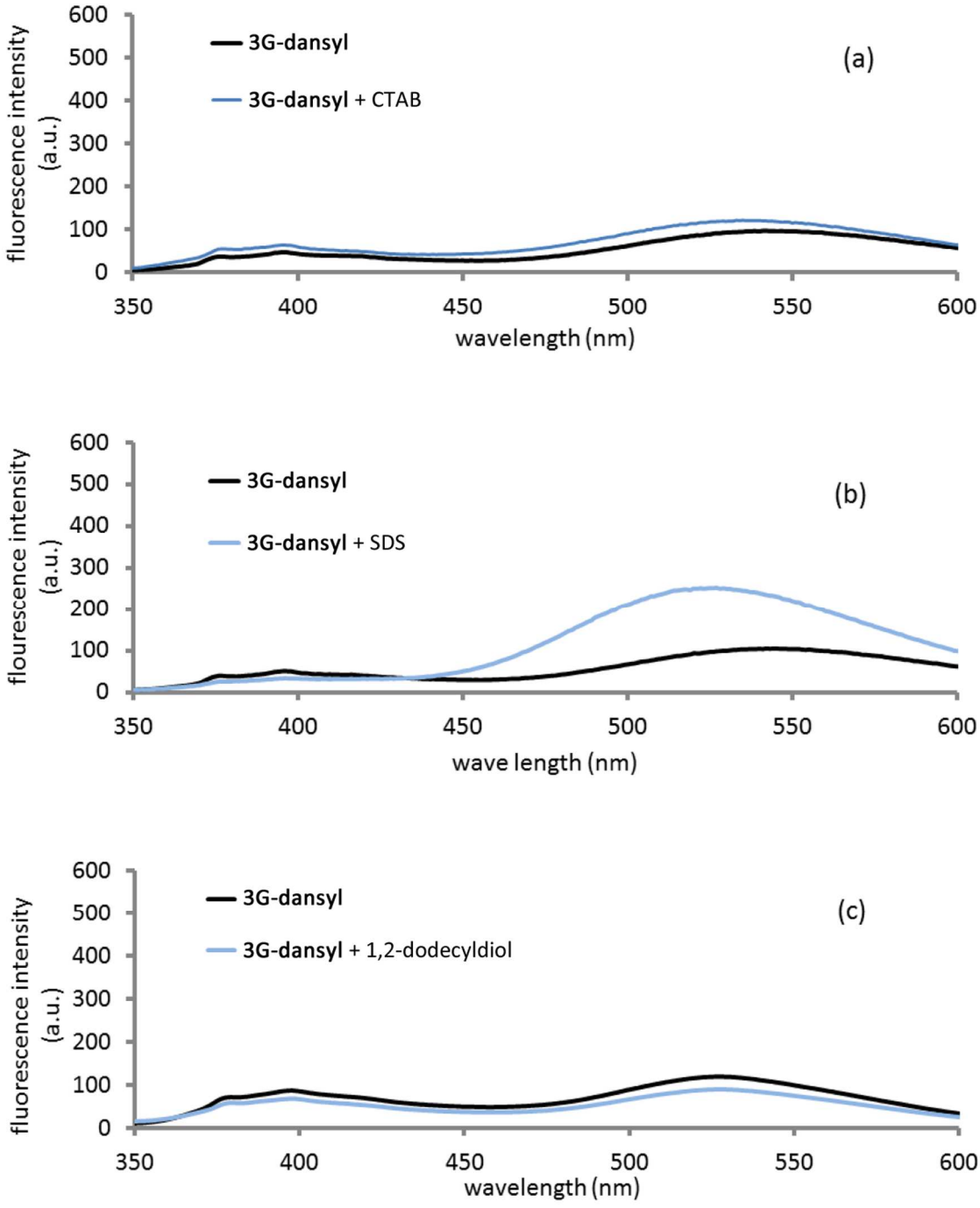

Figure 45 Changes in the fluorescence intensity (a.u.) and wavelength (nm) when introducing various surfactants vesicles to 3rd generation PAMAM dendrimer marked with dansyl (40 μM in water). Mixing ratio 1:75 dendrimer:surfactant. (a) Introducing CTAB did not show a significant change; (b) An increase in the fluorescence intensity was observed when introducing SDS; (c) Introducing 1,2-dodecyldiol did not show any increase in fluorescence intensity.

The increase in the fluorescence intensity in the case of SDS happens because of the attraction between the positively charged surface amines of the **3G-dansyl** dendrimer and the negatively charged polar head of SDS. This attraction leads to the water solvent molecules being forced away from the area nearby the amine head groups and being replaced by SDS molecules (which are less polar). In the case of CTAB the absence of the negatively charged polar head does not encourage a similar attraction and therefore there are no major changes in fluorescence intensity. In the case of 1,2-dodecyldiol, while no attraction depending on the charge differences is expected, it was noted that mimicking the two hydroxyl groups present in POPG without the negatively charged polar head does not cause a large increase in the fluorescence intensity of compound **3G-dansyl**. This suggests that the attraction between POPG and the **3G-dansyl** dendrimer is mainly down to the negative charge of the polar headgroup.

In summary, the increase in fluorescence intensity when adding anionic lipids and surfactants provides clear evidence for the interaction between negatively charged polar headgroups and 3rd generation PAMAM dendrimers. While the changes in fluorescence intensity with neutral or positively charged species are minimal, all cases studied show a shift in the emission maximum wavelength. This shift varies, but the largest shift was observed in the presence of negatively charged lipids and surfactants and the smaller shifts in the presence of positively charged polar head lipids and surfactants. By running more experiments with a larger variety of differently charged lipids and surfactants and by analysing the data it would be possible to explore a wide spectrum of their interaction with dendrimers. Furthermore, widening the spectrum to test against more PAMAM dendrimer generations would provide better insight into the affinities between PAMAM dendrimers and various lipids and could help gain a deeper understanding of and help optimise the role that PAMAM dendrimers play in drug and gene delivery

2.4 Molecular Dynamic Simulations

The solid state ^{31}P and ^{1}H-^{1}H NOESY NMR, as well as the fluorescence studies discussed in the previous sections have indicated that especially third generation PAMAM dendrimers are able to interact with phospholipid bilayers. This interaction was shown to be more pronounced in the presence of anionic lipids (POPG) compared to neat zwitterionic lipid bilayers (POPC). This suggests that the interaction is driven by electrostatic interactions between the positively charged dendrimers and negatively charged phosphate-containing headgroups of the lipid. However, the ^{1}H-^{1}H NOESY NMR results also showed the **3G** PAMAM interacts with the apolar interior of the lipid and therefore appears to be embedded within the membrane. This suggests a mechanism where the dendrimer spans the membrane bilayer, allowing electrostatic interactions between the dendrimer surface groups and the phospholipid headgroups at both sides of the membrane while the interior of the dendrimer is in close contact with the interior of the membrane (see **Figure 19**, mechanism D). Theoretically such an interaction should be possible given that the typical bilayer thickness of a POPC membrane is 39 Å (thickness of hydrocarbon region only is 29 Å),[148] while the average diameter of **3G** PAMAM dendrimers has been calculated to be around 36 Å,[149] indicating that an extended conformation of third generation PAMAM is able to span the membrane. **0G** PAMAM on the other hand is a lot smaller (14 Å) than **3G** PAMAM and is thus unable to span a phospholipid bilayer.

In an attempt to understand how **3G** PAMAM can interact with POPC/POPG membranes and can potentially be embedded within the bilayer, molecular dynamics (MD) simulations were performed. However, the study of dendrimer-lipid bilayer interaction using atomistic MD simulations can be difficult as a result of the high number of atoms and interactions that need to be calculated and therefore coarse-grained (CG) models were used. In CG simulations a small group of atoms are represented by a single interaction site (or 'bead') with similar mass and properties. This reduces the number of degrees of freedom in the system and thus allows the modelling of larger and more complex systems as well as longer time-scales. Marrink and co-workers were the first to design a

CG-MD system for the semi-quantitative simulation of lipids such as DPPC.[150] In their simulations, lipids were modelled by a combination of four types of beads (that each correspond to on average four atoms): polar (P), i.e. uncharged water soluble groups of atoms, apolar (C), i.e. hydrophobic groups of atoms, nonpolar (N), i.e. groups of atoms partly polar and partly apolar and charged (Q), i.e. ionized groups of atoms.[150] The beads are also assigned information about their potential hydrogen bond donating (d) or accepting (a) ability to allow fine-tuning of the interactions. Lee *et al.* have used this CG model to investigate the interactions of a number of dendrimers with neutral (zwitterionic) DPPC bilayers and these 0.5-μs-long simulations have shown that **3G** PAMAM is able to insert itself into the bilayer.[115] In order to see if the same holds true for the interaction of PAMAM dendrimers with anionic lipid bilayers (2:1 POPC:POPG), a similar set of CG-MD simulations were performed in association with Jamie Parkin and Dr. Syma Khalid.

For these MD simulations, the PAMAM dendrimers are modelled using three different types of beads following the method by Lee *et al.*[115] (see **Figure 46**): beads representing the nodes or branching points that have no hydrogen bonding ability (N_0), beads representing the branches that possess both hydrogen bond donating and accepting ability (N_{da}) and beads representing the terminal amine groups which are assumed to be positively charged and possessing hydrogen bond donating ability (Q_d). The terminal amines are assigned a positive charge because Tomalia and co-workers have previously shown that at neutral pH the majority of the terminal amine functionalities are protonated.[15] The lipid molecules were modelled using the system developed by Marrink and colleagues[150] (see **Figure 47**): a number of apolar beads for the lipid tails (C), two nonpolar beads with hydrogen bond accepting ability for the glycerol ester linkage (N_a), a negatively charged bead with hydrogen bond accepting ability representing the phosphate group (Q_a^-) and either a positively charged bead for the POPC choline unit (Q_0^+) or a polar bead with hydrogen bond donating and accepting ability for the POPG glycol unit (P_{da}).

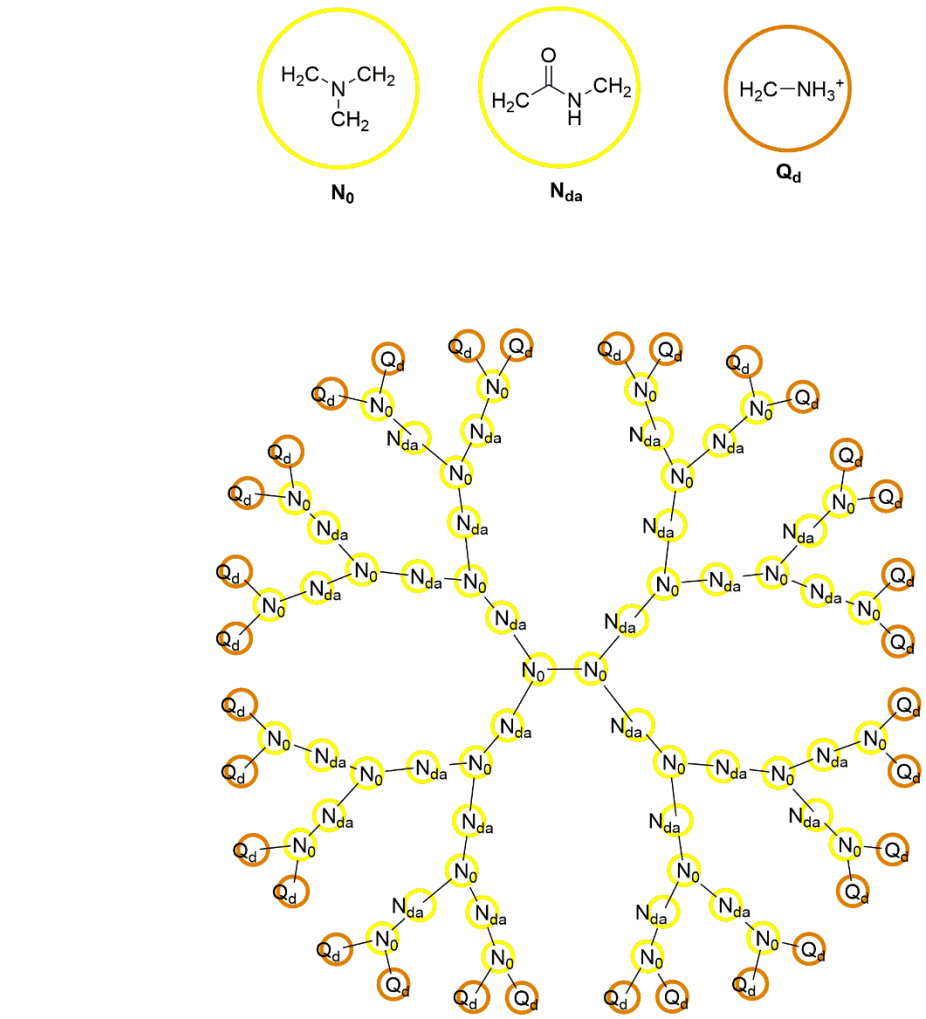

Figure 46 Representation of the dendrimer CG beads used for the MD simulations, as well as the CG representation of **3G** PAMAM.

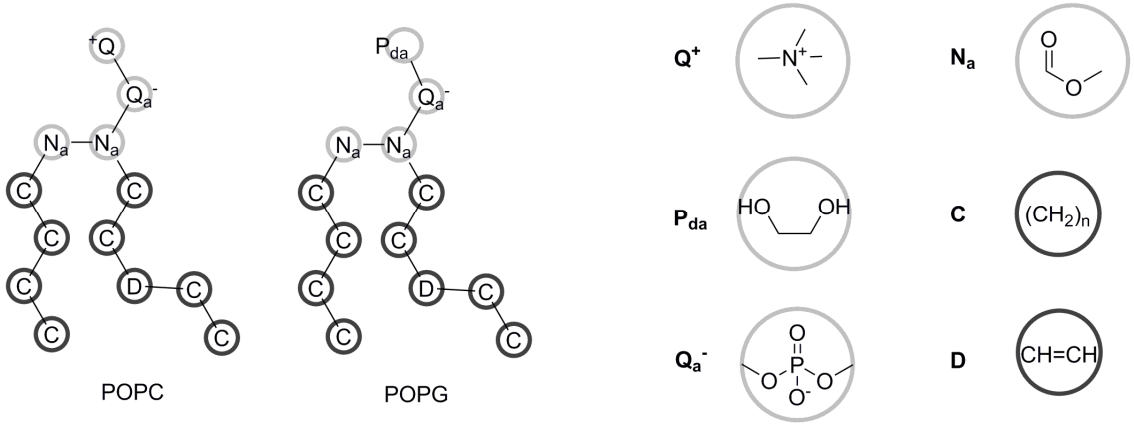

Figure 47 Representation of the lipid CG beads used for the MD simulations, as well as the CG representation of POPC and POPG.

The CG molecular dynamics simulations were run with a time step of 30 fs and for an overall duration of 300 ns using the GROMACS simulation package.[151] Each simulation contained four dendrimer molecules, 300 lipid molecules (200 POPC and 100 POPG molecules) and was solvated with 11,800 CG water molecules (each CG water bead corresponds to four water molecules) in a periodic box of size 10.4 x 9.3 x 16 nm^3. Na^+ and Cl^- ions were also added to maintain the charge balance. The temperature was maintained at 323 K by applying a Berendsen thermostat.[152]

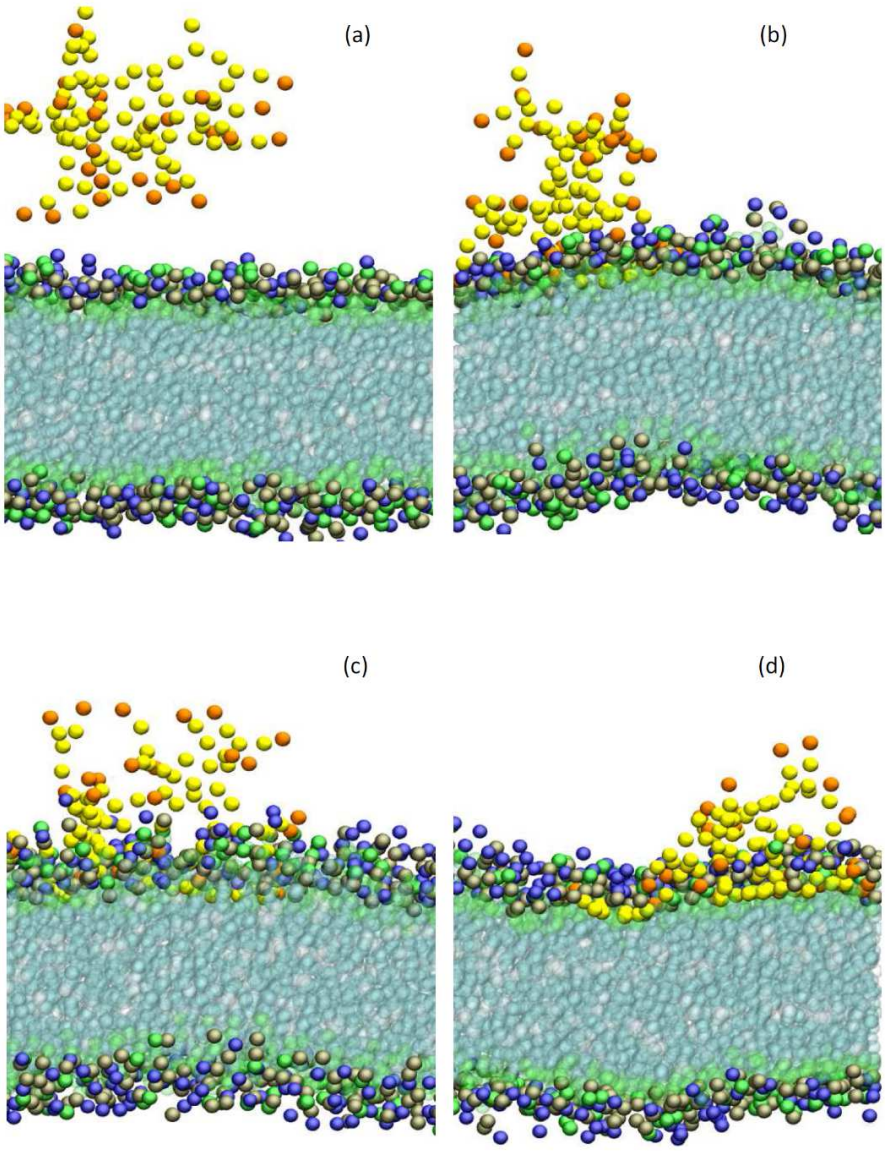

Figure 48 Coarse-grained MD simulation of the interaction between 3rd generation PAMAM and 2:1 POPC:POPG with snapshots at (a) t = 0 ns, (b) t = 75 ns, (c) t = 150 ns and (d) t = 300 ns. The following colour coding is used: terminal amine groups (orange beads), internal PAMAM moieties (yellow beads), phospholipids (green and blue beads with the membrane interior opaque).

Figure 48 shows a number of snapshots that were taken during the simulation of the interaction of **3G** PAMAM and 2:1 POPC: POPG lipids. It can be seen that the dendrimer approaches the lipid bilayer during the simulation and eventually flattens on top of the membrane, thereby maximising the number of electrostatic interactions between the dendrimer surface amines and the lipid head groups. Unlike the MD simulations by Lee *et al.* that showed insertion of **3G** PAMAM into DPPC lipids after 500 ns,[115] no insertion was seen in these simulations. However, at the end of the simulation the dendrimer is deeply embedded in the polar region of the bilayer and also comes into contact with the apolar interior of the bilayer (which agrees with ^{1}H-^{1}H NOESY NMR results that showed close contact between the dendrimer and the membrane interior). This suggest that insertion of the dendrimer might be possible if the simulations are run for a longer time period.

To investigate the nature of the interaction in more detail, the number of contacts between the dendrimer and either the lipid headgroup or the whole lipid was calculated (a contact was counted when the distance between any of the dendrimer beads and the lipid beads (either the Q^{+} or P_{da} bead for the lipid headgroup, or all of the lipid beads for the whole lipid) was within 6 Å. It can be seen from **Figure 49** that the number of contacts between the dendrimer and the lipid gradually increases over time. It also appears that the number of contacts has not yet reached an equilibrium as it is still increasing at the end of the simulation. This might indicate that the **3G** PAMAM dendrimers could possibly insert into the lipid bilayer if the simulation was run for a longer period of time. Furthermore, the number of contacts between the POPC and POPG headgroups are surprisingly similar given that there are twice as many POPC molecules than POPG molecules. This could indicate that the positively charged PAMAM dendrimers favour interactions with the negatively charged POPG molecules and thus that the contacts are driven by electrostatic forces, which agrees with the fluorescence studies were the largest changes in fluorescence intensities were seen with negatively charged lipids and surfactants (see **Section 2.3**). Additionally, **Figure 49** reveals that there are significantly more contacts between the dendrimer and the whole lipids than with the lipid headgroups alone. This suggests, that there are also contacts with the apolar region of the lipids and thus that at least some parts of the

dendrimer are inserted within the bilayer (this can also be observed in **Figure 48(d)**). This agrees with the solid state NMR studies were cross peaks were seen between the dendrimer protons and the protons of the lipid tails (see **Section 2.2**). Overall, this CG molecular dynamics simulation suggests that third generation PAMAM dendrimers can interact with negatively charged membranes through electrostatic interactions, but some insertion of the dendrimer into the apolar region is also observed. Combined with the solid state NMR and fluorescence studies, these result indicate that the most likely interaction between PAMAM dendrimers and membranes is mechanism D (see **Figure 19**), where the dendrimer is [partly] embedded within the lipid bilayer whilst maintaining electrostatic interactions with the lipid headgroups

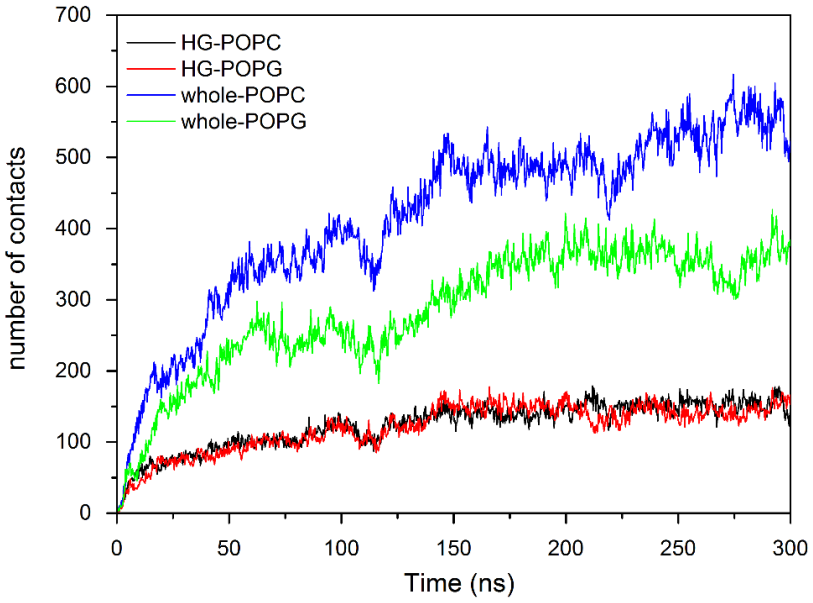

Figure 49 Number of contacts between **3G** PAMAM dendrimers and POPC or POPG lipids during a 300 ns CG MD simulation. The results are the average of three independent runs.

While it is generally believed that the primary amino groups on the surface of PAMAM dendrimers are protonated at neutral pH,[149] it is unlikely that all amines are protonated. The protonation of one surface amine group will reduce the protonation ability of a neighbouring amine functionality, as there would, for example, be charge repulsion if both amines are protonated. The pK_a values of dendrimers can therefore not be given as a single value, but are better presented as a range of values (Tomalia and co-workers have estimated the pK_a

of the primary surface amines to be in the region pK_a = 7-9)[15, 153]. This charge repulsion effect on the pK_a of neighbouring amines should be more pronounced for higher generation PAMAM dendrimers, as the surface is more crowded and the amines are situated closer to each other. In this respect, Ottaviani *et al.* have calculated that the pH at which protonation begins is pH 8.5 (and lower) for **3G** PAMAM, while it is only pH 8.0 for **5G** PAMAM.[154] It is therefore possible that not all of the surface amine groups of **3G** PAMAM are protonated at neutral pH. The CG MD simulation were therefore also repeated for 'half charged' dendrimers, where some of the beads corresponding to $-NH_3^+$ groups were replaced with beads corresponding to $-NH_2$ groups. As a control, the simulations were also repeated with uncharged, i.e. neutral, dendrimers. If the interactions with the lipids are the result of electrostatic interactions, no interactions are expected under these conditions. Furthermore, the effect of the size of the dendrimer was investigated by repeating all of the simulations with **0G** PAMAM dendrimers. The results are shown in **Figure 50** (snapshots representing the situation at the end of each simulation) and **Figure 51** (number of contacts versus simulation time).

It can be seen from **Figure 50** that full insertion of the dendrimer into the bilayer has not occurred during any of the CG MD simulations. Furthermore, the Figures show that in the case of **3G** PAMAM dendrimer electrostatic interactions appear to be important. This can be derived from the observation that the number of contacts between **3G** PAMAM and the lipids decreases when the overall positive charge on the dendrimer is decreased (**Figure 51**). Additionally, the snapshots in **Figure 50** show that the fully charged **3G** PAMAM dendrimers flatten out onto the surface of the membrane to maximise the number of contacts, the four half charged **3G** PAMAM dendrimers cluster together and come into contact with the membrane surface without flattening out, while the uncharged **3G PAMAM** dendrimers do not interact with the membrane at all. It must be noted that in the case of the half charged 3rd generation PAMAM dendrimer the number of contacts between the dendrimer and the whole lipid is still higher than the number of contacts between the dendrimer and the lipid headgroups, indicating that there is also some degree of insertion and contact with the apolar membrane interior under these conditions (in agreement with the solid state NMR results).

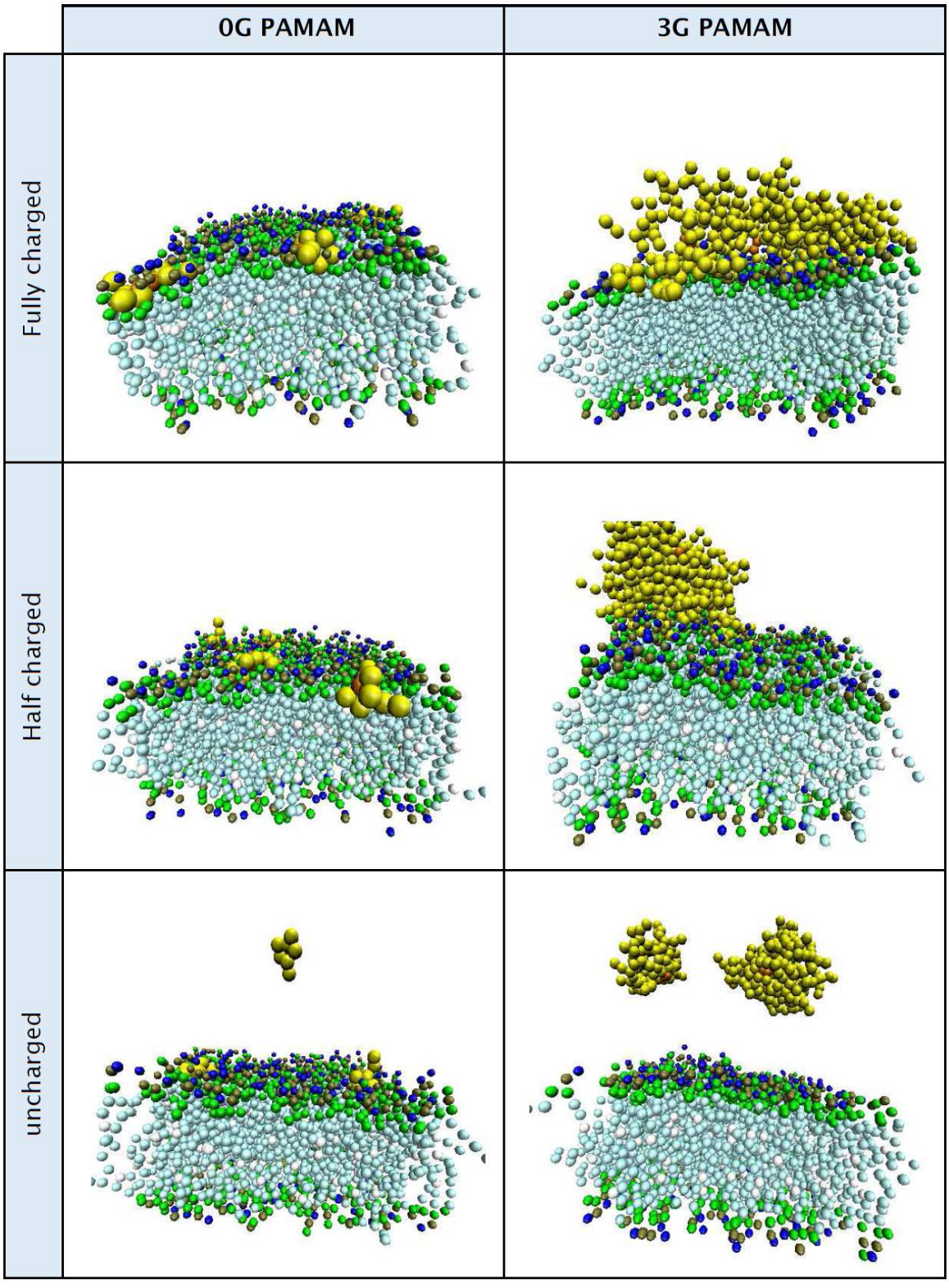

Figure 50 Snapshots taken at the end of various coarse-grained MD simulations (t = 300 ns), showing the interaction between fully charged, half charged and uncharged 0th and 3rd generation PAMAM dendrimers and 2:1 POPC:POPG. Each simulation contains four PAMAM dendrimers and the following colour coding is used: PAMAM moieties (yellow beads), phospholipids (green and blue beads with the membrane interior opaque). Water molecules and Na^+/Cl^- ions are omitted for clarity.

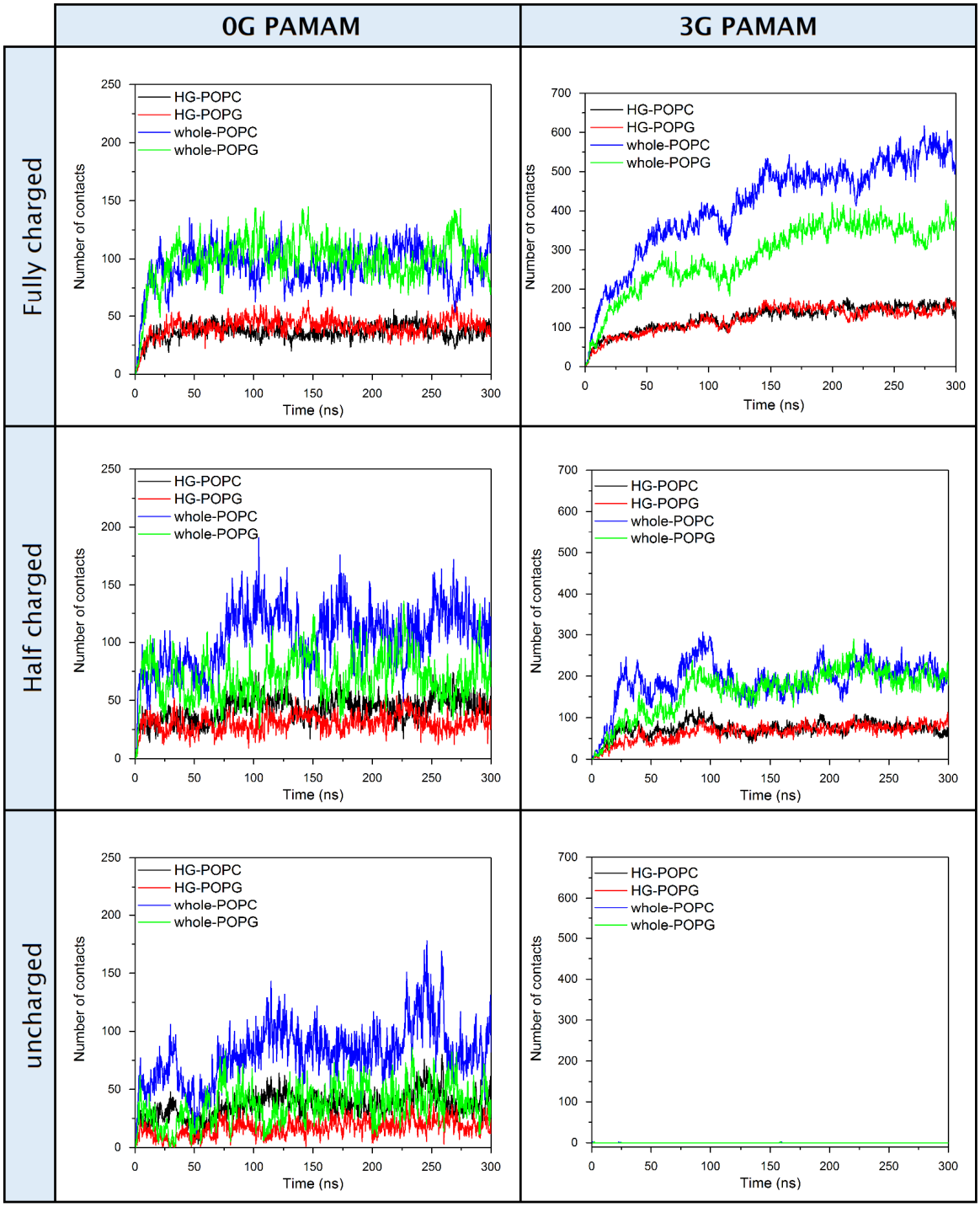

Figure 51 Overview of the number of contacts between fully positively charged, half positively charged and uncharged **0G** or **3G** PAMAM dendrimers and POPC or POPG lipids during a 300 ns CG-MD simulation. The results are the average of three independent runs. The y-axes are kept the same to allow easier comparison between the fully charged, half charged and uncharged conditions.

The situation is slightly different in the case of **0G** PAMAM. Compared to the fully charged third generation PAMAM, the zero generation PAMAM dendrimers

have a smaller number of contacts with the lipids which can be attributed to their smaller size. Furthermore, the interaction between **0G** PAMAM dendrimers and 2:1 POPC:POPG lipid bilayers appears to reach an equilibrium faster than is the case for **3G** PAMAM dendrimers (see **Figure 51**). This could be a result of faster diffusion of the smaller **0G** PAMAM dendrimers compared to the larger 3G PAMAM dendrimers. Once again, a larger number of contacts is seen with the whole lipid than with the lipid head group alone, suggesting some degree of insertion for the fully charged 0th generation PAMAM. In contrast to the simulations with third generation PAMAM dendrimers, the difference in interaction between fully charged, half charged and uncharged **0G** PAMAM are not that pronounced. The largest difference can be seen in **Figure 50** which shows that not all of the uncharged **0G** PAMAM dendrimers come into contact with the anionic lipid bilayer, indicating that electrostatic interactions also play a role for zero generation PAMAM dendrimers. Furthermore, the differences in the number of contacts between the whole lipid and **0G** PAMAM as opposed to only the headgroups and **0G** PAMAM are less pronounced for the half-charged and uncharged dendrimers (see **Figure 51**). This could indicate that [partial] insertion of **0G** PAMAM dendrimers into the lipid bilayer is less favourable than insertion of **3G** PAMAM dendrimers (which was also seen during the ^{1}H-^{1}H NOESY NMR experiments were only few cross peaks were observed between **0G** PAMAM and POPC/POPG lipids).

Overall, the coarse-grained MD simulations have suggested that electrostatic interactions might play an import role in the interaction between protonated PAMAM dendrimers (be it fully protonated or partially protonated) and negatively charged lipid bilayers. While full insertion of the dendrimers into the bilayer or dendrimer-induced pore formation was not observed during these simulations, combined with the solid state NMR results and the fluorescence studies, the simulations hint that **3G** PAMAM dendrimers can interact with the surface headgroups of the membrane through electrostatic interactions and can gradually be inserted into the bilayer to maximise these electrostatic interactions (see mechanism D in **Figure 19**). However, it must be noted that during the solid state NMR studies the dendrimer samples were pre-mixed with the lipids before the formation of bilayers (by the addition of water), whilst

during the fluorescence and simulation studies the dendrimers were added in the aqueous phase surrounding existing membranes. This could mean that the insertion of the dendrimer into the bilayer is stable (as suggested by the solid state NMR results), but might be hard to achieve when the dendrimer is added externally and might only occur over a longer period of time. Future simulations over a longer time window might be able to shed light on this.

Chapter 3: Conclusions and Future Work

In this project, the successful synthesis and characterisation of a series of PAMAM dendrimers up to the 3rd generation have been undertaken, as well as a detailed study of the interaction of low generation PAMAM dendrimers (0th and 3rd generations) with various lipids (POPC and mixture of POPC/POPG) based on ^{1}H-^{1}H NOESY NMR, ^{31}P NMR, fluorescence spectroscopy and coarse-grained MD simulations. It was observed from the ^{31}P NMR experiments that both 0th and 3rd generation PAMAM dendrimers can interact with the lipid bilayer headgroups. However, NOESY NMR spectra showed an interaction between all dendrimers and the chains of both POPC and POPC:POPG lipid bilayers in non-controlled conditions. However, when the NOESY experiments were repeated in a controlled Tris buffer (pH=7.2) 3rd generation PAMAM dendrimers interacted more strongly with the chains of the lipid bilayers than the 0th generation, which might be due to the relatively small size of the 0th generation. Furthermore, this interaction was found to be more pronounced for 2:1 POPC:POPG bilayers than for pure POPC bilayers. The observed interaction between the 3rd generation PAMAM dendrimer and the chain in the lipid bilayer suggests either the formation of a dendrimer-lipid micelle whereby the lipid chain intercalates into the core of the dendrimer, or the insertion of the dendrimer into the membrane. It is currently not possible to distinguish between these two types of dendrimer-lipid interaction based on the results obtained during this study. Additional experiments based on different experimental techniques could be employed to distinguish between the two proposed mechanisms (*e.g.* AFM or other types of micoscopy can be used to see if dendrimer-micelles are formed).

Conclusions

Fluorescence studies were also carried out to explore the interaction between dansyl-labelled 3rd generation PAMAM dendrimers and various lipids and surfactants (POPC, a mixture of POPC/POPG, CTAB, SDS and 1,2-dodecyldiol). It was observed that the fluorescence intensity of a dansyl-labelled 3rd generation PAMAM dendrimer dramatically increased upon the addition of anionic lipids and surfactants, while a much smaller change in the fluorescence intensity occurred upon the addition of neutral or positively charged species. A shift in the emission wavelength was also observed in all cases with the highest shift in the presence of negatively charged lipids and surfactants and a lower shift in the presence of positively charged polar head lipids and surfactants. The fluorescence studies further confirmed the presence of the interaction between 3rd generation PAMAM dendrimers and negatively charged POPG bilayers that had been observed from the solid state NMR experiments. The importance of electrostatic interactions was also further highlighted by the coarse-grained MD simulation which showed that these dendrimers can interact with the surface of the membrane when they are positively charged, but not when the dendrimers are uncharged.

By running more experiments with a larger variety of differently charged lipids and surfactants, or even by testing against membrane extracts of bacterial or mammalian cells, it would be possible to obtain a wider spectrum of data relating to the interaction of various biologically relevant lipids with PAMAM dendrimers. Furthermore, testing against more PAMAM dendrimer generations or against functionalised PAMAM dendrimers with different surface properties would provide better information about the affinities between PAMAM dendrimers and various lipids and could help in optimising the use of PAMAM dendrimers for gene and drug delivery purposes (e.g. by finding the optimal dendrimer size for interaction with lipids).

Chapter 4: Experimental Section

4.1 Synthesis

Chemicals were purchased from *Sigma-Aldrich* or *Fisher Scientific*. Solvents were dried by distilling over drying agent; toluene and EDA were dried over calcium hydride, methanol was dried over calcium sulphate. DCM was dried by passing it twice through a silica plug. ^{1}H and ^{13}C NMR spectra were collected using either a Bruker AV300 or Bruker DPX400 spectrometer as solutions in a deuterated solvent and were reported at 300 MHz or 400 MHz. ^{13}C NMR spectra were collected fully ^{1}H decoupled. Chemical shift data are given in ppm with multiplicities abbreviated as follows; s (singlet), d (doublet), t (triplet), q (quartet), qu (quintet), br (broad) and m (multiplet). Coupling constants (J) are quoted in Hz. Analysis was carried out using ACD labs. Infrared (IR) were recorded on a Matterson Satellite (ATR) and are reported in wavenumbers (cm^{-1}). Low resolution mass spectra (LRMS) were recorded on a walters ZMD single quadrupole spectrometer. High resolution mass spectra (HRMS) were recorded by the mass spectrometry service at the University of Southampton on a Bruker Apex III or Bruker maXis ESI spectrometer. All mass spectra are reported as m/z (relative intensity). Elemental analysis was performed by *Medac Ltd*. Results are accurate to ±0.30%. All characterisations were compared to literature values and found in good agreement (differences can be attributed to the presence of methanol in the samples).[15, 155]

General procedure for half generation dendrimers. Half generations PAMAM dendrimers were synthesised by adding methyl acrylate (2.8 moles per dendrimer end group) dropwise to a stirred solution of whole generation

dendrimer in dried methanol (20 mL). The reaction was covered and stirred for about 6 days at room temperature, on reaction completion the solvent was removed under reduced pressure. Purification by column chromatography was carried on for generations up to 1.5 giving viscous yellow oils. An azeotropic distillation was carried out by dissolving the product in methanol (10 mL), then adding toluene (120 mL), followed by removing the solvents under reduced pressure. Azeotropic distillations were repeated for a further two times. The product was then dissolved in methanol (10 mL) and concentrated *in vacuo* to yield the product.

General procedure for full generation dendrimers. The whole generation PAMAM dendrimers were synthesised by dissolving half generation dendrimers in dried methanol (10%). The solution and EDA were deoxygenated by bubbling nitrogen through for 30 minutes. The dendrimer solution was added slowly to EDA cooled over ice and the reaction was stirred over ice at 5°C. The solvent and excess EDA were removed under reduced pressure and an azeotropic distillation was executed as described for the half generation dendrimers. The product was then dissolved in methanol and subsequently concentrated under reduced pressure to end up with a pale yellow oil. 3rd generation dendrimer was purified by dialysis in de-ionised water for 5 days, followed by azeotropic distillation to produce a viscous oil.

PAMAM -0.5G ($^{b}CH_2{}^{b}CH_2$)[N($^{c}CH_2{}^{a}CH_2CO_2{}^{d}CH_3$)$_2$]$_2$. ^{1}H NMR (300 MHz, $CDCl_3$) δ ppm 2.42 (8 H, t, *J*=7.0 Hz, a), 2.47 (4 H, s, b), 2.75 (8 H, t, *J*=7.0 Hz, c), 3.65 (12 H, s, d); ^{13}C NMR (75 MHz, $CDCl_3$) δ ppm: 32.6 (a), 49.7 (c), 51.5 (d), 52.2 (b), 172.9 (C=O); FTIR (neat) ν_{max}/cm^{-1} 2950, 2820, 1730; LRMS (ESI+) m/z: 405.2 $[M+H]^+$, 427.1 $[M+Na]^+$; Elemental analysis (%) for $C_{18}H_{32}N_2O_8$: C, 53.5; H, 8.0; N, 6.9 (calcd), C, 53.3; H, 7.7; N, 7.0 (found).

PAMAM 0G ($^{b}CH_2{}^{b}CH_2$)[N($^{d}CH_2{}^{a}CH_2CONH^{e}CH_2{}^{c}CH_2NH_2$)$_2$]$_2$. ^{1}H NMR (300 MHz, D_2O) δ ppm: 2.45 (8 H, t, *J*=7.3 Hz, a), 2.61 (4 H, s, b), 2.73 (8 H, t, *J*=6.2 Hz, c), 2.82 (8 H, t, *J*=8.0 Hz, d), 3.25 (8 H, t, *J*=6.2 Hz, e); ^{13}C NMR (75 MHz, $CDCl_3$) δ ppm: 34.4 (a), 41.5 (c), 42.4 (e), 50.6 (d), 52.1 (b), 173.1 (C=O); FTIR (neat)

ν_{max}/cm^{-1} 3270, 2920, 2850, 1640, 1550; HRMS (ESI+) m/z for $C_{22}H_{49}N_{10}O_4$ $[M+H]^+$ 517.3933 (calc), 517.3932 (found), for $C_{22}H_{48}N_{10}NaO_4$ $[M+Na]^+$ 539.3752 (calc), 539.3743 (found); Elemental analysis (%) for $C_{22}H_{48}N_{10}O_4$: C, 51.1; H, 9.3; N, 27.1 (calcd), C, 41.6; H, 10.5; N, 21.5 (found).

PAMAM 0.5G ($^cCH_2{}^cCH_2$) [N($^eCH_2{}^aCH_2CO^iNH^gCH_2{}^dCH_2N(^fCH_2{}^bCH_2CO_2{}^hCH_3)_2)_2]_2$. ^{1}H NMR (300 MHz, $CDCl_3$) δ ppm 2.41 (24 H, m, a, b), 2.54 (12 H, m, c, d), 2.74 (24 H, m, e, f), 3.25 (8 H, q, *J*=5.6 Hz, g), 3.65 (24 H, s, h), 7.16 (4 H, br. s, i); ^{13}C NMR (75 MHz, $CDCl_3$) δ ppm: 32.6 (b), 33.6 (a), 37.2 (g), 49.3 (f), 51.1 (e), 51.5 (h), 52.9 (c, d), 172.1 (C=O), 172.9 (CO_2); FTIR (neat) ν_{max}/cm^{-1} 3290, 2950, 2830, 1730, 1640, 1540 LRMS (ESI+) m/z: 1205.7 $[M+H]^+$, 1227.1 $[M+Na]^+$, 603.5$[M+2H]^{++}$; Elemental analysis (%) for $C_{54}H_{96}N_{10}O_{20}$: C, 53.8; H, 8.1; N, 11.6 (calcd), C, 53.1; H, 8.2; N, 11.5 (found).

PAMAM 1.0G

($^cCH_2{}^cCH_2$)[N($^eCH_2{}^aCH_2CONH^hCH_2{}^dCH_2N(^fCH_2{}^bCH_2CONH^iCH_2{}^gCH_2NH_2)_2)_2]_2$.

^{1}H NMR (300 MHz, D_2O) δ ppm 2.39 (24 H, m, a, b), 2.61 (12 H, m, c, d), 2.78 (40 H, m, e, f, g), 3.25 (24 H, m, h, i); ^{13}C NMR (75 MHz, $CDCl_3$) δ ppm: 32.5 (a), 33.2 (b), 37.2 (h),45.6(g), 49.1(i), 50.0(e), 51.5 (f), 52.6 (c), 62.7(d), 173.0 (C=O); FTIR (neat) ν_{max}/cm^{-1} 3340, 3270, 3190, 2920, 2860, 1640, 1550; LRMS (ESI+): m/z Calcd for $C_{62}H_{128}N_{26}O_{12}$ [M]: 1429.02. Found: 715.5 $[(M+2H)/2]^{++}$, 1430.02 $[M+H]^+$; Elemental analysis (%) for $C_{62}H_{128}N_{26}O_{12}$: C, 52.1; H, 8.9; N, 25.5 (calcd), C, 44.1; H, 9.9; N, 21.4 (found).

PAMAM 1.5G

($^dCH_2{}^dCH_2$)[N($^gCH_2{}^cCH_2CONH^jCH_2{}^eCH_2N

($^hCH_2{}^bCH_2CONH^kCH_2{}^fCH_2N(^iCH_2{}^aCH_2CO_2{}^lCH_3)_2)_2)_2]_2$.

^{1}H NMR (300 MHz, $CDCl_3$) δ ppm 2.44 (56 H, t, J=6.59 Hz, a, b, c), 2.58 (28 H, m, d, e, f), 2.78 (56 H, m, g, h, i), 3.29 (24 H, m, j, k), 3.67 (54 H, s, l); ^{13}C NMR (75 MHz, $CDCl_3$) δ ppm: 32.4 (a), 33.5 (b, c), 37.0 (k),37.3 (j), 49.0 (i), 49.5 (h), 49.6 (g), 50.0 (l), 51.4 (l), 52.2 (e), 52.6 (f), 172.4 (C=O), 172.9 (CO_2); FTIR (neat) ν_{max}/cm^{-1} 2940, 2820, 1730, 1640, 1540; LRMS (ESI+): m/z Calcd for $C_{126}H_{224}N_{26}O_{44}$ [M]: 2805.61. Found: 951.2 $[(M+H+2Na)/3]^{+++}$, 1415.3

$[(M+H+Na)/2]^{++}$, 2807.3$[M+H]^{+}$, 2828,6 $[M+Na]^{+}$; Elemental analysis (%) for $C_{126}H_{224}N_{26}O_{44}$: C, 53.9; H, 8.1; N, 12.9 (calcd), C, 50.2; H, 9.1; N, 12.0 (found).

PAMAM 2.0G

($^{d}CH_2{}^{d}CH_2$)[N($^{h}CH_2{}^{a}CH_2CONH^{l}CH_2{}^{e}CH_2N$
($^{i}CH_2{}^{b}CH_2CONH^{m}CH_2{}^{f}CH_2N(^{j}CH_2{}^{c}CH_2CONH^{k}CH_2{}^{g}CH_2NH_2)_2)$ $_2)_2]_2$.

^{1}H NMR (300 MHz, D_2O) δ ppm 2.44 (56 H, m, a, b, c), 2.62 (28 H, t, J=6.40 Hz, d, e, f), 2.72 (32 H, m, g), 2.84 (56 H, m, h, i, j), 3.26 (56 H, m, k, l, m); ^{13}C NMR (75 MHz, D_2O) δ ppm: 32.7 (a), 32.8 (b, c), 36.7 (l, m),39.8 (g), 41.6 (k), 49.1 (h, i), 51.3 (d, e), 174.4 (C=O), 174.6 (C=O), 175.6 (C=O); FTIR (neat) ν_{max}/cm^{-1} 3320, 3270, 3190, 3060, 2920, 2860, 1640, 1550.

PAMAM 2.5G

($^{l}CH_2{}^{l}CH_2$)[N($^{k}CH_2{}^{d}CH_2CO^{s}NH^{m}CH_2{}^{g}CH_2N$
($^{j}CH_2{}^{c}CH_2CO^{r}NH^{n}CH_2{}^{f}CH_2N(^{i}CH_2{}^{b}CH_2CO^{q}NH^{o}CH_2{}^{e}CH_2N(^{h}CH_2{}^{a}CH_2CO_2{}^{p}CH_3)_2)_2)$ $_2)_2]_2$.

^{1}H NMR (300 MHz, $CDCl_3$) δ ppm 2.42 (120 H, m, a, b, c, d), 2.51 (56 H, m, e, f, g), 2.73 (124 H, m, h, i, j, k, l), 3.24 (56 H, m, m, n, o), 3.62 (96 H, s, p), 7.12 (14 H, m (br), g), 7.71 (12 H, m (br), r, s); ^{13}C NMR (75 MHz, $CDCl_3$) δ ppm: 32.9, 34.1, 37.5, 37.8, 49.6, 50.1, 50.3, 50.8, 51.9, 52.8, 53.2, 172.6-172.7 (C=O), 173.4 (C=O); FTIR (neat) ν_{max}/cm^{-1} 2950, 2820, 1730, 1650, 1540; LRMS (ESI+): m/z Calcd for $C_{270}H_{480}N_{58}O_{92}$ [M]: 6007.47. Found: 1227.9 $[(M+K+4Na)/5]^{+5}$.

PAMAM 3.0G

($^{h}CH_2{}^{h}CH_2$)[N($^{m}CH_2{}^{d}CH_2CONH^{q}CH_2{}^{g}CH_2N(^{l}CH_2{}^{c}CH_2CONH^{p}CH_2{}^{f}CH_2N$
($^{k}CH_2{}^{b}CH_2CONH^{o}CH_2{}^{e}CH_2N(^{j}CH_2{}^{a}CH_2CONH^{n}CH_2{}^{i}CH_2NH_2)_2)_2)_2)_2]_2$.

^{1}H NMR (300 MHz, D_2O) δ ppm 2.45 (120 H, m, a, b, c, d), 2.63 (60 H, m, e, f, g, h), 2.74 (64 H, m, i), 2.83 (120 H, m, j, k, l, m), 3.28 (120 H, n, o, p, q); ^{13}C NMR (75 MHz, $CDCl_3$) δ ppm: 32.8, 36.7, 39.8, 41.4, 49.1, 51.3, 53.2, 174.6 (C=O), 174.6 (C=O); FTIR (neat) ν_{max}/cm^{-1} 3340, 3270, 3170, 2920, 2850, 1730, 1640, 1560.

4.2 Solid state NMR

4.2.1 Preparation of lipid samples (negative controls)

1-palmitoyl-2-oleoyl-*sn*-glycero-3-phosphocholine (POPC) and 1-palmitoyl-2-oleoyl-*sn*-glycero-3-phospho-(1`-rac-glycerol) (POPG) powder were obtained from *Avanti Polar Lipids, INC*. POPC samples were prepared by dissolving 7 mg in a 1:1 mix of chloroform and methanol and lyophilised overnight. POPC/POPG samples in ratio 2:1 POPC: POPG were prepared by dissolving 4.66 mg of POPC and 2.34 mg of POPG in a mix 1:1 of chloroform and methanol and lyophilised overnight. Samples then were dissolved in 23 µL deuterium oxide. Homogeneity was achieved by cycling between freeze and thaw states at least six times, using liquid nitrogen for freezing. These negative controls were used for Nuclear Overhauser Effect (NOE) and for testing the relaxation times of the phosphorus nuclei.

4.2.2 Preparation of dendrimers in lipids samples

The 0^{th} generation and 3^{rd} generation PAMAM dendrimers (0.126 µmol) were added in molar ratio (1:75) to the POPC or the mixture (POPC:POPG 2:1) (9.45 µmol) in methanol. The mixture was lyphophilised overnight and then 23 µL of deuterium oxide was added. Then the samples went into cycles of freeze (using liquid nitrogen) and thawing at room temperature. This preparation is believed to provide a uniform dendrimer distribution throughout the membrane.[124].

4.2.3 ^{31}P phosphorous NMR

Phosphorus nuclei scans were run on a Chemagnetix ICS 400 MHz with a 4 mm double resonance magic angle spinning tube. One dimensional scans acquired at a spectral frequency of 161.824 MHz, a spectral width of 100 KHz and 512 acquisitions took place with a pulse sequence consisting of: 90° pulse, $50*10^{-6}$ second wait, 180° pulse, $30*10^{-6}$ second wait and then the acquisition

period. Phosphorus nuclei examined on an Adjuvant DDRZ 600 MHz with 3.2 mm triple resonance MAS tubes, at frequency 243.0608 MHz and spectral width of 100 KHz and 1024 acquisitions. All phosphorus nuclei samples are referenced to a phosphoric acid standard (aligned to 0 ppm on the spectra) and are proton decoupled at 50 KHz.

To observe the phase transition temperature of the lipids and the behaviour of the phosphates in the lipids phosphorus nuclei were examined across a range of temperatures (-20°C to 40°C). The second moment of these spectra were calculated and plotted against temperature, which allowed an estimation of phase transition temperature. Determination of the spin-lattice and spin-spin relaxation times at 25°C were carried out on a Chemagnetic ICS 400 MHz at the frequency and spectral width given above. The spin-lattice relaxation times were measured using 7197 acquisitions and mixing times of 1 ms, 500 ms, 750 ms 1 s, 1.5 s, 2s and 4 s. The spin-spin relaxation times were measured using CPMG sequence with mixing times of 25 μs, 50 μs, 100 μs, 150 μs, 200 μs, 400 μs and 800 μs.

4.2.4 Nuclear Overhauser Effect (NOE)

The NOE was studied at 25°C on an Adjuvant DDRZ 600 MHz with 3.2 mm triple resonance MAS tubes. The sample was spun at a rate of 10 KHz with 872 complex points in the acquisition dimension and 256 in the indirect dimension. 16 scans were acquired for each mixing time at a frequency 600.445 MHz and spectral width 7267.44 Hz.

Each acquisition was obtained using a pulse sequence of: 90° pulse, an incremental delay period, another 90° pulse, a wait for the mixing time and finally another 90° pulse, followed by a wait and an acquisition period. The mixing times used were increments of 100 ms between 100 ms and 500 ms. NOEs were estimated by using an initial rate approximation.

4.3 Fluorescence studies

Synthesis of compound 3G-dansyl. 3rd generation PAMAM dendrimer (129.15 mg, 0.0187 mmol) was stirred in a distilled dry methanol (3 mL) with two drops of triethylamine. Dansyl chloride (10.2 mg, 0.0378 mmol) was added to the previous solution and stirred overnight at room temperature. Purifications were carried out by dialysis to the finished reaction products in deionised water. The excess of water was removed on rotary vacuum at 50-55˚C.

UV/Vis absorption spectra were recorded on Shimadzu UV-1601 UV/Vis spectrophotometer. Fluorescence intensity was measured Cary Eclipse and Hitachi F-2500 FL Spectrophotometer. The extinction coefficient of compound **3G-dansyl** was calculated by measuring the absorbance at 330 nm for various concentrations of aqueous solutions of **3G-dansyl**. The results were subsequently plotted as absorbance versus concentration and fitted using the Lambert-Beer equation (A=εlc, with A= absorbance, ε= extinction coefficient, l= length of cuvette (1cm), c=concentration) using Excel 2010 as shown in **Figure 52**.

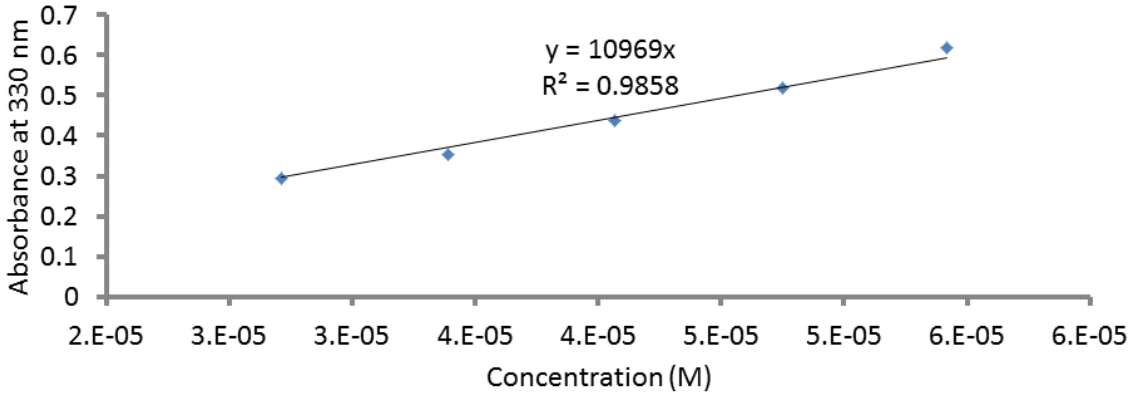

Figure 52. Linearity between the concentrations of the 3rd generation PAMAM dendrimer marked with dansyl and the absorbance values at 330 nm in aqueous solution. The extinction coefficient of **3G-dansyl** shows the value 10,969 $M^{-1}cm^{-1}$, about twice the value for the single dansyl and as there is a linear relation between the number of the dansyls attached to the PAMAM dendrimer,[146] this suggests that the ratio in **3G-dansyl** is 2:1 dansyl:dendrimer.

4.4 Molecular dynamics simulations

Dendrimers were defined by coarse-grained beads according to the method described by Lee *et al,*[115] while lipids and water molecules were described according to the method by Marrink *et al.*[150] The MARTINI CG force field was used for the dendrimers, lipids, water and ions.[156] The CG molecular dynamics simulations were run with a time step of 30 fs and for an overall duration of 300 ns using the GROMACS simulation package.[151] Each simulation contained four dendrimer molecules, 300 lipid molecules (200 POPC and 100 POPG molecules) and was solvated with 11,800 CG water molecules (each CG water bead corresponds to four water molecules) in a periodic box of size 10.4 x 9.3 x 16 nm^3. Na^+ and Cl^- ions were also added to maintain the charge balance. The temperature was maintained at 323 K by applying a Berendsen thermostat.[152] A cut-off of 1.2 nm was used for van der Waals interactions, to which a standard shift function was applied to smoothly shift the Lennard-Jones potential to zero between 0.9 nm and 1.2 nm. Electrostatic interactions were modelled with a particle mesh Ewald summation which allows long-rang interactions.

Contacts were defined as an interaction when the distance between any of the dendrimer beads and the lipid beads (either the Q^+ or P_{da} bead for the lipid headgroup, or all of the lipid beads for the whole lipid) was less than 6 Å. Contacts were calculated using the VMD software and were further analysed and plotted using Origin 9.1.

List of References

1. O. E. Dictionary, "*polymer, n.*", Oxford University Press.
2. M. L. Miller, *The structure of polymers*, Reinhold New York, 1966.
3. J. C. Salamone, *Concise polymeric materials encyclopedia*, CRC press, 1998.
4. H. Aliyar, R. Huber, G. Loubert and G. Schalau, *J. Pharm. Sci.*, 2014.
5. K. Ito, Y. Tomi and S. Kawaguchi, *Macromol. Theory Simul.*, 1992, **25**, 1534-1538.
6. S. K. Rhodes, R. H. Lambeth, J. Gonzales, J. S. Moore and J. A. Lewis*, *Langmuir*, 2009, **25**, 6787-6792.
7. N. Du, J. Song, G. P. Robertson, I. Pinnau and M. D. Guiver, *Macromol. Rapid Commun.*, 2008, **29**, 783-788.
8. H. Kudo, K. Shigematsu, K. Mitani, T. Nishikubo, N. C. Kasuga, H. Uekusa and Y. Ohashi, *Macromol. Theory Simul.*, 2008, **41**, 2030-2036.
9. J. F. Stoddart, *Chem. Soc. Rev.*, 2009, **38**, 1802-1820.
10. T. Takata, N. Kihara and Y. Furusho, in *Polymer Synthesis*, Springer Berlin Heidelberg, 2004, vol. 171, pp. 1-75.
11. G. Sforazzini, A. Kahnt, M. Wykes, J. K. Sprafke, S. Brovelli, D. Montarnal, F. Meinardi, F. Cacialli, D. Beljonne, B. Albinsson and H. L. Anderson, *J. Phys. Chem. C*, 2014, **118**, 4553-4566.
12. N. Watanabe, Y. Ikari, N. Kihara and T. Takata, *Macromol. Theory Simul.*, 2004, **37**, 6663-6666.
13. C. Hamers, F. M. Raymo and J. F. Stoddart, *Eur. J. Org. Chem.*, 1998, **1998**, 2109-2117.
14. E. Buhleier, W. Wehner and F. Vogtle, *Synthesis*, 1978, 155-158.
15. D. A. Tomalia, H. Baker, J. Dewald, M. Hall, G. Kallos, S. Martin, J. Roeck, J. Ryder and P. Smith, *Polym. J.*, 1985, **17**, 117-132.
16. D. A. Tomalia, H. Baker, J. Dewald, M. Hall, G. Kallos, S. Martin, J. Roeck, J. Ryder and P. Smith, *Macromol. Theory Simul.*, 1986, **19**, 2466-2468.
17. D. A. Tomalia, A. M. Naylor and W. A. Goddard, *Angew. Chem., Int. Ed. Engl.*, 1990, **29**, 138-175.
18. G. R. Newkome, Z. Yao, G. R. Baker and V. K. Gupta, *J. Org. Chem.*, 1985, **50**, 2003-2004.
19. G. R. Newkome, Z. Yao, G. R. Baker, V. K. Gupta, P. S. Russo and M. J. Saunders, *J. Am. Chem. Soc.*, 1986, **108**, 849-850.
20. D. McIntyre, L. J. Fetters and E. Slagowski, *Science*, 1972, **176**, 1041-1043.

21. B. Zhang, R. Wepf, K. Fischer, M. Schmidt, S. Besse, P. Lindner, B. T. King, R. Sigel, P. Schurtenberger, Y. Talmon, Y. Ding, M. Kröger, A. Halperin and A. D. Schlüter, *Angew. Chem. Int. Ed.*, 2011, **50**, 737-740.
22. P. Ge and Z. H. Zhou, *Proc. Natl. Acad. Sci. U. S. A.*, 2011, **108**, 9637-9642.
23. K. Namba, R. Pattanayek and G. Stubbs, *J. Mol. Biol.*, 1989, **208**, 307-325.
24. J. N. Culver, *Annu. Rev. Phytopathol.*, 2002, **40**, 287-308.
25. P. T. Callaghan and D. N. Pinder, *Macromol. Theory Simul.*, 1981, **14**, 1334-1340.
26. P.-G. De Gennes, *Scaling concepts in polymer physics*, Cornell university press, 1979.
27. A. M. Naylor, W. A. Goddard, G. E. Kiefer and D. A. Tomalia, *J. Am. Chem. Soc.*, 1989, **111**, 2339-2341.
28. R. G. Denkewalter, J. Kolc and W. J. Lukasavage, Google Patents, 1981.
29. S. M. Aharoni, C. R. Crosby and E. K. Walsh, *Macromol. Theory Simul.*, 1982, **15**, 1093-1098.
30. J. Fréchet, Y. Jiang, C. Hawker and A. Philippides, Proc. IUPAC Int. Symp., Macromol. pp, 1989.
31. C. J. Hawker and J. M. J. Frechet, *J. Am. Chem. Soc.*, 1990, **112**, 7638-7647.
32. T. M. Miller and T. X. Neenan, *Chem. Mater.*, 1990, **2**, 346-349.
33. Y. Yamakawa, M. Ueda, R. Nagahata, K. Takeuchi and M. Asai, *J. Chem. Soc., Perkin Trans. 1*, 1998, 4135-4140.
34. O. Haba, K. Haga, M. Ueda, O. Morikawa and H. Konishi, *Chem. Mater.*, 1999, **11**, 427-432.
35. J.-F. Nierengarten, T. Habicher, R. Kessinger, F. Cardullo, F. Diederich, V. Gramlich, J.-P. Gisselbrecht, C. Boudon and M. Gross, *Helv. Chim. Acta*, 1997, **80**, 2238-2276.
36. C. Bingel, *Chem. Ber.*, 1993, **126**, 1957-1959.
37. R. Esfand and D. A. Tomalia, *Drug Discovery Today*, 2001, **6**, 427-436.
38. S. Svenson and D. A. Tomalia, *Adv. Drug Delivery Rev.*, 2012, **64, Supplement**, 102-115.
39. M. Najlah and A. D'Emanuele, *Curr. Opin. Pharmacol.*, 2006, **6**, 522-527.
40. M. Liu and J. M. J. Fréchet, *Pharm. Sci. Technol. Today*, 1999, **2**, 393-401.
41. V. Biricova and A. Laznickova, *Bioorg. Chem.*, 2009, **37**, 185-192.
42. S. H. Medina and M. E. El-Sayed, *Chem. Rev.*, 2009, **109**, 3141-3157.
43. C. M. Paleos, D. Tsiourvas, Z. Sideratou and L.-A. Tziveleka, *Expert Opin. Drug Delivery*, 2010, **7**, 1387-1398.
44. M. A. Mintzer and M. W. Grinstaff, *Chem. Soc. Rev.*, 2011, **40**, 173-190.
45. S. Svenson, *Eur. J. Pharm. Sc*, 2009, **71**, 445-462.
46. S. Mignani, S. El Kazzouli, M. Bousmina and J.-P. Majoral, *Adv. Drug Delivery Rev.*, 2013, **65**, 1316-1330.
47. J. Recker, D. J. Tomcik and J. R. Parquette, *J. Am. Chem. Soc.*, 2000, **122**, 10298-10307.
48. J.-M. Lehn and J. Sanders, *Angew. Chem.*, 1995, **34**, 2563.
49. V. Balzani, *Tetrahedron*, 1992, **48**, 10443-10514.
50. T. S. Ahn, A. L. Thompson, P. Bharathi, A. Müller and C. J. Bardeen, *J. Phys. Chem. B*, 2006, **110**, 19810-19819.

51. T. Hori, N. Aratani, A. Takagi, T. Matsumoto, T. Kawai, M.-C. Yoon, Z. S. Yoon, S. Cho, D. Kim and A. Osuka, *Chem. Eur. J.*, 2006, **12**, 1319-1327.
52. M. Cotlet, S. Masuo, M. Lor, E. Fron, M. Van der Auweraer, K. Müllen, J. Hofkens and F. De Schryver, *Angew. Chem. Int. Ed.*, 2004, **43**, 6116-6120.
53. P. Furuta, J. Brooks, M. E. Thompson and J. M. J. Fréchet, *J. Am. Chem. Soc.*, 2003, **125**, 13165-13172.
54. N. Georgiev, V. Bojinov and A. Venkova, *J Fluoresc*, 2013, **23**, 459-471.
55. D. Yamaji and Y. Takaguchi, *Br. Polym. J.*, 2009, **41**, 293-296.
56. J.-M. Liu, Z.-B. Liu, G.-H. Zhu, X.-L. Li, X.-M. Huang, F.-M. Li, X.-M. Shi and L.-Q. Zeng, *Talanta*, 2008, **74**, 625-631.
57. A. Foucault-Collet, C. M. Shade, I. Nazarenko, S. Petoud and S. V. Eliseeva, *Angew. Chem., Int. Ed.*, 2014, **53**, 2927-2930.
58. H. Kobayashi, K. Reijnders, S. English, A. T. Yordanov, D. E. Milenic, A. L. Sowers, D. Citrin, M. C. Krishna, T. A. Waldmann, J. B. Mitchell and M. W. Brechbiel, *Clin. Cancer Res.*, 2004, **10**, 7712-7720.
59. A. T. Yordanov, H. Kobayashi, S. J. English, K. Reijnders, D. Milenic, M. C. Krishna, J. B. Mitchell and M. W. Brechbiel, *J. Mater. Chem.*, 2003, **13**, 1523-1525.
60. A. Puzari, *Liq. Cryst. Org. Compd. Polym. Mater. XXI Century: Synth. Appl.*, 2011, 95-124.
61. P. K. S. Antharjanam, M. Jaseer, K. N. Ragi and E. Prasad, *J. Photochem. Photobiol., A*, 2009, **203**, 50-55.
62. L. Balogh and D. A. Tomalia, *J. Am. Chem. Soc.*, 1998, **120**, 7355-7356.
63. L. Balogh, D. R. Swanson, D. A. Tomalia, G. L. Hagnauer and A. T. McManus, *Nano Lett.*, 2000, **1**, 18-21.
64. M. Zhao, L. Sun and R. M. Crooks, *J. Am. Chem. Soc.*, 1998, **120**, 4877-4878.
65. M. F. Ottaviani, R. Daddi, M. Brustolon, N. J. Turro and D. A. Tomalia, *Langmuir*, 1999, **15**, 1973-1980.
66. M. Zhao and R. M. Crooks, *Adv. Mater.*, 1999, **11**, 217-220.
67. M. Zhao and R. M. Crooks, *Angew. Chem., Int. Ed.*, 1999, **38**, 364-365.
68. R. Breslow, S. Wei and C. Kenesky, *Tetrahedron*, 2007, **63**, 6317-6321.
69. S. Wei, J. Wang, S. Venhuizen, R. Skouta and R. Breslow, *Bioorg. Med. Chem. Lett.*, 2009, **19**, 5543-5546.
70. J. J. Chruma, L. Liu, W. Zhou and R. Breslow, *Biorg. Med. Chem.*, 2005, **13**, 5873-5883.
71. D. A. Tomalia, M. Hall and D. M. Hedstrand, *J. Am. Chem. Soc.*, 1987, **109**, 1601-1603.
72. A. Sharma and U. S. Sharma, *Int. J. Pharm.*, 1997, **154**, 123-140.
73. A. Samad, Y. Sultana and M. Aqil, *Current drug delivery*, 2007, **4**, 297-305.
74. S. H. Battah, C.-E. Chee, H. Nakanishi, S. Gerscher, A. J. MacRobert and C. Edwards, *Bioconjugate Chem.*, 2001, **12**, 980-988.
75. N. Nishiyama, H. R. Stapert, G.-D. Zhang, D. Takasu, D.-L. Jiang, T. Nagano, T. Aida and K. Kataoka, *Bioconjugate Chem.*, 2002, **14**, 58-66.
76. G.-D. Zhang, A. Harada, N. Nishiyama, D.-L. Jiang, H. Koyama, T. Aida and K. Kataoka, *J. Controlled Release*, 2003, **93**, 141-150.
77. Y. Gong, B. Matthews, D. Cheung, T. Tam, I. Gadawski, D. Leung, G. Holan, J. Raff and S. Sacks, *Antiviral Res.*, 2002, **55**, 319-329.

78. M. Witvrouw, V. Fikkert, W. Pluymers, B. Matthews, K. Mardel, D. Schols, J. Raff, Z. Debyser, E. De Clercq, G. Holan and C. Pannecouque, *Mol. Pharmacol.*, 2000, **58**, 1100-1108.
79. U. Boas, A. J. Karlsson, B. F. M. de Waal and E. W. Meijer, *J. Org. Chem.*, 2001, **66**, 2136-2145.
80. N. Malik, E. G. Evagorou and R. Duncan, *Annu. Rev. Phytopathol.*, 1999, **10**, 767-776.
81. R. Duncan and N. Malik, US Patents US6585956 B2, 1998.
82. C. Kojima, K. Kono, K. Maruyama and T. Takagishi, *Bioconjugate Chem.*, 2000, **11**, 910-917.
83. D. Bhadra, S. Bhadra, S. Jain and N. K. Jain, *Int. J. Pharm.*, 2003, **257**, 111-124.
84. A. E. Beezer, A. S. H. King, I. K. Martin, J. C. Mitchel, L. J. Twyman and C. F. Wain, *Tetrahedron*, 2003, **59**, 3873-3880.
85. P. Kolhe, E. Misra, R. M. Kannan, S. Kannan and M. Lieh-Lai, *Int. J. Pharm.*, 2003, **259**, 143-160.
86. Y. Zhou, J. Yang, Z. Lin, J. Li, K. Liang, H. Yuan, S. Li and J. Li, *Colloids Surf., B*, 2014, **115**, 237-243.
87. K. Winnicka, M. Wroblewska, P. Wieczorek, P. Sacha and E. Tryniszewska, *Molecules*, 2013, **18**, 8607-8617.
88. B. Devarakonda, R. A. Hill and M. M. de Villiers, *Int. J. Pharm.*, 2004, **284**, 133-140.
89. A. U. Bielinska, C. Chen, J. Johnson and J. R. Baker, *Bioconjugate Chem.*, 1999, **10**, 843-850.
90. J. D. Eichman, A. U. Bielinska, J. F. Kukowska-Latallo and J. R. Baker Jr, *Pharm. Sci. Technol. Today*, 2000, **3**, 232-245.
91. C. R. Dass, *J. Pharm. Pharmacol.*, 2002, **54**, 3-27.
92. P. Ferruti, M. A. Marchisio and R. Duncan, *Macromol. Rapid Commun.*, 2002, **23**, 332-355.
93. J. A. Hughes, A. I. Aronsohn, A. V. Avrutskaya and R. L. Juliano, *Pharm. Res.*, 1996, **13**, 404-410.
94. I. Jääskeläinen, S. Peltola, P. Honkakoski, J. Mönkkönen and A. Urtti, *Eur. J. Pharm. Sci.*, 2000, **10**, 187-193.
95. R. L. Juliano, S. Alahari, H. Yoo, R. Kole and M. Cho, *Pharm. Res.*, 1999, **16**, 494-502.
96. S. C. W. Richardson, N. G. Pattrick, Y. K. Stella Man, P. Ferruti and R. Duncan, *Biomacromolecules*, 2001, **2**, 1023-1028.
97. D. S. Shah, T. Sakthivel, I. Toth, A. T. Florence and A. F. Wilderspin, *Int. J. Pharm.*, 2000, **208**, 41-48.
98. V. A. Bloomfield, *Curr. Opin. Struct. Biol.*, 1996, **6**, 334-341.
99. M. X. Tang, C. T. Redemann and F. C. Szoka, *Bioconjugate Chem.*, 1996, **7**, 703-714.
100. M. Tang and F. Szoka, *Gene Ther.*, 1997, **4**, 823-832.
101. H. Arima, F. Kihara, F. Hirayama and K. Uekama, *Bioconjugate Chem.*, 2001, **12**, 476-484.
102. H. Yoo and R. L. Juliano, *Nucleic Acids Res.*, 2000, **28**, 4225-4231.
103. A. V. Maksimenko, V. Mandrouguine, M. B. Gottikh, J.-R. Bertrand, J.-P. Majoral and C. Malvy, *J. Gene Med.*, 2003, **5**, 61-71.
104. T. Takahashi, K. Kono, T. Itoh, N. Emi and T. Takagishi, *Bioconjugate Chem.*, 2003, **14**, 764-773.
105. E. R. Figueroa, A. Y. Lin, J. Yan, L. Luo, A. E. Foster and R. A. Drezek, *Biomaterials*, 2014, **35**, 1725-1734.

106. D. Cao, L. Qin, H. Huang, M. Feng, S. Pan and J. Chen, *Mol. BioSyst.*, 2013, **9**, 3175-3186.
107. C. Peetla, A. Stine and V. Labhasetwar, *Mol. Pharmaceutics*, 2009, **6**, 1264-1276.
108. S. Hong, P. R. Leroueil, E. K. Janus, J. L. Peters, M.-M. Kober, M. T. Islam, B. G. Orr, J. R. Baker and M. M. Banaszak Holl, *Bioconjugate Chem.*, 2006, **17**, 728-734.
109. A. Mecke, I. J. Majoros, A. K. Patri, J. R. Baker, M. M. Banaszak Holl and B. G. Orr, *Langmuir*, 2005, **21**, 10348-10354.
110. A. Mecke, D.-K. Lee, A. Ramamoorthy, B. G. Orr and M. M. Banaszak Holl, *Langmuir*, 2005, **21**, 8588-8590.
111. B. Erickson, S. C. DiMaggio, D. G. Mullen, C. V. Kelly, P. R. Leroueil, S. A. Berry, J. R. Baker, B. G. Orr and M. M. Banaszak Holl, *Langmuir*, 2008, **24**, 11003-11008.
112. C. V. Kelly, M. G. Liroff, L. D. Triplett, P. R. Leroueil, D. G. Mullen, J. M. Wallace, S. Meshinchi, J. R. Baker, B. G. Orr and M. M. Banaszak Holl, *ACS Nano*, 2009, **3**, 1886-1896.
113. S. Hong, A. U. Bielinska, A. Mecke, B. Keszler, J. L. Beals, X. Shi, L. Balogh, B. G. Orr, J. R. Baker and M. M. Banaszak Holl, *Bioconjugate Chem.*, 2004, **15**, 774-782.
114. R. Jevprasesphant, J. Penny, D. Attwood and A. D'Emanuele, *J. Controlled Release*, 2004, **97**, 259-267.
115. H. Lee and R. G. Larson, *J. Phys. Chem. B*, 2006, **110**, 18204-18211.
116. A. Mecke, S. Uppuluri, T. M. Sassanella, D.-K. Lee, A. Ramamoorthy, J. R. Baker Jr, B. G. Orr and M. M. Banaszak Holl, *Chem. Phys. Lipids*, 2004, **132**, 3-14.
117. Y. Cheng, Q. Wu, Y. Li, J. Hu and T. Xu, *J. Phys. Chem. B*, 2009, **113**, 8339-8346.
118. Z.-Y. Zhang and B. D. Smith, *Bioconjugate Chem.*, 2000, **11**, 805-814.
119. P. E. S. Smith, J. R. Brender, U. H. N. Dürr, J. Xu, D. G. Mullen, M. M. Banaszak Holl and A. Ramamoorthy, *J. Am. Chem. Soc.*, 2010, **132**, 8087-8097.
120. A. Akesson, K. M. Bendtsen, M. A. Beherens, J. S. Pedersen, V. Alfredsson and M. C. Gomez, *PCCP*, 2010, **12**, 12267-12272.
121. C. V. Kelly, P. R. Leroueil, E. K. Nett, J. M. Wereszczynski, J. R. Baker, B. G. Orr, M. M. Banaszak Holl and I. Andricioaei, *J. Phys. Chem. B*, 2008, **112**, 9337-9345.
122. A. Mecke, I. Lee, J. R. B. jr, M. M. B. Holl and B. G. Orr, *Eur. Phys. J. E*, 2004, **14**, 7-16.
123. H. Lee and R. G. Larson, *J. Phys. Chem. B*, 2008, **112**, 7778-7784.
124. B. Klajnert and R. M. Epand, *Int. J. Pharm.*, 2005, **305**, 154-166.
125. K. Gardikis, S. Hatziantoniou, K. Viras, M. Wagner and C. Demetzos, *Int. J. Pharm.*, 2006, **318**, 118-123.
126. N. Karoonuthaisiri, K. Titiyevskiy and J. L. Thomas, *Colloids Surf., B*, 2003, **27**, 365-375.
127. R. Jevprasesphant, J. Penny, R. Jalal, D. Attwood, N. B. McKeown and A. D'Emanuele, *Int. J. Pharm.*, 2003, **252**, 263-266.
128. D. Fischer, Y. Li, B. Ahlemeyer, J. Krieglstein and T. Kissel, *Biomaterials*, 2003, **24**, 1121-1131.
129. D. A. Tomalia and J. M. J. Fréchet, *J. Polym. Sci., Part A: Polym. Chem.*, 2002, **40**, 2719-2728.
130. S. Ghosh, A. K. Banthia and Z. Chen, *Tetrahedron*, 2005, **61**, 2889-2896.

131. D. B. Amabilino, Royal Holloway, University of London, 1991.
132. D. Pavia, G. Lampman and G. Kriz, *Introduction to spectroscopy*, Second edn., Harcourt Brace College Publishers, Fort Worth, 1996.
133. H. W. Dudley and I. Fleming, *Spectroscopic methods in organic chemistry*, Fifth edn., McGraw-Hill Publishing Company, Berkshire, England, 1995.
134. L. M. Jackman and S. Sternhell, *Applications of nuclear magnetic resonance spectroscopy in organic chemistry*, 1972.
135. B. Bechinger, *Biochim. Biophys. Acta*, 1999, **1462**, 157-183.
136. D. Huster and K. Gawrisch, *J. Am. Chem. Soc.*, 1999, **121**, 1992-1993.
137. K. J. Hallock, K. Henzler Wildman, D.-K. Lee and A. Ramamoorthy, *Biophys. J.*, 2002, **82**, 2499-2503.
138. M. Bruch, *NMR spectroscopy techniques*, CRC Press, 1996.
139. P. J. Davis, B. D. Fleming, K. P. Coolbear and K. M. W. Keough, *Biochemistry*, 1981, **20**, 3633-3636.
140. V. S. Bryantsev, M. S. Diallo and W. A. Goddard, *J. Phys. Chem. A*, 2007, **111**, 4422-4430.
141. G. van Meer, D. R. Voelker and G. W. Feigenson, *Nat. Rev. Mol. Cell Biol.*, 2008, **9**, 112-124.
142. W.-M. Yau, W. C. Wimley, K. Gawrisch and S. H. White, *Biochemistry*, 1998, **37**, 14713-14718.
143. U. P. Strauss and G. Vesnaver, *J. Phys. Chem.*, 1975, **79**, 2426-2429.
144. B. Ren, F. Gao, Z. Tong and Y. Yan, *Chem. Phys. Lett.*, 1999, **307**, 55-61.
145. F. M. Winnik, *Chem. Rev.*, 1993, **93**, 587-614.
146. F. Vögtle, S. Gestermann, C. Kauffmann, P. Ceroni, V. Vicinelli, L. De Cola and V. Balzani, *J. Am. Chem. Soc.*, 1999, **121**, 12161-12166.
147. V. P. Torchilin and V. Weissig, *Liposomes: a practical approach*, Oxford University Press, 2003.
148. N. Kučerka, M.-P. Nieh and J. Katsaras, *Biochim. Biophys. Acta*, 2011, **1808**, 2761-2771.
149. R. Esfand and D. A. Tomalia, in *Dendrimers and Other Dendritic Polymers*, John Wiley & Sons, Ltd, 2002, pp. 587-604.
150. S. J. Marrink, A. H. de Vries and A. E. Mark, *J. Phys. Chem. B*, 2004, **108**, 750-760.
151. B. Hess, C. Kutzner, D. Van Der Spoel and E. Lindahl, *Journal of chemical theory and computation*, 2008, **4**, 435-447.
152. H. J. Berendsen, J. P. M. Postma, W. F. van Gunsteren, A. DiNola and J. Haak, *J. Chem. Phys.*, 1984, **81**, 3684-3690.
153. M. H. Kleinman, J. H. Flory, D. A. Tomalia and N. J. Turro, *J. Phys. Chem. B*, 2000, **104**, 11472-11479.
154. M. F. Ottaviani, F. Montalti, M. Romanelli, N. J. Turro and D. A. Tomalia, *J. Phys. Chem.*, 1996, **100**, 11033-11042.
155. W.-I. Hung, C.-B. Hung, Y.-H. Chang, J.-K. Dai, Y. Li, H. He, S.-W. Chen, T.-C. Huang, Y. Wei, X.-R. Jia and J.-M. Yeh, *J. Mater. Chem.*, 2011, **21**, 4581-4587.
156. S. J. Marrink, H. J. Risselada, S. Yefimov, D. P. Tieleman and A. H. de Vries, *J. Phys. Chem. B*, 2007, **111**, 7812-7824.